TAMPEREEN TEKNILLINEN YLIOPISTO
TAMPERE UNIVERSITY OF TECHNOLOGY

ALEXANDRA SHAKUN

SOFT ELASTOMERIC MATERIAL WITH IMPROVED DIELECTRIC PERMITTIVITY

Master of Science Thesis

Examiners: Professor Jyrki Vuorinen
FiDiPro Fellow Amit Das

Examiner and topic approved by the Faculty Council of the Faculty of Engineering Sciences on 15 January 2014

Abstract

TAMPERE UNIVERSITY OF TECHNOLOGY
International Master's Degree Programme in Materials Science
SHAKUN, ALEXANDRA: Soft elastomeric material with improved dielectric permittivity
Master of Science Thesis, 84 pages, 2 Appendix pages
April 2014
Major subject: Polymeric Materials
Examiners: Professor Jyrki Vuorinen, FiDiPro Fellow Amit Das
Keywords: dielectric elastomers, acrylic rubber, epichlorohydrin rubber, high dielectric constant fillers, dielectric permittivity

Dielectric elastomeric actuators (DEAs) tend to have good perspectives in artificial muscle applications. This class of materials has properties similar to the natural muscles. However, DEAs generally need very high actuation voltage that limits the possible applications and decreases the lifetime of an actuator. Although much research has been conducted to overcome the mentioned problems, efficient ways of lowering the working voltage are still in demand. Utilization of dielectric rubber composites is one of the popular approaches showing positive results. Namely, higher overall relative permittivity of the material allows reducing the actuation voltage if the mechanical properties are maintained at the initial level.

The aim of the current work is to modify acrylic and epichlorohydrin rubbers by addition of dielectric and ferroelectric fillers, as well as two types of dielectric oils, in order to obtain a material with enhanced dielectric permittivity and low modulus. Moreover, attention is paid to the mechanical properties, especially Young's modus and stress at 100 % elongation of the initial elastomers and obtained composites. The effect of crosslink densities of the vulcanizates is also taken into consideration. While the actuation tests are outside the scope of this thesis, actuation behaviour of the materials can be estimated theoretically based on mechanical and dielectric properties. As a result, some improvement was gained in material performance; number of important conclusions about fabrication, sample preparation, dielectric measurements and directions of further research was drawn. Finally, theoretical and experimental knowledge obtained during the preparation of the thesis can be valuable for the further development of the research project.

Preface

The studies underlying this thesis were conducted at the Department of Materials Science, Tampere University of Technology, during April – December 2013 as the part of ECoBi (Bio-inspired Elastomeric Composites) project. The project is undertaken in co-operation with industrial companies and funded by Finnish Funding Agency for Technology and Innovations (Tekes) and industrial partners. ECoBi project is aiming to develop novel elastomeric composite materials with enhanced dielectric actuation properties for application as an actuator in various fields, including robotics, vibration and sound dampening, portable electro-optic and microelectronic devices.

Part of the research was conducted in Saint-Petersburg at the laboratory of Mechanics of Polymer and Composite Materials in the Institute of Macromolecular Compounds, Russian Academy of Sciences during September - November 2013 as a part of bilateral exchange between Academy of Finland and Russian Academy of Sciences. I thank Professor Jyrki Vuorinen and Vladimir Yudin for making my exchange possible and productive, as well as for their advices and valuable recommendations. Moreover, I would like to thank members of Laboratories 8 and 10 of IMC RAS, especially Nadezhda Afanas'eva and Andrei Khayrullin for the revision and comments on dielectric part of my MSc thesis and for assistance in practical work.

I am grateful for the experience and knowledge that I have got during the preparation of this thesis. Therefore I would like to thank Minna Poikelispää and Amit Das for their patient guidance and valuable advices. Moreover, some experiments would be impossible without help of Kari Lahti, Meri Honkanen and Essi Sarlin. Finally, I thank my family for their support and inspiration during my studies.

Tampere, 21 March 2014

Alexandra Shakun

Contents

Abstract ii
Preface iii
List of symbols and abbreviations vi
List of figures ix
List of tables xii
1. Introduction 1
1.1. Aim and scope of the work 2
1.2. Thesis outline 3
2. Theoretical background 4
2.1. Dielectricity 4
2.1.1. Dielectric constant and relative permittivity 5
2.1.2. Polarization 6
2.1.3. Complex relative permittivity and dielectric loss 8
2.1.4. Dielectric relaxation 9
2.1.5. Dielectric strength and dielectric breakdown 11
2.1.6. Actuation 12
2.2. Dielectric elastomers 14
2.2.1. Effect of crosslinking on properties of elastomer 16
2.2.2. Acrylic rubber (ACM) 17
2.2.3. Epichlorohydrin rubber (CO, ECO, GECO) 19
2.3. Dielectric composite materials 20
2.3.1. Dielectric composite mixing rules 21
2.3.2. Filler systems 22
2.3.2.1. Titanium dioxide 23
2.3.2.2. Barium titanate 25
2.3.2.3. Tantalum pentoxide 26
2.3.3. Plasticizers 26
2.4.4. Alternative approach 27
3. Experimental 28
3.1. Materials 28
3.2. Preparation of elastomeric thin films 30
3.2.1. Solution casting 30
3.2.2. Mixing in internal mixer 31

3.2.3. Mixing on mill 33
3.3. Curing and determination of curing time 34
3.4. Determination of crosslink density 35
3.4.1. Determination of bound rubber 37
3.5. Mechanical testing 37
3.6. Electrical testing 38
3.6.1. Determination of dielectric constant 39
3.6.2. Testing for breakdown strength 40
3.7. Microscopy 40
4. Results and discussions 42
4.1. Preparation techniques 42
4.1.1. Tensile properties 43
4.1.2. Dielectric properties 44
4.1.3. Conclusions 45
4.2. Neat rubbers 45
4.2.1. Determination of curing time 46
4.2.2. Tensile properties 47
4.2.3. Dielectric properties 49
4.2.4. Conclusions 51
4.3. Composites 51
4.3.1. Curing 52
4.3.2. Tensile properties 53
4.3.3. Breakdown strength 58
4.3.4. Dielectric constant 59
4.3.5. Fitting to dielectric composite mixing rules 63
4.3.6. Conclusions 64
4.4. Effect of crosslink density 65
4.4.1. Conclusions 67
4.5. Microscopy 68
4.5.1. Conclusions 70
4.6. Evaluation of materials 71
4.6.1. Conclusions 73
5. General conclusions and further work 74
References 76
Appendix 1: Comparison of biological muscles and available actuator materials 85

List of symbols and abbreviations

A	polarizability of the molecule
α_a	atomic (ionic) polarizability
α_d	dipolar (orientational) polarizability
α_e	electronic polarizability
α_i	interfacial polarizability
α_π	hyperelectronic (nomadic) polarization
Δ	loss angle (phase lag)
δ_p	Hildebrand solubility parameter of polymer
δ_s	Hildebrand solubility parameter of solvent
ε_0	dielectric permittivity of vacuum
ε_c	permittivity of composite
ε_f	permittivity of filler particle
ε_s	static (relaxed) permittivity
ε_m	permittivity of isotropic matrix
ε_∞	high frequency (unrelaxed) permittivity
ε^*	complex relative permittivity
ε' (ε_r)	relative permittivity
ε''	loss factor (energy dissipated per cycle)
Θ	phase
K	dielectric constant
Λ	deformation ratio
λ_{break}	critical stretch at breakdown
M	permanent dipole moment
v_f	filler load (volume fraction)
v_m	volume fraction of matrix
v_r	volume fraction of rubber
v_{rf}	volume fraction of filled rubber in the swollen gel
$+\sigma/-\sigma$	charge density
Σ	Maxwell pressure
P	density
σ_f	conductivity of filler
σ_m	conductivity of matrix
Y	number of effective network chains
T	relaxation time
Φ	mass fraction of insoluble components
X	Flory-Huggins polymer-solvent interaction parameter
Ω	frequency of the alternating field
Φ	volume fraction of filler in the unswollen filled rubber
$+A\sigma/-A\sigma$	surface charge concentration
A	area of electrode
A_a, A_b, A_c	depolarizing factors along the three axes
a,b	fitting parameters of Havriliak – Negami equation for dielectric relaxation
C	capacitance
C	filler-rubber interaction parameter

D	electric flux density
d_0	initial sample thickness
E	electric field
E_{break}	breakdown strength
E_L	local electric field intensity
F	formula weight
F	frequency
F_L	indentation force
K	constant
k_B	Boltzmann constant
M	molecular weight
M_{100}	stress at 100% elongation
M_{200}	stress at 200% elongation
m_o	initial weight of the specimen
m_d	weight of the dried specimen
M_H	maximum torque
M_L	minimum torque
m_s	weight of the swollen specimen
N	Avogadro's number
N'	crosslink density
$\bar{p}$	dipole moment
$+p/-p$	bound charge density
P	electric polarization vector
Q	swelling value
Q_f	quality factor
R	gas constant
S'	elastic torque
S^*	complex torque
S_p	planar actuation strain
S_z	compressional strain in thickness direction
T	temperature
T_c	Curie temperature
t_{Cx}	time to a given percent state-of-cure
V	potential difference, applied voltage
V_{break}	breakdown voltage
V_s	molar volume of solvent
X	electric susceptibility of the material
X	percent state-of-cure
Y	Young's modulus (elastic modulus)
Z^*	complex impedance
Z_c	impedance of capacitor

AC	alternating electric field
ACM	acrylic rubber (polyacrylate elastomer)
AGE	allyl glycidyl ether
BRV	bound rubber value
BT	barium titanate
CAS	(CAS No.) numerical unique identifier of a chemical substance given by the Chemical Abstracts Service (CAS)
CBS	N-cyclohexyl-2-benzothazolesulfenamide

CCTO	calcium copper titanate
CNT	carbon nanotube
CO	epichlorohydrin homopolymer
CR	chloroprene rubber
CuPc	copper phthalocyanine
DC	static electric field
DE	dielectric elastomer
DEA	dielectric elastomer actuator
DOP	dioctyl phthalate
EAP	electroactive polymer
ECH	epichlorohydrin
ECO	epichlorohydrin/ethylene oxide/allyl glycidyl ether co-polymer
EM	electromagnetic motor
EMI	electromechanical instability
EO	ethylene oxide
EPDM	ethylene-propylene-diene rubber
GCO	epichlorohydrin/allyl glycidyl ether co-polymer
GECO	epichlorohydrin/ethylene oxide/allyl glycidyl ether ter-polymer
IMC RAS	Institute of Macromolecular Compounds, Russian Academy of Sciences
MWCNT	multiwall carbon nanotube
NCV	neat chamber volume
NBR	acrylonitrile-butadiene rubber
NR	natural rubber
P3HT	poly(3-hexylthiophene)
PBPSSI	poly(1,4-butanediol/1,3-propanediol/sebacate/succinate/itaconate)
PDMS	polydimethylsiloxane
PEG	polyethylene glycol
Phr	parts per hundred rubber
PMN	lead magnesium niobate
PMN-PT	lead magnesium nibobate-lead titanate
PPO	polypropylene oxide
PPy	polypyrrole
PT	lead titanate
PVDF	poly(vinylidene fluoride)
P(VDF-TrFE)	poly(vinylidene fluoride) copolymerized with trifluoroethylene
SBR	styrene-butadiene rubber
SEBS	polystyrene-b-poly(ethylene-co-butylene)-b-polystyrene
SIS	poly(styrene-isoprene-styrene)
TMTD	tetramethylthioram disulfide
TO	titanium dioxide (titania)
TP	tantalum pentoxide
TPE	thermoplastic elastomer
XNBR	carboxylated nitrile rubber

List of figures

Figure 2.1. Charges on a parallel-plate capacitor in static field a) with vacuum between the plates; b) with dielectric material between the plates [13]. 5

Figure 2.2. Dependence of the dielectric constant and polarization mechanisms on frequency [14] 8

Figure 2.3. AC losses in dielectric material: a) circuit diagram; b) phasor current [13]. 9

Figure 2.4. Dependence of low-frequency dielectric permittivity (a) and dielectric loss (b) on temperature [21]. 10

Figure 2.5. Possible scheme of experiment for breakdown strength determination [13]. 12

Figure 2.6. Operational principles of DEAs [2]......13

Figure 2.7. Effect of crosslink density on the mechanical properties of vulcanizate [60]. 17

Figure 2.8. Chemical structures of a) AMC rubber and b) available cure sites [66]. ...18

Figure 2.9. Chemical structures of epichlorohydrin elastomers [69]. 19

Figure 2.10. Unit cells of rutile and anatase; the bond lengths and angles of octahedrally coordinated Ti atoms are shown. On the right side the stacking of the octahedra is presented [86]. 24

Figure 2.11. Scheme of ionic displacement within barium titanate crystal leading to polarization in applied electric field [13]......25

Figure 2.12. Schematic structure of barium titanate [15]......26

Figure 3.1. The example of curing curve and curing time determination [60]. 34

Figure 3.2. Measuring cell with sample in assembly......39

Figure 4.1. ACM samples with dual cure-sites fabricated by a) solution casting; b) mixing in internal mixer; c) mixing on two-roll mill. 42

Figure 4.2. Tensile properties (with standard deviations) of ACM with dual cure-sites prepared by different methods. 43

Figure 4.3. Relative dielectric permittivity and dielectric losses (solid lines of corresponding colours) of a) solution-casted sample b) sample mixed in internal mixer and c) milled sample. 44

Figure 4.4. Resistivity (logarithmic scale) of ACM samples with dual cure-sites of a) solution-casted sample, b) sample mixed in internal mixer and c) milled sample. 45

Figure 4.5. Unfilled rubbers: a) ACM (dual); b) ACM (chlorine); c) CO; d) GECO....46

Figure 4.6. Curing curve at 175 ˚C of unfilled a) ACM with dual cure-sites; b) CO; c) GECO with TMTD accelerator......47

Figure 4.7. Curing curves of GECO samples at 160 ˚C (dashed line) and 175 ˚C (solid line) with different curatives: a, b) TMTD; c, d) CBS. 47

Figure 4.8. Tensile properties (with standard deviations) of neat rubbers. 48

Figure 4.9. Tensile properties (with standard deviations) of ACM with dual cure-sites prepared on mill depending on the curing time. 49

Figure 4.10. Relative dielectric permittivity (ε′) and dielectric losses (ε″, solid lines of corresponding colours) of a) ACM with dual cure-sites, b) ACM with chlorine cure-sites and c) CO sample. 49

Figure 4.11. Relative dielectric permittivity (a) and dielectric losses (c) of GECO with TMTD accelerator; relative dielectric permittivity(b) and dielectric losses (d) of GECO with CBS accelerator. 50

Figure 4.12. Volume resistivity (logarithmic scale) of neat rubber samples: a) ACM with dual cure-sites, b) ACM with chlorine cure-sites, c) CO, and GECO with d) TMTD accelerator or e) CBS accelerator. 51

Figure 4.13. Curing curves of acrylic rubber at 175 ˚C with a) no oil; b) 5 phr of MIDEL® oil c) 5 phr of Fomblin® oil. 52

Figure 4.14. Curing curves of GECO with TMTD accelerator at 175 ˚C with a) no oil; b) 5 phr of Fomblin oil; c) 5 phr of MIDEL oil. 53

Figure 4.15. Curing curves of GECO with TMTD accelerator at 175˚C with a) no filler; and with 20 phr of b) BT; c) TP; d) TO. 53

Figure 4.16. Tensile properties of ACM (dual) composites prepared by sonication-assisted solution casting method. 54

Figure 4.17. Tensile properties (with standard deviations) of ACM with dual cure-sites depending on the BT load. 55

Figure 4.18. Tensile properties (with standard deviations) of ACM with chlorine cure-sites with 5 phr of fillers/oils. 56

Figure 4.19. Young's modulus of various rubbers at 5 phr filler or oil load. 56

Figure 4.20. Maximum elongation of various rubbers with 5 phr filler or oil load. 57

Figure 4.21. Mechanical properties of filler-loaded GECO rubbers. 57

Figure 4.22. Mechanical properties of oil-filled GECO. 58

Figure 4.23. Maximum elongation of GECO samples. 58

Figure 4.24. Breakdown strength of solution-casted samples (with standard deviation). 59

Figure 4.25. Relative dielectric permittivity (a) and losses (b) of various composites containing 5 phr of fillers; measured at 1 kHz. 60

Figure 4.26. Relative dielectric permittivity (a, b) and losses (c, d) of various composites containing transformer oils; measured at 1 kHz. 61

Figure 4.27. Relative dielectric permittivity (a, b) and losses (c, d) of various GECO composites; measured at 1 kHz. 62

Figure 4.28. Volume resistivity of GECO rubbers filled with a) BT; b) TP; c) TO depending on a frequency and a filler load. 62

Figure 4.29. Volume resistivity of GECO rubbers filled with a) MIDEL® oil; b) Fomblin® oil depending on a frequency and a filler load. 63

Figure 4.30. Fitting experimental dielectric permittivity of BT-filled ACM with dual cure-sites to classical dielectric mixing rules. 64

Figure 4.31. Mechanical properties of ACM with dual cure-sites in relation to curing times and accompanying change in crosslink density. 65

Figure 4.32. Mechanical properties of ACM with dual cure-sites loaded with 0, 5, 10, 20 phr of BT in relation to the crosslink density. 66

Figure 4.33. Mechanical properties of ACM (chlorine) with various fillers/oils in relation to the crosslink density. 66

Figure 4.34. Mechanical properties of GECO with 5 phr of different fillers in relation to crosslink density. 67

Figure 4.35. Effect of curing time on crosslink density and relative dielectric permittivity (at 1 kHz) of ACM unfilled rubber with dual cure-sites. 67

Figure 4.36. SEM images of unfilled ACM (a, e) and ACM with 5 phr (b, f); 10 phr (c, g); 20 phr (d, h) of barium titanate. 69

Figure 4.37. SEM images of ACM compound containing 10 phr of BT (a, d), TP (b, e) and TO (c, f) with different magnification. 70

Figure 4.38. Evaluation of unfilled elastomers of different types. 72

Figure 4.39. Evaluation of selected elastomers with 5 phr fillers/oils; a) ACM(chlorine); b) CO. 72

List of tables

Table 2.1 Dielectric and mechanical properties of some elastomers [43]. 15
Table 2.2. Designations of epichlorohydrin rubbers. 20
Table 2.3. Dielectric constants of some selected inorganic fillers. 23
Table 3.1. ACM grades and their properties. 28
Table 3.2. Epichlorohydrin grades and their properties. 28
Table 3.3. Fillers. 29
Table 3.4. Dielectric oils. 29
Table 3.5. ACM neat compound recipe. 30
Table 3.6. Filler amounts. 30
Table 3.7. Sample fabrication order. 31
Table 3.8. ACM compound recipes. 32
Table 3.9. GECO compound recipes. 32
Table 3.10. CO compound recipe. 32
Table 3.11. Compounding order. 33
Table 3.12. Recipe of ACM compound prepared on mill. 34
Table 3.13. Curing times in press at 175 ˚C. 35

Table A. 1. Comparison of actuator materials [3] 85
Table A. 2. Comparison of classes of muscle-like materials with natural muscles [2] 86

1. Introduction

The nature provides ideas how to create new functional materials resembling those already existing in the biosphere. Bio-inspired and bio-mimetic materials have recently gained a huge interest in the scientific community. [1] Although it seems impossible to surpass the creations of Mother Nature, much development is going on in the field of artificial muscles [2]. In this case "artificial muscle" is synonymous to "muscle-like material", and such materials are being developed for non-biomedical applications rather than for substitution of natural muscles. The possible applications of artificial muscles include refreshable braille displays, robotic arms and other moving part, loudspeakers, optical zoom lenses, active damping and force-feedback systems, energy generators and others. [3]

In the past decades, researchers have attempted to reproduce the performance of natural muscles by conventional electromagnetic motor (EM) - based actuators, pneumatic systems and "smart material" actuators[*]. EM-based and pneumatic systems are usually large, heavy and noisy, while lighter and smaller "smart materials", which are conventionally shape memory alloys, piezoelectrics or magnetostrictive alloys, can give only small strains. [3] Electroactive polymers (EAPs) appeared as an alternative to the previously mentioned actuators [3-5]. It is stated that EAP actuators have properties most resembling those of biological muscles and being truly bio-inspired [6]. Although there are other ways of classification, electroactive polymers can be divided into major groups based on their actuation method: ionic and field-activated EAPs. Ionic EAPs include ionic polymer-metal composites, ionic gels, carbon nanotubes (CNTs) and various conductive polymers. Under the field-activated classification fall ferroelectric, electrostrictive and relaxor ferroelectric polymers, polymer electrets, liquid crystal elastomers and dielectric elastomers that will be discussed in more details in the current work. [3]

As for ferroelectric EAPs, best actuator performance to date has been obtained from poly(vinylidene fluoride)-based (PVDF) polymers copolymerized with trifluoroethylene, or P(VDF-TrFE). The application of an electric field perpendicular to the P(VDF-TrFE) chains leads to a transition between nonpolar and polar forms resulting in a contraction in the direction of polarization and an expansion perpendicular to it. This transition can be facilitated by irradiation, or when a small mass fraction of a bulky monomer (e.g., chlorofluoroethylene) is added to P(VDF-TrFE). The resulting material is a relaxor ferroelectric. [7] Limitations of the discussed EAPs are low strain

[*] In this case, actuator is a device that is capable of transforming the applied energy (electrical, thermal, etc.) into the reversible mechanical deformation.

level and strain energy, fatigue of the electrodes, need for high electric fields, and high heat dissipation. Moreover, the e-beam irradiation process for curing the fluorocarbons is expensive. [8] Electrostrictive graft elastomers have a flexible backbone with polar side chains, which are aggregated and form polar crystalline regions. Application of an electric field aligns crystalline regions thus changing the polymer dimensions. [3] Liquid crystals are known to change the phase and orientation when electric field is applied. By incorporation of liquid crystals into a polymer backbone or side chains, field-induced changes may be used to produce actuation. However, both modulus and actuator strains of such polymers are low. [7]

Finally, dielectric elastomers (DEs) are insulators that become polarized in applied electric field thus being subjected to an active electrostatic pressure [9]. Among the other "smart materials" used to obtain muscle-like action, dielectric elastomers most resemble the natural muscles in strain, actuation pressure, density, efficiency and response speed. Compared to other electroactive polymers, dielectric elastomers offer good overall performance, high strains and decent cost. [2]

Dielectric elastomer actuators (DEAs) can offer "muscle-like" behaviour, but due to certain limitations of the existing dielectric elastomers, new materials are in demand. Same as for other EAPs, the main drawback of the contemporary DEAs is very high operating voltage that can reach 10 kV for 10-100 μm thick films. [3] Such actuation voltages limit their applications, and, therefore, need to be reduced [10;11]. Increasing the dielectric constant with control on the elastic modulus of a material is one of the possible methods to lower the operating voltage [9;12], and such approach is applied in the current work.

1.1. Aim and scope of the work

This thesis work is dealing with speciality elastomer compounds possessing considerably high relative dielectric permittivity to allow their application in dielectric elastomer actuators. The current work evaluates the effect of processing methods, type and amount of incorporated fillers, as well as addition of plasticizers on the dielectric and mechanical properties of selected rubbers.

This study utilizes different grades of acrylic and epichlorohydrin rubbers filled with titanium oxide, tantalum pentoxide, or barium titanate in various concentrations. The samples were fabricated by solution casting (conventional and assisted by sonication), on two-roll mill or in laboratory internal mixer. Furthermore, two different types of commercial dielectric oils were incorporated into the rubbers in order to obtain plasticizing effect.

The aim of this work is to:

a) Study the effect of rubber type and grade on the electrical and mechanical properties of the material

b) Study the effect of fabrication method (conventional solvent casting, sonication assisted solvent casting, mixing in an internal mixer or on two-roll mill) on the dielectric constant and tensile properties of acrylic rubbers
c) Study the effect of the type of dielectric filler and filler load on the permittivity and mechanical properties of elastomers
d) Study the compatibility and effect of different dielectric oils on processing, dielectric and mechanical properties of the chosen elastomers

1.2. Thesis outline

The current Master of Science thesis consists of five chapters. Theoretical part in **Chapter 2** covers three major topics: dielectricity, dielectric elastomers and composites. The phenomena of dielectricity and related conceptions, as well as, principles of dielectric actuation are introduced with the focus on elastomers in **Chapter 2.1**. In **Chapter 2.2**, the main types of dielectric elastomers are revised, and polymers used in the current work are introduced in more details. Moreover, the approaches to the dielectric elastomeric composites are discussed briefly in **Chapter 2.3**.

Experimental part of the work is presented in **Chapter 3**. It contains descriptions of the applied materials, recipes, apparatus, sample fabrication techniques, and testing methods used in the work. The results of experiments are discussed in **Chapter 4**, and each of the sub-chapter is followed by conclusion. Finally, **Chapter 5** contains general conclusions, suggestions and recommendations for the further work.

2. Theoretical background

Among the various actuator materials presented briefly in **Chapter 1**, DEAs are one of the most promising materials for artificial muscle applications. The comparison between important properties of natural muscles and various mimicking materials is shown in **Appendix 1**. Understanding the nature of dielectricity and physical basis of actuation, as well as, selection of materials and critical evaluation of available engineering approaches are crucial for creation of new DEA.

The current chapter will shortly discuss main physical, chemical and engineering aspects and phenomena involved in the functioning of DEAs. Moreover, this chapter will introduce the structure and properties of the materials involved during this work in compounding new dielectric elastomer. Furthermore, suitable methods of prediction of dielectric constant of such composites will be shortly reviewed. And finally, alternative approaches for the creation of functional DEA will be discussed briefly.

2.1. Dielectricity

Dielectricity is a physical model focusing on interaction between the electric field and atoms/molecules of the material. All materials respond to the external disturbance in the way offsetting its effects. Likewise, all materials are polarized in response to an applied electric field, when all the dipoles in it align in the applied field so that negative end is turned towards higher potential, and positive ends – towards lower. Other mechanisms also contribute to the polarization of the material and they will be discussed in the corresponding chapter. In the current work, the effect of electric field will be discussed mainly for dielectric materials. *Dielectrics* are *insulators* - material that contains no free charge carriers that can be moved in electric field. To be precise, dielectrics are able to conduct electricity due to the impurities and imperfections within the material, but their conductivity is ranging from 10^{-18} to 10^{-6} S/m. [13;14]

In a static electrical field dielectric model can be illustrated with an example of a primitive parallel plate capacitor. In ***Figure 2.1a***, the capacitor is built from two parallel metallic plate electrodes of an area A separated by distance d in vacuum. At a constant potential difference *V*, surface charge concentrations $+A\sigma$ and $-A\sigma$ start to build up on the opposite plates. Capacitance is expressed as a ratio of the charge on the plate to the difference in potential [13]:

$$C_0 = \frac{A\sigma}{V} \tag{2.1}$$

A uniform electric flux density D_0 arising from the charge density $+\sigma$ is directly proportional to the acting electric field *E*:

$$D_0 = \varepsilon_0 E \tag{2.2}$$

where ε_0 is the dielectric permittivity of vacuum and has a value of 8.854 pF/m. As $E=V/d$, formula (2.1) can be written as:

$$C_0 = \frac{\varepsilon_0 A}{d} \tag{2.3}$$

When a dielectric material is placed between the electrodes (***Figure 2.1b***), the charge density on the plates then includes bound charge densities $\pm p$ due to the effect of polarization. Hence, total charge density becomes $(\sigma+p)$, and the capacitance of such system expressed from (2.1) will be:

$$C = \frac{A(\sigma+p)}{V} \tag{2.4}$$

The described increase in charge densities will lead to increase in flux density, or electric displacement vector:

$$\bar{D} = \varepsilon_0 \bar{E} + \bar{P} \tag{2.5}$$

where $\bar{P}$ is electric polarization vector.[15]

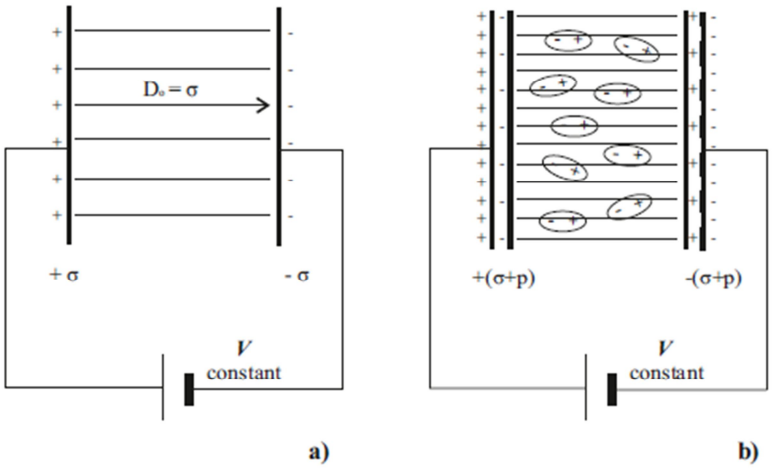

Figure 2.1*. Charges on a parallel-plate capacitor in static field a) with vacuum between the plates; b) with dielectric material between the plates [13].*

2.1.1. Dielectric constant and relative permittivity

Dielectric constant of a material is a unitless measure of the material's ability to polarize in presence of an electric field [16]. In static fields the relative (real) dielectric constant can be defined as a ratio between flux density in dielectric and in vacuum, or ratio of corresponding permittivities, when equations (2.2) and (2.5) are applied [14]:

$$\varepsilon' = \frac{\bar{D}}{D_0} = \frac{\varepsilon}{\varepsilon_0} \tag{2.6}$$

where ε is dielectric permittivity of the material. Moreover, relative dielectric constant (permittivity) can be expressed as [13]:

$$\varepsilon' = \frac{C}{C_0} = 1 + X \tag{2.7}$$

where $X = \frac{\bar{P}}{\varepsilon_0 \bar{E}}$ is the electric susceptibility of the material; the expression is derived from equations (2.1) and (2.4).

In literature, references are not usually made to the "dielectric constant" of the material, but to "relative dielectric permittivity", ε' or ε_r, that is synonymous to it. Moreover, the terms "relative dielectric constant" and "relative permittivity" are often substituted. [14] Although some authors still use traditional κ' [16], it is more often replaced by ε' or ε_r. "Relative dielectric permittivity", as well as "ε'", will be used further in this work because such designation is most common in the literature related to DEAs.

2.1.2. Polarization

On a macroscopic level, material responds to an applied electric field by becoming polarized, and the energy is stored in the dielectric medium. Macroscopic polarization *P* is obtained from the polarization of *n* molecular dipoles with induced dipole moment $\bar{p}$ in the unit volume ($P = n\bar{p}$). On a microscopic level, magnitude of a dipole moment is proportional to a local electric field intensity E_L [13;15;17]:

$$\bar{p} = \alpha E_L \tag{2.8}$$

where α is polarizability of the molecule. Dielectric permittivity ε' and molar polarizability $N\alpha$ were first related to each other in Clausius-Mosotti equation [15]:

$$\frac{N\alpha}{3\varepsilon_0} = \frac{(\varepsilon'-1)M}{(\varepsilon'+2)\rho} \tag{2.9}$$

where *N* is Avogadro's number, *M* – molecular weight, ρ – density. Molecular polarizability is a combination of distinct values based on different mechanisms responsible for microscopic polarization [13;15]:

a) Electronic polarizability α_e. In the applied electric field electrons in the atoms are displaced to the opposite direction than E with respect to the positive nucleus. Electronic polarizability dominates in materials consisting of only one type of atom (C, Si, etc.). The effect is more pronounced for heavy atoms.
b) Atomic (ionic) polarizability α_a. In this case, valence electron cloud is displaced in the region of the chemical bonds of a molecule. Moreover, this mechanism is responsible for displacement of centres of positively charged ions relative to negatively charged ions leading to a high polarizability. This mechanism is important for inorganic solids, for example, NaCl and various metal oxides.
c) Dipolar (orientational) polarizability α_d arises in the presence of molecular groups containing atoms with different electronegativity. If these molecules are independent, they easily align in the applied electric field. Therefore, this mechanism is important mostly for liquids due to the weak physical bonds

between the molecules. However, polarization may also arise from rotation of side polar groups and can be observed in some polymers, such as, poly(vinylchloride) and poly(vinilydene fluoride).

d) Hyperelectronic (nomadic) polarization α_π appears in π-conjugated molecules and show displacement over the extended regions that are limited just by the size of the molecule. Such a mechanism is typical for some organic solids and is valid for low frequencies.
e) Interfacial polarizability α_i. In contrast to the previous mechanisms, it is not a molecular phenomenon and occurs at the interface of microscopic boundaries where the charges are built up. The charge is accumulated and can move through the material in electric field showing the increase in conductivity.

However, Clausius-Mosotti equation is valid for static fields and takes into account only distortional polarization mechanisms (a and b) thus being applicable only for gases having no permanent dipoles. Equation (2.9) was later modified by Debye, Fröhlich, Onsager, Kirkwood and other scientists with added effects of orientational polarization and local field. Modern polarization theories developed for polymers should also include all intra- and intermolecular interactions of the chains that lead to overloaded formulas and long computations, and cannot be generalised. [18] Therefore, they will stay outside the scope of this work.

Each of polarizability mechanisms contributes to the dielectric constant and their related characteristic relaxation frequencies, as shown in ***Figure 2.2***.

In case of static electric fields (DC) and alternating electric fields (AC) with low frequency, total polarizability of material is the sum of the involved polarization mechanisms. Molecular mechanisms depend on the displacement of charges bound to atoms or molecules. They are acting similarly in the material bulk and have the same value for the same materials. However, interfacial polarizability depends a lot on inhomogeneities and defects within the material. Hence, α_i will be different in different areas of the same material. Finally, Maxwell-Wagner polarization is can arise only in heterogeneous systems like polymer blends or composite materials. [13;15] Moreover, thermal motion affects dielectric polarizability by distortion of aligned dipoles. Thus, dielectric permittivity of a system with dominant orientational polarization is also dependent on temperature [19].

In case of AC with certain frequency *f*, the effect of certain mechanisms will be excluded from the total, if *f* is higher than characteristic relaxation frequency of the mechanism. Relaxation phenomena will be discussed in more details in further chapters. Polarization induced in normal dielectric materials is small, with ε' less than 100, but some crystals with asymmetric structure can be largely polarized in the applied electric field [20].

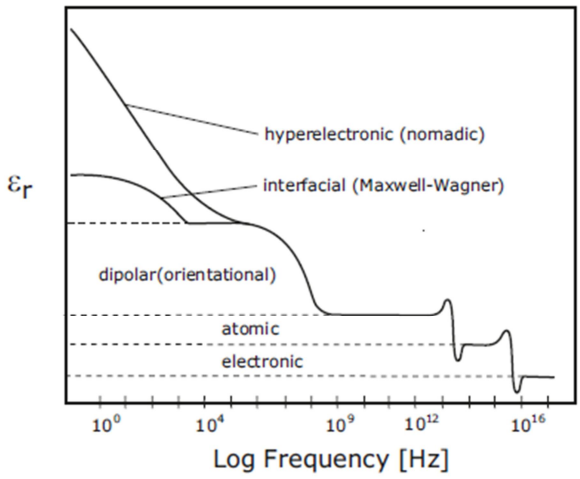

Figure 2.2. *Dependence of the dielectric constant and polarization mechanisms on frequency [14].*

According to [17;21], molecular polarization can be determined by only two major mechanisms: distortional and orientational polarization. The change of electric charge distribution in a molecule including induced dipoles under applied electric field belongs to distortional polarisation, while orientational polarization is related only to permanent dipoles. Permanent dipoles exist in the absence of an electric field, and they rotate to the direction of the applied electric field. As already mentioned above, such dipoles will never completely align with the field because of thermal agitation. Thus, total molecular polarizability equals to the sum of distortional polarizability and the contribution from rotation of permanent dipoles that is proximately $\mu^2/(3k_BT)$, where μ – is permanent dipole moment of the molecule (expressed in debye units D; 1 D = 3.33564×10^{-30} C m), k_B – Boltzmann constant and T – absolute temperature.

2.1.3. Complex relative permittivity and dielectric loss

If we consider an ideal dielectric parallel-plate capacitor, like the one in ***Figure 2.1b***, the current in the external circuit leads applied voltage by 90˚ and no component of the current is in phase with V. In alternating fields dielectric response of the real material depends on the frequency. [15]

As it was mentioned earlier in **Chapter 2.1.2**, interfacial polarization mechanism leads to increase in charge flow within the material meaning that angle between current and voltage phasor will be $(90^\circ\text{-}\delta)$. In that case stronger polarization means more pronounced phase lag. Moreover, part of the energy is dissipated and transferred, for instance, into heat build-up. It is referred to as *dielectric loss* (ε''), while relative dielectric permittivity ε' represents the energy stored in cycle. Phase lag δ is also known as the *loss angle*. As seen from ***Figure 2.3b***, the loss angle can be expressed by *dissipation factor* showing how much energy was lost in a cycle compared to the energy stored [13]:

$$\tan\delta = \frac{\varepsilon''}{\varepsilon'} \qquad (2.10)$$

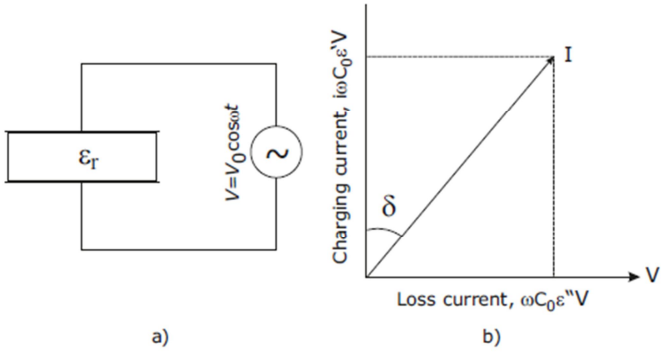

***Figure 2.3**. AC losses in dielectric material: a) circuit diagram; b) phasor current [13].*

Therefore, actual permittivity of the material is a complex parameter:

$$\varepsilon(\omega) = \varepsilon^* = \varepsilon' - i\varepsilon'' \qquad (2.11)$$

where $\omega=2\pi f$ – is frequency of the alternating field. Real and imaginary components are important for the study of relaxation processes. [13] Relative permittivity of material depends on its chemical composition and structure, while loss factor is also influenced by the peculiarities of molecular motion and purity of the polymer [21].

2.1.4. Dielectric relaxation

Dielectric relaxation processes are similar to the mechanical ones, and dielectric relaxation model is analogue to mechanical model with Voigt–Kelvin element in series with a spring [17]. For chemists, dielectric relaxation corresponds to molecular dynamics when viewed as the temperature dependence of the permittivity and loss factor and their frequency dependence at a constant temperature. Such measurements are also used to observe the progress of chemical reactions, if dipoles are being created or lost in those. [22] Dielectric relaxation curves for polar polymer are shown in ***Figure 2.4***.

When loss factor is plotted against the temperature at constant frequency, it is possible to distinguish different processes denoted by Greek letters α, β, γ, etc. For example, α-processes are more pronounced and seen at temperatures above the glass transition temperature T_g, while other processes are below T_g. Generally, α-peaks are narrower than others and are related to the segmental dynamics (rotation) under applied electric field. Finally, β-peaks and others can almost be flat. Processes of β and γ relaxation are related only to the motion of side-groups and some small elements of polymer chains (for example, several CH_2- or CF_2- groups in polyvinylchloride) respectively. Possibly, “crankshaft”-like motion of linear hydrocarbon chain is responsible for γ-relaxations. Finally, additional relaxation peak above T_g can be related to the Maxwell-Wagner polarization in composite materials, but if only both relative

dielectric permittivities and volume conductivities of the materials are much different thus leading to an accumulation of charge between media. [21;22]

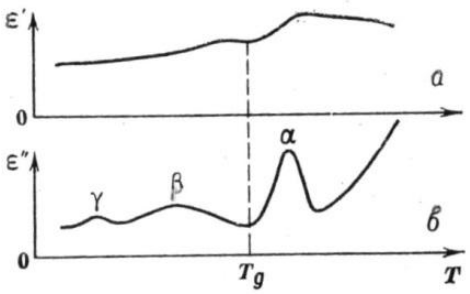

***Figure 2.4**. Dependence of low-frequency dielectric permittivity (a) and dielectric loss (b) on temperature [21].*

Material's response to the applied electric field consists of at least two steps: instantaneous and time-dependent. Instantaneous step occurs at very high frequencies or very short times and is associated with the atomic and electronic displacements in the dielectric material. [23] Dipoles in the dielectric material do not align instantaneously with the applied electric field and can be characterized by a time τ required for the alignment. Each polarization mechanism has its own *relaxation time*, that is $\tau_e<\tau_a<\tau_d<\tau_\pi<\tau_i$. [15] In general, deformation polarization requires about 10^{-13}-10^{-14} s to settle down, but relaxation time of orientational constituent of polarization is dependent on temperature, shape and form of molecules or other elements forming permanent dipoles in the material, molecular interactions, etc. [21] This so-called relaxation or respond time affects dynamic performance of dielectrics [14].

If material has only one relaxation time, complex relative permittivity ε^* quantifies its response to the AC induced field and can be expressed by Debye formula [23]:

$$\varepsilon^*(\omega) = \varepsilon_\infty + \frac{\varepsilon_S-\varepsilon_\infty}{1+i\omega\tau}, \text{ from where } \begin{cases} \varepsilon'(\omega) = \varepsilon_\infty + \frac{\varepsilon_S-\varepsilon_\infty}{1+\omega^2\tau^2} \\ \varepsilon''(\omega) = \varepsilon_\infty + \frac{(\varepsilon_S-\varepsilon_\infty)\omega\tau}{1+\omega^2\tau^2} \end{cases} \quad (2.12)$$

where $\varepsilon_\infty$is high frequency (unrelaxed) permittivity and ε_S is static (relaxed) permittivity. According to this model, the loss spectrum is symmetric and ideal, while the real loss peak is often broad and asymmetric, which is not always true. Therefore, some improvements to the theory were developed by Cole and Cole (C-C), Cole and Davidson (C-D), Havriliak and Negami (H-N). Among those, H-N equation describes relaxation processes more fully than others and can be transformed into Debye (2.12), C-C and C-D formulas for certain values of fitting parameters *a* and *b* [23]:

$$\varepsilon^*(\omega) = \varepsilon_\infty + \frac{\varepsilon_S-\varepsilon_\infty}{[1+(i\omega\tau)^a]^b} \quad (2.13)$$

Relaxation time τ is dependent on the temperature T based on equation: $\tau = \tau_0 e^{\frac{U}{RT}}$, where U – activation energy, R – universal gas constant. For more detailed relaxation analysis, it can be applied to the formula (2.13). [21]

Real polymeric dielectrics commonly have multiple relaxation times because of different relaxation velocities in different parts of molecular chains and different possible relaxation mechanisms. Moreover, long-chain structure and intermolecular interactions contribute to the appearance of relaxation time spectra. Leaving major part of relaxation theory of dielectrics off the scope of the current work, it is worth mentioning some of its consequences: at very low temperatures (or very high frequencies) dielectric permittivity and loss factor are expected to be reduced, and at very low frequencies (or high temperatures) relative permittivity increases. [21]

2.1.5. Dielectric strength and dielectric breakdown

Dielectric (electrical) *breakdown* is a destruction of a material as the result of subjecting it to an electric field. It generally depends on the local electric stresses within the dielectric material. However, premature failure often occurs before the intrinsic dielectric breakdown. Possible causes include thermal breakdown, mechanical failure due to the electrostatic forces, discharges, effect of electrode type, etc. Thermal breakdown ultimately happens due to thermal instability generally caused by joule heating. Joule heating is continuously generated inside the dielectric material mainly as the result of electrical conduction and polarization. It is said that series of short-time application of high electric fields remove ionic impurities and other charge carriers from dielectrics thus improving its insulation and breakdown properties. [15;24] In practice, *dielectric strength* of the material is calculated according to the equation that takes into account any failure of the material subjected to an electric field regardless of its nature:

$$E_{break} = \frac{V_{break}}{d_0} \tag{2.14}$$

where V_{break} is the breakdown voltage and d_0 is the initial thickness of the sample. Generally, dielectric strength of the material can be roughly estimated by assuming that elastomer is fully homogenous and purely elastic at low strains. According to this simple model, dielectric strength of the material is [12]:

$$E_{break} \cong 0.6\sqrt{\frac{Y}{2\varepsilon_0\varepsilon'}} \tag{2.15}$$

where Y is Young's modulus of the material. Such an idealized model surprisingly fits to the major experimental data and can be applied to estimate the breakdown field for the random (unstructured) composites. Dielectric breakdown strength is known to increase with increasing strain, and decrease with increasing the concentration of inclusions (filler, acid absorber, plasticizer, etc.). [4] Reduction of breakdown field is often related to the reduced resistivity of composite containing small plasticizer molecules leading to a larger leakage current [25].

Decrease in dielectric strength is typical problem for random composites, meaning that higher values of dielectric constant normally correlate with lowered values of breakdown electric field. However, this drawback can be neglected if increase in

actuation performance is obtained for low-voltage applications. Supported by numerous experimental evidences, this reduction of breakdown strength can be explained by Maxwell-Wagner interfacial polarization phenomena, when the losses increase. [12]

However, these simple equations (2.14-2.15) cannot be applied for pre-strained electrically-actuated polymers. It is known, that breakdown voltage decreases with increased pre-stretching [26]. Equation (2.16) and experimental setup shown in ***Figure 2.5*** suggested by Kollosche and Kofod [27] is more suitable for testing DEAs. During the experiment, a spherical electrode with radius of curvature R is pushed into soft elastomer (Y=156-320 kPa) with a force F_L, while the initial thickness of the sample is d_0. The proposed model includes the effects of load, boundary conditions and mechanical stresses:

$$\frac{F_L}{2\pi R d_0(1-\lambda)^2} - \frac{\varepsilon_r \varepsilon_0}{\lambda^3}\left(\frac{V_{break}}{d_0}\right)^2 = -\frac{Y}{3}\left(2\lambda - \frac{1}{\lambda^2}\right) \qquad (2.16)$$

where λ is a deformation ratio. From this equation critical stretch at breakdown λ_{break} can be derived.

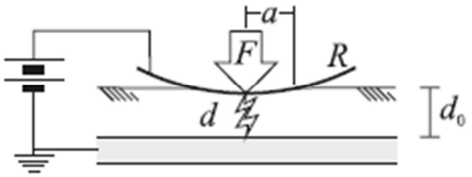

Figure 2.5*. Possible scheme of experiment for breakdown strength determination [13].*

2.1.6. Actuation

Actuation is an action of bringing a static body into motion. In case of electrical actuation of elastomers, *dielectric elastomer actuator* is a device utilizing material that deforms in response to applied electric field. DEAs are also known as deformable capacitors or electrically stretchable devices. When voltage is applied, actuator surface area increases with decreased thickness. After electric field is removed, actuator restores its original dimensions. [2]

Basic operation principle of DEA shown in ***Figure 2.6*** is the same as of two-plate capacitor. Such actuator is made of thin dielectric elastomer with compliant electrodes on its both sides. Carbon or silver grease electrodes are more frequently used, although it is possible to utilize silver and gold paint, copper, CNTs [28;29], printed Ag-CNTs [30], CNT-rubber gels [31] and many others described in [32]. Moreover, conductive elastomers [33] and even thin metallic films [34] can be used for such purposes. [3] When the voltage is applied, charge is built up on the electrodes. The attraction of opposite charges “presses” the elastomeric film in thickness direction. As the material is not compressible, the film area increases simultaneously facilitated by the repulsion of same charges. As the film thickness decreases, electrical energy E is converted into

mechanical energy in the form of electrostatic pressure across the material given by the Maxwell pressure (σ) equation [14]:

$$\sigma = \varepsilon' \cdot \varepsilon_0 \cdot E^2 \tag{2.17}$$

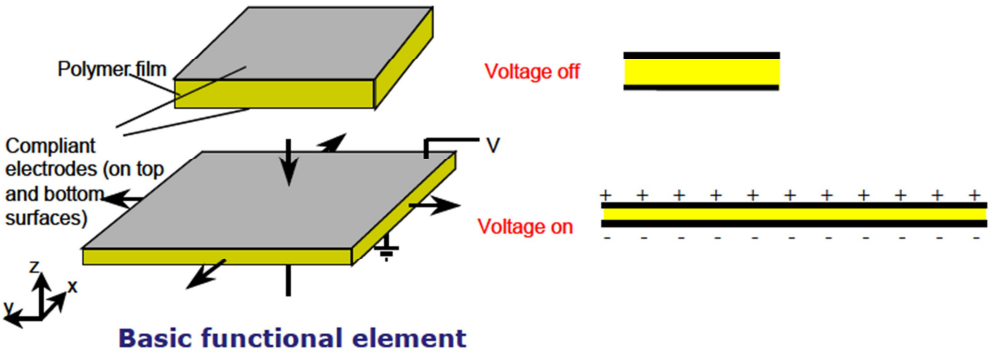

***Figure 2.6**. Operational principles of DEAs [2].*

Electrical energy can be expressed by applied voltage and distance between electrodes $E=V/d$. Therefore, from equation (2.17) we get final expression for the Maxwell pressure:

$$\sigma = \varepsilon' \cdot \varepsilon_0 \cdot \left(\frac{V}{d}\right)^2 \tag{2.18}$$

Maxwell pressure can be used to obtain compressional strain in thickness direction (s_z) that also depends on the elastic modulus of the material (Y):

$$s_z = -\frac{\sigma}{Y} \tag{2.19}$$

Planar strain can be estimated by the following equation [35]:

$$s_p = \frac{1}{1+s_z} - 1 = \frac{\varepsilon' \varepsilon_0 E^2}{Y - \varepsilon' \varepsilon_0 E^2} \tag{2.20}$$

Maxwell model is frequently used in literature related to dielectric elastomer actuators. However, Maxwell pressure theory is valid only for ideal dielectric elastomers meaning that its behaviour is liquid-like and not affected by deformation. [26] It is known, that elastomers show such behaviour when their polarizable groups have little restrictions in motion that is achievable at low crosslink densities and/or small deformations [36].

Non-linear field theory and electromechanical coupling for dielectrics proves the validity of Maxwell pressure equation for the cases mentioned above and aims to explain actuation phenomena in more details [37]. But in experiments DEAs sometimes show poorer actuation properties than ones calculated based on Maxwell pressure theory [38]. This can be explained by planar actuation strain being often[†] limited by

[†] For some materials, dielectric breakdown occurs before actuator enters the instability region. Moreover, some of the elastomers are able to survive the instability and reach the stable state.

arising electromechanical instability (EMI). Also known as pull-in instability, it leads to unequal reduction of thickness of elastomeric film after certain increase in electric field. Thus, some parts of the film suffer a significant reduction of thickness that in most cases lead to a breakdown. Numerical model for the process is recently available. [36;39]

Nevertheless, Maxwell pressure model is still often used in order to estimate actuator behaviour of the material at the early development stage. Regardless of the actuation model, certain requirements are imposed upon material properties in order to obtain DEAs with good functionality: large actuation strain, low applied voltage, high energy density, good efficiency and high response speed. Moreover, light and inexpensive would be preferable from economical viewpoint. [3;38;40] Finally, most of the current DEAs require pre-straining in order to show suitable performance thus having limitations and complications related to the design of actuator. Thus, high performance materials without pre-strain could be beneficial. [41]

2.2. Dielectric elastomers

Elastomers are polymers that have high degree of flexibility and low modulus after being crosslinked, and are capable of significant and reversible deformations under applied mechanical stress [42]. Elastomers are generally dielectrics with dielectric constant ranging from about 2 to 25 [43;44]. Crosslinked elastomers, alone or together with other compounding ingredients, are referred to as rubbers. Rubbers more frequently studied for DEA applications include silicone (PDMS), polyacrylate and polyurethane [3]. Moreover, some research has been conducted on DEAs utilizing acrylonitrile-butadiene rubber (NBR) [45], natural rubber (NR) [46], chloroprene (CR) [47], ethylene-propylene-diene (EPDM) [48;49], fluorinated rubbers [43] and polyester-based elastomer [35;50]. Dielectric chloroprene rubber is stated to have a number of advantages including high dielectric constants, good electrical properties, high chemical resistance, low modulus 1-3 MPa and comparably easy processing [47]. NR is believed to have future in DEA application, for example, when filled with alumina and crosslinked with dicumyl peroxide [46].

Thermoplastic elastomers, for example, polypropylene oxide (PPO, $\varepsilon'=5.6$ at 100 Hz) [51], styrene-isorpene (SIS) block copolymer with $\varepsilon'=2$ [52] and polystyrene-b-poly(ethylene-co-butylene)-b-polystyrene (SEBS, $\varepsilon'=2.3$ at 100 Hz) [13;53] are also capable of electrically induced recoverable deformations. Thermoplastic elastomers (TPE) are obviously suitable actuator materials allowing the adjustment of mechanical and dielectric properties by varying their composition. For instance, the properties of TPE can be controlled by changing the ratio of the monomers and the lengths of their hard and soft segments. [13] Bio-based elastomers, like poly(1,4-butanediol/1,3-propanediol/sebacate/succinate/itaconate) (PBPSSI) with very low elastic modulus have good actuation performance [35].

Finally, grafting high-ε groups and oligomers to the elastomeric chain is also promising way of adjusting dielectric properties of actuator materials. Acrylic elastomer ACM-g-copper phthalocyanine (CuPc) with very high dielectric constant (ε'=303 at 100 Hz) was synthesised by Liu et al. [54] by graphting CuPc oligomer onto the backbone of acrylic rubber. Such polymer was beneficial over same physically blended composite, for example, by the size of CuPc particles. Some dielectric and mechanical properties of these and other elastomers are presented in ***Table 2.1***.

Table 2.1. *Dielectric and mechanical properties of some elastomers [43].*

	Dielectric constant at 1kHz	Dielectric loss factor at 1kHz	Young's modulus [x10^6 Pa]	Eng. stress [MPa]	Break stress [MPa]	Ultimate strain [%]
Polyisoprene, natural rubber(IR)	2.68	0.002–0.04	1.3	15.4	30.7	470
Poly(chloroprene)(CR)	6.5–8.1	0.03/0.86	1.6	20.3	22.9	350
Poly(butadiene)(BR)	–	–	1.3	8.4	18.6	610
Poly(isobutene–co–isoprene)butyl rubber	2.42	0.0054	1	–	17.23	–
Poly(butadiene–co–acrylonitrile)(NBR, 30% acrylonitrie constant)	5.5 (10^6 Hz)	35 (10^6 Hz)		16.2	22.1	440
Poly(butadiene–co–styrene) (SBR, 25% styrene constant)	2.66	0.0009	1.6	17.9	22.1	440
Poly(isobutyl–co–isoprene rubber)(IIR)	2.1–2.4	0.003	–	5.5	15.7	650
Chlorosulfonated polyethylene(CSM)	7–10	0.03–0.07	–	–	24.13	–
Ethylene–propylene rubber(EPR)	3.17–3.34	0.0066–0.0079	–	–	20.68	–
Ethylene–propylene diene monomer (EPDM)	3.0–3.5	0.0004 at 60 Hz	2	7.6	18.1	420
Urethane	5–8	0.015–0.09	–	–	20–55	–
Silicone	3.0–3.5	0.001–0.010	–	–	2–10	80–500

As reported, acrylic and silicone elastomers are beneficial in actuator performance when compared to other elastomers. Acrylic rubber applied in DEAs is typically a commercial uncured double-sided adhesive tape with a thickness of 1 mm. This type of material shows high strain, Maxwell pressure and energy density, while silicones provide better thermal stability and are more efficient due to higher response speed. In addition, unlike acrylic elastomer silicone-based actuator is time history independent. [4;5;55] The time history dependence means that behaviour of the material depends on strain history, for instance, when radial strain increases with increased number of actuation cycles [56]. The reduced response time of silicones is related to lower viscosity of the material. Furthermore, pre-straining plays an important role in this

phenomenon for all elastomer types due to the reduction in elastic modulus and is believed to reduce arising EMI. Generally, silicone is beneficial material for low-strain (<10%) applications, while acrylic actuator is better for higher strains. [55;57]

Acrylic rubber is a well-studied polymer that already showed good actuation performance. Its dielectric constant is about 4.7 at 1 kHz with Young's modulus of 1-2 MPa and elongation at break up to 600% [58]. Nevertheless, most of the experiments were conducted with commercial adhesive tape VHB 4910 by 3M, and just few studies involved preparation of polyacrylate composition and its vulcanization. Epichlorohydrin rubber is known for its high polarity and thus relatively high dielectric constant, and presence of polyethylene oxide groups in terpolymer that can even make such polymer conductive [59]. However, polyepichlorohydrin rubber has not been applied in DEAs yet.

Due to the reasons discussed above, several grades of acrylic and polyepichlorohydrin elastomers were chosen for the current work. Although polar NBR and carboxylated nitrile rubber (XNBR) are expected to have properties suitable for high-performance actuator material, they will not be included into the scope of this work.

2.2.1. Effect of crosslinking on properties of elastomer

Adjusting the crosslink density in rubber allows tuning its mechanical and electrical properties. The degree of crosslinking affects the mechanical properties of elastomers including elastic modulus, elongation at break, tensile strength and others shown in ***Figure 2.7***. [25] The rough estimation of the effect of crosslink density on elastic modulus can be expressed by formula [35]:

$$Y = 3N'k_BT \tag{2.21}$$

where N' is crosslink density. Thus, lower elastic modulus can be obtained by reducing the crosslink density of the vulcanizate. However, tensile strength and resilience of the material will be negatively affected. These properties are important for performance and life-time of the future actuator and need to be maintained at suitable level.

Crosslink density is known to be among the factors influencing both relative permittivity and loss factor of a compound. For the temperatures above T_g, both properties will decrease with increase in crosslink density that can be related to better-ordered molecular system. That effect can be seen in PDMS [61], although some researchers [4] mention that change in crosslink density has no significant effect on dielectric constant of material. However, in some cases increased amount of crosslinks negatively affect interaction of neighbouring polymer chains thus increasing ε' and ε''. [21]

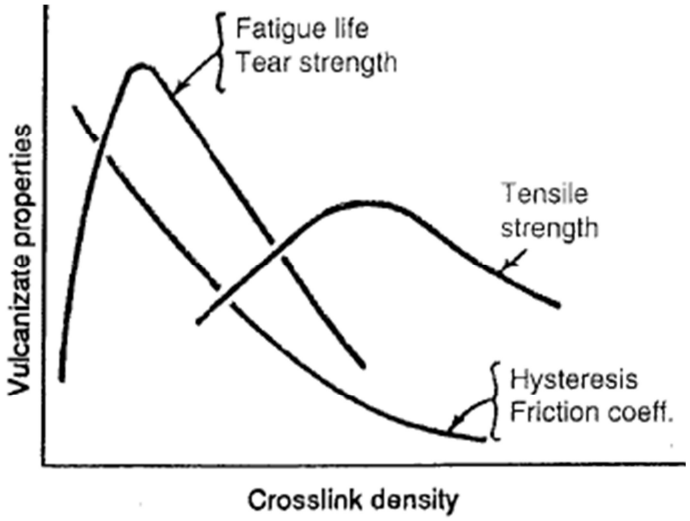

Figure 2.7. *Effect of crosslink density on the mechanical properties of vulcanizate [60].*

2.2.2. Acrylic rubber (ACM)

Acrylic rubber (polyacrylate elastomer, ACM) belongs to a class of polar speciality rubbers showing very good oil- and heat-resistance. Two major types of ACM are available, namely, conventional and ethylene/acrylic ACMs. Conventional acrylic rubbers include alkyl (ethyl acrylate, butyl acrylate) and alkoxy (methoxy ethyl acrylate, ethoxy ethyl acrylate) polyacrylates, while ethylene/acrylic rubber is presented by the co-polymer of ethylene and methyl acrylate. [62-64]

Properties of acrylic elastomers depend a lot on a number of carbon atoms in a side-chain: lager the number (up to 10) means lower T_g of the polymer, but worse oil-resistance. The latter property improves when one carbon atom is replaced by oxygen. Higher is the polarity of the side-chain, better is the heat and oil-resistance of polymer, but in this case low temperature flexibility decreases a lot. [42] Dielectric properties of acrylic, like of any other rubbers depend on the chemical structure and its polarity, exact composition of the compound, presence of plasticizers and softeners, and many other aspects. Being most studied and reported in multiple articles, acrylic 1 mm thick adhesive tape VHB 4910 produced by 3M company can be used as a reference with ε'=4.2 - 4.8 at 1kHz [3;52;65], although some researcher report higher value $\varepsilon' = 7$ [44].

Generally, as the saturated polymer backbone does not allow conventional crosslinking, acrylic elastomers are not homopolymers, but contain a small percentage (1–5%) of reactive side-chains. These cure-sites can be chlorine- (2-chroloethyl vinyl ether, vinyl chloroacetate), carboxyl- groups, combination of those, or epoxy-group containing side-chains. [63] Chemical structures of ACM elastomers and possible cure-sites are presented in ***Figure 2.8***. Polymers with dual cure sites are cure faster, and reduce the need to post-cure [64].

a)

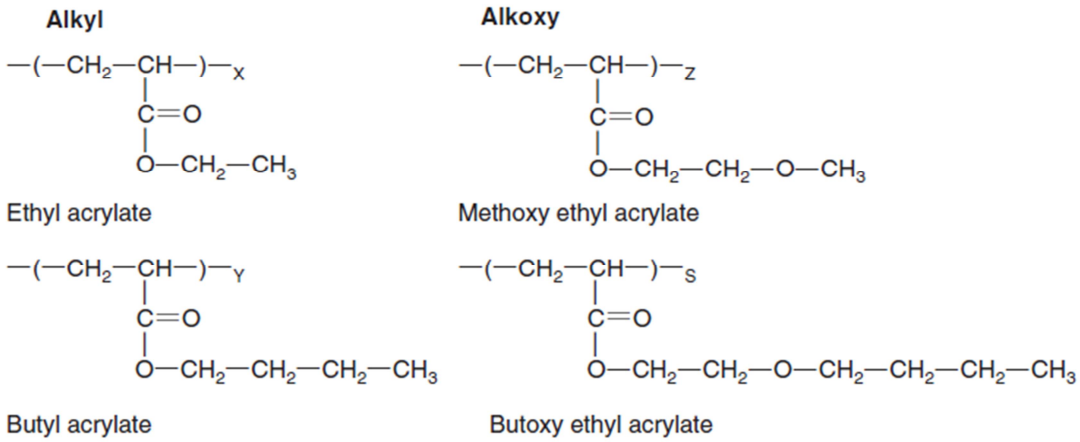

b)

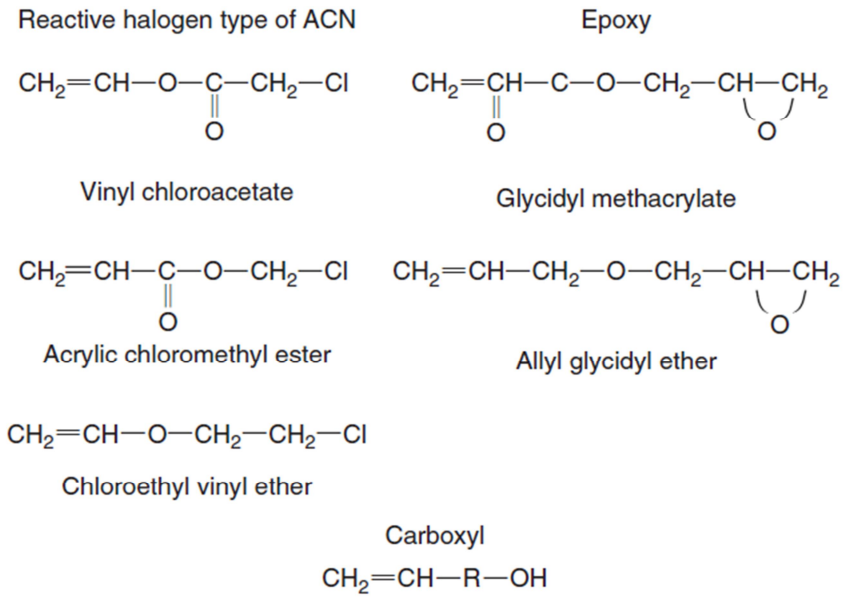

***Figure 2.8**. Chemical structures of a) AMC rubber and b) available cure sites [66].*

The chlorine and mixed type ACM cure systems may include soap/sulphur, soap/amine, lead/thiourea, activated thiols, polyamines, diamines, and many others [63]. Among those systems, metal soap (metal stearate)/ sulphur combination in 10 : 1 ratio is widely used, with potassium stearate being more active than sodium stearate [62]. When comparing elastomers with chlorine and dual cure-sites, soap/sulphur curing system is more recommended for chlorine/carboxyl cure-site ACMs. It is stated that when used with acrylic rubber containing only chlorine groups, such system gives just moderate shelf stability and slow cure rates. [66] Soap is mentioned to have a function of curing agent, while elemental sulphur, or sulphur donor, like tetramethylthiuram disulphide, being an activator [62;64]. Moreover, Wootthikanokkhan et al. [67] mentioned that sodium stearate serves as acceptor of the released chlorine; polysulphide vulcanization bonds are formed. In other source [68], it is stated that metal stearate performs as a

polymer soluble base. However, none of the sources elucidated vulcanization mechanism.As most of the curing systems used with ACMs are basic in nature, vulcanization can be accelerated by bases and retarded by acids. Stearic acid, for example, can be not only a retarder, but a processing aid. Post-cure is recommended for most of the ACM grades. [62;63]

2.2.3. Epichlorohydrin rubber (CO, ECO, GECO)

Epichlorohydrin rubbers are presented by homo- co- and ter- polymers in a large variety of grades. The classes of epichlorohydrin elastomers and abbreviations of their repeating units are shown in ***Table 2.2***, while the chemical structures are presented in . Generally, epichlorohydrin elastomers possess a good balance of certain properties from NR, NBR, ACM and CR rubbers, including oil-, heat- and ozone-resistance, excellent low-temperature properties, vibration damping and low gas permeability. Most of these properties owe to the saturated backbone of epichlorohydrin elastomers, but presence of chlorine side-groups is responsible for reduced permeability.

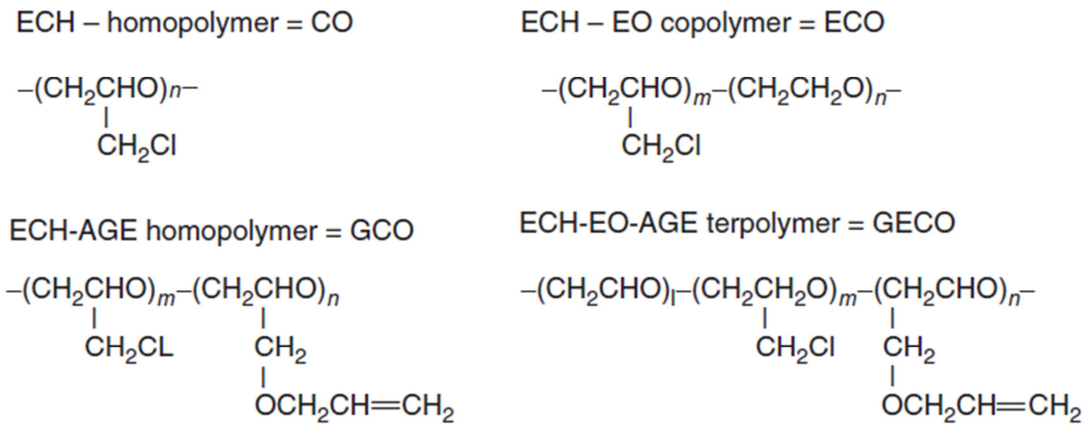

Figure 2.9. *Chemical structures of epichlorohydrin elastomers [69].*

Homopolymers of epichlorohydrin have great gas and solvent permeation resistance [63]. Addition of allyl glycidyl group is known to improve high temperature resistance and enlarge the range of suitable curatives. Presence of ethylene oxide groups improves side-chain mobility and, therefore, is responsible for enhanced low-temperature flexibility and good ageing resistance. Finally, terpolymer combines the benefits of co-polymers, and is known for its fair electrical conductivity. [69] Conductivity of commercial ter-polymers can reach maximum of 1.1×10^{-9} S/cm depending on polyethylene oxide content (up to 56 mol %), while conductivity of homopolymer is about 5×10^{-12} S/cm [59].

As mentioned in literature [62;69], CO and ECO elastomers were originally cured with systems containing lead oxide. However, non-lead systems are available now, such as, triazine, thiadiazole, and bis-phenol based curatives. In comparison to CO and ECO

types, which are fully saturated, GCO and GECO elastomers have unsaturation in side-chain (allyl), and can be cured by sulphur, peroxide or other curing systems.

***Table 2.2**. Designations of epichlorohydrin rubbers.*

Type	**Abbreviation**	**Repeating unit(s)**
Homopolymer	CO	Epichlorohydrin (ECH)
Co-polymer	GCO	Epichlorohydrin/allyl glycidyl ether (ECH/AGE)
	ECO	Epichlorohydrin/ethylene oxide (ECH/EO)
Terpolymer	GECO	Epichlorohydrin/ethylene oxide/allyl glycidyl ether (ECH/EO/AGE)

Being chlorine-containing elastomer, epichlorohydrin rubber requires an acid acceptor to bind free chlorine atoms released during vulcanization. For triazine curatives, precipitated calcium carbonate, sometimes combined with magnesium oxide, is conventionally used, while peroxide systems utilize calcium oxide with potassium stearate. Antioxidant can be used in order to improve ageing resistance. [69]

2.3. Dielectric composite materials

DEAs, like most of EAPs, require a high operating voltage (up to 10 kV for 10-100 μm thick films meaning up to ~100kV/mm) that limits possible commercial applications of such actuators. Therefore, acting electric field needs to be reduced. From the Maxwell pressure equations (2.18-2.19), discussed in **Chapter 2.1.6**, it is clear that voltage reduction can be obtained by increasing dielectric constant and reducing elastic modulus of dielectric elastomer.

Dielectric constant of the material may be increased by incorporation of fillers with high dielectric constant, or by polymer modification. However, neither incorporation of high-ε' fillers nor introduction of polar functional groups along the polymer backbone that generally increase the overall dielectric constant does not necessarily lead to the improvement of actuation properties of the composite. Accompanying changes in elastic modulus (due, for instance, to the method or extent of crosslinking) and chain entanglement, as well as specific inter- and intra-molecular interactions, may negatively affect the respond of the polymer to electrical stimulation. [5]

As mentioned previously in **Chapter 2.2**, pure elastomers have too low dielectric constant for superior actuation performance that limits their possible commercial applications. Therefore, DEAs are often composite materials, where high-ε′ dielectric, ferroelectric or even highly conductive particles (conductive carbon blacks, carbon nanotubes, polyaniline, polythiophene and others in concentrations below percolation threshold) are distributed in the elastomeric matrix. Although conductive fillers increase dielectric permittivity of the composite at concentrations close to percolation threshold, dielectric losses also increase and breakdown strength of the material decreases significantly. [35] According to the classification given by Carpi and co-authors [12],

methods of increasing dielectric permittivity of elastomers may be divided into creation of random composite, field-structured composite, and novel synthetic polymer. The current work is dealing only with the first group of methods.

2.3.1. Dielectric composite mixing rules

Several theoretical approaches are available for the estimation of the dielectric constant of dielectric composite material under the name “dielectric composite mixing rules”. In this part, only mixing rules for spherical particles will be discussed. Classical mixing rules consider isotropic matrix with permittivity ε_m and volume fraction v_m filled with particles of permittivity ε_f and volume fraction $v_f = 1 - v_m$. It is assumed that both components have no dielectric losses in the described frequency region. Some models have equations for the effective permittivity at high frequencies (ε_∞) that take into account arising Maxwell-Wagner relaxation. [12;13]

In general, the permittivity of the obtained composite lies between extremes $\varepsilon_{c,min}$ and $\varepsilon_{c,max}$ that are obtained from equivalent series connection and parallel circuit respectively:

$$\varepsilon_{c,min} = \frac{\varepsilon_m \varepsilon_f}{\varepsilon_m v_f + \varepsilon_f v_m} \tag{2.22a}$$

$$\varepsilon_{c,max} = \varepsilon_m v_m + \varepsilon_f v_f \tag{2.22b}$$

Intermediate form was proposed by Lichtenecker in logarithmic form:

$$\ln \varepsilon_c = v_m \ln \varepsilon_m + v_f \ln \varepsilon_f \tag{2.23}$$

At filler volume fraction lower than *0.1*, the consideration is made that electric potential arises from a distribution of filler in dielectric matrix and from distribution of the hypothetical larger spheres with dielectric constant ε_c in the same matrix. Sillars (also known as Landau-Lifshitz) mixing rule is obtained by equating these considerations:

$$\varepsilon_c = \varepsilon_m \left[1 + \frac{3v_f(\varepsilon_f - \varepsilon_m)}{2\varepsilon_m + \varepsilon_f}\right] \tag{2.24}$$

The above equation is valid only if matrix has much lower electrical resistivity than the filler particles. Such restriction is avoided in more accurate Maxwell-Garnett equation $\varepsilon_c = \varepsilon_m \left[1 + \frac{3v_f(\varepsilon_f - \varepsilon_m)}{(1 - v_f)(\varepsilon_f - \varepsilon_m) + 3\varepsilon_m}\right]$ or the equivalent Maxwell-Wagner (also known as Rayleigh, Lorentz-Lorenz or Kerner-Böttcher) formula:

$$\frac{\varepsilon_c - \varepsilon_m}{\varepsilon_c + 2\varepsilon_m} = v_f \frac{\varepsilon_f - \varepsilon_m}{\varepsilon_f + 2\varepsilon_m} \tag{2.25}$$

For a higher filler load (up to $v_f = 0.2$) Wagner-Rayleigh theory can be applied:

$$\varepsilon_c = \varepsilon_m \frac{2\varepsilon_m+\varepsilon_f+2v_f(\varepsilon_f-\varepsilon_m)}{2\varepsilon_m+\varepsilon_f-v_f(\varepsilon_f-\varepsilon_m)} \tag{2.26}$$

Furthermore, Bruggeman's equation is valid up to $v_f = 0.5$ or for disorded systems on the stipulation that the dispersed particles do not form percolative paths:

$$\frac{\varepsilon_f-\varepsilon_c}{\varepsilon_c^{1/3}} = \frac{(1-v_f)(\varepsilon_f-\varepsilon_m)}{\varepsilon_m^{1/3}} \tag{2.27}$$

Jayasundere and Smith provided the following formula when taking into consideration polarization of the neighbouring filler particles:

$$\varepsilon_c = \frac{\varepsilon_m v_m+\varepsilon_f v_f \frac{3\varepsilon_m}{(2\varepsilon_m+\varepsilon_f)}\left[1+3v_f\frac{\varepsilon_f-\varepsilon_m}{2\varepsilon_m+\varepsilon_f}\right]}{v_m+v_f\frac{3\varepsilon_m}{(2\varepsilon_m+\varepsilon_f)}\left[1+3v_f\frac{\varepsilon_f-\varepsilon_m}{2\varepsilon_m+\varepsilon_f}\right]} \tag{2.28}$$

Finally, Fricke proposed a pair of mixing rules for spheroids for the relaxed and unrelaxed permittivity:

$$\begin{cases} \varepsilon_{c,s} = \varepsilon_m + \frac{1}{3}v_f \sum_{i=a,b,c}\frac{\sigma_f-\sigma_m}{[\sigma_m+A_i(\sigma_f-\sigma_m)]} + \sigma_m \sum_{i=a,b,c}\frac{\sigma_m\varepsilon_f-\sigma_f\varepsilon_m}{[\sigma_m+A_i(\sigma_f-\sigma_m)]^2} \\ \varepsilon_{c,\infty} = \varepsilon_m\left\{1+\frac{1}{3}v_f\sum_{i=a,b,c}\frac{\varepsilon_f-\varepsilon_m}{[\varepsilon_m+A_i(\varepsilon_f-\varepsilon_m)]}\right\} \end{cases} \tag{2.29}$$

where A_a, A_b and A_c are depolarizing factors along the three axes, and σ_m and σ_f are the conductivities of matrix and filler. At small filler loads there is no significant difference between the models, but they appear at v_f over *0.1*. For such loads, Sillars model tends to underestimate the effective permittivity, and Böttcher model on the contrary overestimates it. [12;70]

2.3.2. Filler systems

As was mentioned in **Chapter 2.3**, various fillers are used for increasing dielectric constants of rubbers. However, at the same time fillers usually decrease the breakdown strength of the material and lead to an increase in dielectric loss. [4] Moreover, inorganic filler particles tend to increase stiffness of composites [71]. Hence, it is important to choose suitable filler with high permittivity and limited drawbacks.

According to Carpi et al. [12], various random composites were obtained by mixing elastomers with organic and inorganic fillers. Apart from dielectric oxides (titanium, tantalum) and ferroelectric ceramic particles, such as, barium titanate and lead magnesium niobate-lead titanate (PMN-PT), conductive inorganic particles (iron, copper, carbon black, carbon nanotubes, etc.) were applied. Some authors [72] report effective use of filler combination leading to increase in dielectric permittivity of PVDF-based composite from 39 (PVDF with barium titanate at 1kHz) to 325, after β-SiC is added. Dielectric constants of some high-ε' inorganic fillers that are frequently used in DEAs are presented in ***Table 2.3***.

***Table 2.3**. Dielectric constants of some selected inorganic fillers.*

Filler	**ε′**	**Reference**
TiO_2	80	[16]
	85	[73]
	90, 100	[15]
	99	[74]
	100	[9;75]
	up to 170[‡]	[76]
Ta_2O_5	26	[16]
	10-27.6; 65; 75[§]	[77]
	90-110[**]	[78]
$BaTiO_3$	100-2500	[79]
	1500	[15]
	2000-3000	[16]
	5000	[9]
$PbTiO_3$ (PT)	51-210	[75]
Lead magnesium niobate (PMN)	4000	[61]
	22000	[80]
PMN-PT	18000	[9]
Calcium copper titanate (CCTO)	Up to 50000	[81]

Among the organic fillers, poly(3-hexylthiophene) (P3HT) [9;82], copper-coated phthalocyanine (both polymeric and oligomeric) [4;12], polyaniline [12], allyl-cyano fillers [83] and others are used for increasing dielectric constant of elastomeric materials. However, only some selected ceramic particles are included into the scope of the current work because of their availability and good overall properties. They will be discussed next in more details.

2.3.2.1. Titanium dioxide

Titanium dioxide (TiO_2, TO, titania) is the first known dielectric material with high relative permittivity, about 100 [15;75]. TO is obtained from titanium containing ores, such as ilmenite, $FeTiO_3$, and rutile minerals. It has relatively low cost and is conventionally used as white pigment [73], although some high-technology applications of titania in photocatalysis, collar cells, etc. are also known [84]. Furthermore, addition of titania into some polymeric compounds lead to some increase in elastic modulus [85].

[‡] For rutile form in *c*-direction
[§] Depending on the frequency, temperature and type of tantalum pentoxide
[**] For specially treated tantalum oxide thin films

Titania can exist in various crystalline forms occurring in nature, such as rutile, anatase and brookite, as well as high pressure structures – similar to those of columbite, baddeleyite, fluorite, pyrite and cotunnite [84]. However, the two widely applied structures are rutile (tetragonal lattice, $a=b$=4.584 Å, c=2.953 Å) and anatase (tetragonal lattice, $a=b$=3.782 Å, c=9.502 Å). Rutile is the stable form of titania, but anatase is metastable and transforms into rutile at elevated temperatures (500-900 ˚C). As presented in ***Figure 2.10***, for both rutile and anatase, the basic cell is built of a titanium atom surrounded by six oxygen atoms that form distorted octahedron. For rutile and anatase octahedron stacking is different, but it equally results in threefold coordinated oxygen atoms. [86] Rutile is made-up from octahedrons connected by their edges, while in anatase the vertices of octahedrons are connected [13].

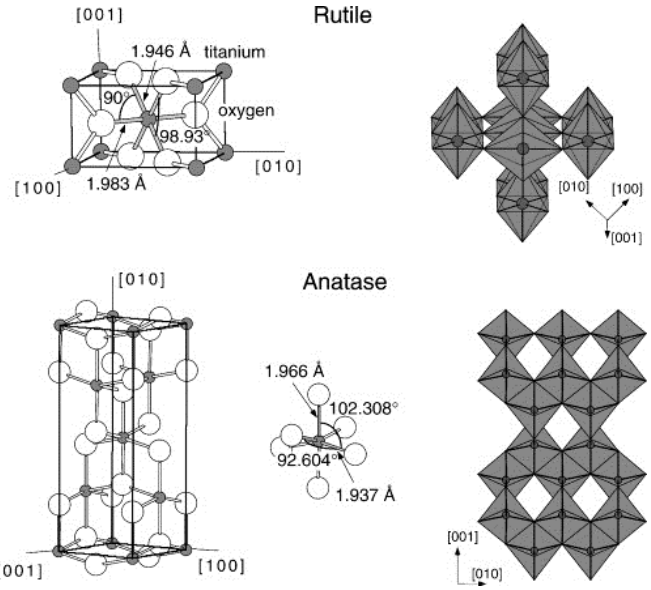

Figure 2.10*. Unit cells of rutile and anatase; the bond lengths and angles of octahedrally coordinated Ti atoms are shown. On the right side the stacking of the octahedra is presented [86].*

As was mentioned in **Chapter 2.1.2**, dielectric properties of the material depend a lot on its crystalline structure. This explains why rutile form of TO possesses a higher static dielectric constant (ε_s~110) than anatase form (ε_s ~30) having different octahedron stacking. [13] Octahedral structure of TiO_2 closely resembles the structure of perovskite crystals, for instance, barium titanate ($BaTiO_3$). In general, comparably high dielectric constant of titania is related to the presence of Ti atom in the material structure. When electric field is applied, titanium ion Ti^{4+} is displaced thus causing more distortion in the octahedral structure and enabling TiO_2 to be polarized (***Figure 2.11***). Due to this distortion TO shows anisotropic dielectric properties meaning that dielectric constant is higher along c-axis compared to a-axes. [16;76] Titania is non-ferroelectric material that means the induced polarization vanishes when the electric field is removed [16].

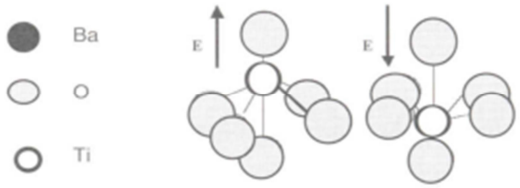

***Figure 2.11**. Scheme of ionic displacement within barium titanate crystal leading to polarization in applied electric field [13].*

Titanium oxide is capable of increasing dielectric constant of elastomeric matrix when properly dispersed. In case of highly polar polymer and nano-sized TO particles with high surface energy, dispersion without agglomeration is challenging. Therefore, real permittivity of such composites may be lower than predicted by theoretical models. Usually titania has some reinforcing effect on polymer networks, but at certain concentration TiO_2 reduces the elastic modulus of composite material. [35]

2.3.2.2. Barium titanate

Barium titanate ($BaTiO_3$, BT) is ferroelectric material with very high dielectric constant and low dielectric losses. It belongs to Perovckite-type minerals with major formula ABO_3, where A and B are metal ions of different sizes and total charge +6. [20] BT is obtained from the fusion of titanic anhydride and barium carbonate. As filler for polymers, it is frequently used to provide low loss, stable dielectric properties and increase in overall dielectric constant of the composite. Polymeric materials containing BT show remarkable increase in insulative properties. [85] Dielectric constant of BT is increasing at higher temperatures because of thermal polarization [19]. Dielectric properties of BT in ferroelectric state are known to be dependent on grain size, production method and temperature [87]. Generally, smaller grain size leads to lower dielectric permittivity [88]. At about 130 ˚C BT undergoes phase transition into paraelectric state, and the grain size has no effect on dielectric properties anymore [89].

The ionic motion is responsible for polarization of BT, when titanium ion is displaced within the oxygen “cage”, as was explained previously for titania. Structurally BT consists of a central Ba atom surrounded by titania octahedrons; the crystalline structure of BT is presented in ***Figure 2.12*.** [16] However, the unit cell of BT may also be presented by central Ti atom surrounded by O atoms forming octahedron placed inside the cage of Ba atoms. The structure of the unit cell is temperature dependent, as at certain temperature T_c (Curie temperature) it transforms to a more stable form. Within 5 - 120 ˚C the unit cell of BT has tetragonal form. In order to obtain this shape from a cubic one, Ba and Ti ions are shifted upwards from their original position, but oxygen atoms move downwards. Such a shift distorts centroids of negative and positive charges thus enabling the spontaneous polarization of barium titanate. As BT is ferroelectric material, the induced polarization does not decay when the electric field is removed.

[20] Barium titanate [72;90;91] and its modifications [79] is frequently used for enhancing dielectric constant of polymeric materials.

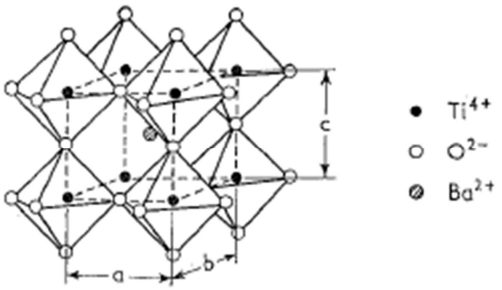

***Figure 2.12**. Schematic structure of barium titanate [15].*

2.3.2.3. Tantalum pentoxide

Tantalum pentoxide (Ta_2O_5, TP) is widely applied in electronics and other fields mainly as a thin film, therefore only little information about its bulk properties and structure is available. TP mainly exists in low-temperature β-form, and high-temperature α-form. [77] High pressure ε-Ta_2O_5 is also existent but will be left outside the scope of this work due to its complicated nature and irrelevant fields of application.

Similarly to crystalline structure of titania, its high polarization is related to the atomic and ionic distortion upon the applied electric field. However, compared to Ti, Ta atom is heavier and tantalum oxide should have higher polarizability. Dielectric loss in high-temperature form, α-TaO_2, is more pronounced at elevated temperatures due to ion migration, while dissipation factor of β-tantalum pentoxide increases a bit with temperature. [92]

2.3.3. Plasticizers

It has been proved by Zhao et al. [93] that incorporation of oil into the dielectric polymer matrix together with high dielectric constant fillers can improve the actuation performance at low electric field. This phenomenon is explained by uniform distribution of the oil between the polymer chain, and good polymer-oil compatibility resulting in the largely reduced Young's modulus of the composite. Same observations were made by Hao et al. [94], as silicone oil also eased alignment if dielectric filler particles during curing with applied electric field. Some researches state that addition of oil (up to 40 phr [61] or up to 80 phr [95]) into elastomeric matrix largely reduces dielectric constant of the obtained composite. However, addition of plasticizer reduced elastic modulus significantly resulting in higher ε′/Y ratio thus improving actuation performance of the composites.

Although the low elastic modulus usually means reduced breakdown strength of the material [4], experiments of Böse et al. [96] with fluorinated silicone and silicone oil showed that such system had no significant changes in electric strength, but resulted in

beneficially lower Young's modulus. For DEAs lower stiffness of the material leads to a more sensitive strain response to the applied field [25].

Transformer oils conventionally utilized as dielectric media in electrical transformers contain some polar groups, and should be compatible with polar elastomers as plasticizers. Low viscosity transformer oils behave more like nonpolar liquids in low frequency electric fields. [21] Moreover, such oils have stable properties and very low losses at low frequencies. However, dielectric properties of transformer oils depend a lot on content of polar and ionizing materials that cause dielectric losses. [15] Finally, polarizability and polarization mechanisms of liquid and solid dielectrics are different because of effect of molecular arrangements, regularity, movement restrictions and other factors [19;21].

2.4.4. Alternative approach

The approach presented previously in **Chapter 2.3** aims to increase dielectric permittivity of rubbers by addition of high-ε′ ceramic particles and obtaining random elastomeric composites. However, many other perspective ways of increasing relative dielectric constant of materials exist in the area of dielectric random composites. Generally, they can be divided into three groups: addition of conductive particles (organic or inorganic), non-conductive particles with high ε′, and mixture of fillers leading to synergy effect.

The incorporation of conductive inorganic nanoparticle into elastomer matrices has been of interest, for example, addition of MWCNTs into styrene butadiene rubber [47]. Filling a dielectric elastomer with conductive polymeric particles is of great interest as well. For instance, effect of polypyrrole (PPy) particles incorporated in ACM copolymers, polydimethylsiloxane (PDMS), styrene-butadiene rubber (SBR) and poly(styrene-isoprene-styrene) (SIS) [97], as well as distribution of polystyrene–isoprene core–shell nanoparticles into SBR matrix have been studied recently. Furthermore, PDMS has been blended with polyethylene glycol (PEG) in order to obtain material with higher dielectric constant and better actuation properties [98].

Long chain amorphous polymers containing covalently bonded electro-negative atoms behave similarly to ferroelectric ceramics in the applied electric field, if they contain embedded crystalline regions. Such polymers can be applied as fillers in elastomeric matrix. [99] Finally, combination of fillers can be successfully used in so-called tree-phase composites with significantly increased dielectric permittivity [72].

3. Experimental

Acrylic and epichlorohydrin rubber composites were fabricated and tested in the current work. Rubbers were filled with different types of powders with high dielectric constants in order to obtain material with enhanced relative permittivity. Plasticizing oils with comparably high dielectric constant were used in order to reduce Young's modulus of materials. The effect of various concentrations of fillers and plasticizing oils was studied with respect to the changes in Young's modulus below 5 % elongation, stress at 100 % and 200 % elongation (M_{100} and M_{200}), dielectric constant, loss factor and breakdown strength. Crosslink density was determined because of its contribution to the electromechanical properties of elastomeric composites.

3.1. Materials

Polyacrylic and epichlorohydrin rubbers produced by Zeon Chemicals L.P. company were used in the work. More details on the ACM elastomers and their properties obtained from [100] are presented in ***Table 3.1***, while ***Table 3.2*** provides characteristics of the utilized epichlorohydrin rubbers.

Table 3.1. *ACM grades and their properties.*

ACM	**Cure-site type**	**T_g [°C]**	**Mooney-Viscosity ML 1+4, 100 °C**	**Specific Gravity [g/cm^3]**	**Characteristics**	**Curing system**
HyTemp® 4051EP	Chlorine/ Carboxyl	– 18	35 – 47	1,10	injection moulding grade	Soap/sulphur
HyTemp® AR 715	Chlorine	– 24	27 – 39	1,10	extrusion grade	Soap/sulphur

Other commercial grade materials used in the ACM compounds were sodium stearate, sulphur, and stearic acid. Acetone was used as dissolving agent for acrylic rubbers in solution casting methods.

Table 3.2. *Epichlorohydrin grades and their properties.*

Type	**Chlorine content**	**T_g [°C]**	**Mooney-Viscosity ML 1+4, 100 °C**	**Specific Gravity [g/cm^3]**	**Structure and characteristics**	**Curing system**
Hydrin® H-45	36	– 48	40 – 50	1,37	Homopolymer	Triazine
Hydrin® T3108	19	– 48	40 – 54	1,28	Terpolymer	Sulphur

Compound materials for epichlorohydrin terpolymer were zinc oxide, stearic acid, N-cyclohexyl-2-benzothazolesulfenamide (CBS) or tetramethylthioram disulfide (TMTD), while in homopolymer compounds triazine and SUPER-PFLEX®100 precipitated calcium carbonate were used. General information on the filler materials is provided in ***Table 3.3***.

Table 3.3. *Fillers.*

Properties/Materials	**AEROXIDE® TiO_2 P 25**	**Tantalum (V)Oxide**	**Barium Titanate (IV)**
Manufacturer	Evonik Industries	Sigma-Aldrich	Sigma-Aldrich
Chemical formula	TiO_2	Ta_2O_5	$BaTiO_3$
Abbreviation	TO	TP	BT
Structure	mixture of crystalline rutile and anatase phases	-	-
Material type	Fine powder	Powder	Powder
Filler size	21 nm	< 250 μm	< 2 μm
Relative density	3.8 g/cm^3	8.0 g/cm^3	6.0 g/cm^3
Dielectric constant[††]	80-100	26–110	100-5000
Toxicity	Category IV, possibly carcinogenic	Category IV	Category IV
Surface modification	no	no	no

Finally, dielectric oils MIDEL® 7131 and Fomblin® Y applied in this work was provided by M&I Materials Ltd and Sigma-Aldrich respectively. Their general information is shown in ***Table 3.4*** according to the information provided by the manufacturer and CAS No. search.

Table 3.4. *Dielectric oils.*

	MIDEL® 7131	**Fomblin® Y**
Chemical name	fatty acids, linear and branched $C_{5\text{-}10}$, mixed esters with pentaerythritol	oxidized and polymerized 1,1,2,3,3,3-hexafluoropropene
Structure	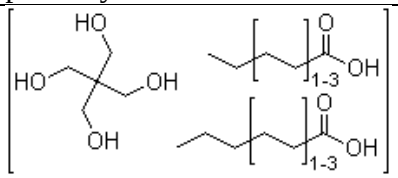 [101]	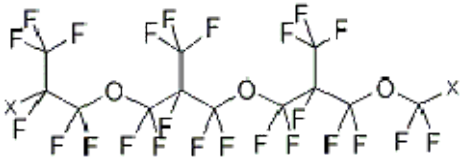 [102]
Relative density	0.97 g/cm^3	1.89 g/cm^3
Dielectric constant	3.2	1.8-2

[††] Average for the material in general according to the information of various sources. See Chapter 2.3.2 for more details.

3.2. Preparation of elastomeric thin films

Two different fabrication methods were employed in the current work – solution casting and mixing in internal mixer or on mill. First method allows obtaining higher purity of the composites and use of small batches, while mixing is faster and easy to scale-up for industrial production. Moreover, mixing require no additional chemicals (solvents). Solution casting was employed only for ACM elastomers, neat and filled with ceramic particles.

3.2.1. Solution casting

ACM films were prepared by solution casting method according to the formulations given in ***Table 3.5*** and ***Table 3.6***. In order to achieve adequate solution homogeneity, two dissolution techniques were suggested as one of the steps of solution casting method: mixing by magnetic stirrer or magnetic stirring assisted by ultrasonication. All dry materials were weighed in plastic weighing pots on a precision laboratory scales; acetone was measured in glassware.

Table 3.5. *ACM neat compound recipe.*

Component	**Content, phr**[‡‡]		**Example amount, g**
	Dual cure-sites (4051EP)	Chlorine cure-sites (AR715)	ACM with dual cure-sites (mechanical mixing)
ACM	100	100	6.55
Sodium stearate	3	3	0.20
Sulphur	0.3	0.3	0.02
Stearic acid	0.5	-	0.03
Total	103.8	103.3	6.8
Dissolved in:			
Acetone	-	-	55 (+10)

Table 3.6. *Filler amounts.*

Filler	**Amount, phr**	
	mechanical mixing	sonication-assisted mechanical mixing
Barium titanate	5	5, 10, 20
Tantalum pentoxide	-	5, 10, 20
Titanium oxide	-	5

The fabrication scheme is shown in ***Table 3.7***. First, rubber was dissolved in acetone by mixing with magnetic stirrer for an hour in closed vessel in order to reduce acetone evaporation rate. Gradual addition of elastomer into the mixing vessel leads to faster dissolution, as swelled rubber tends to form clumps meaning the reduction of ACM

[‡‡] Per hundred parts of rubber

surface area, and gradual addition helps to avoid large clumps. In case of conventional mixing of neat elastomer compound, other recipe components were added directly to homogenous rubber solution and stirred for 25 minutes. In case of sonication-assisted mixing, the rest of recipe ingredients were added into a glass cup containing 20 mL of acetone and placed into ultrasonication bath (FinnSonic m03).

Table 3.7*. Sample fabrication order.*

Process	**Materials**	**Time, min**			
		mechanical mixing		sonication-assisted mechanical mixing	
		neat	filled	neat	filled
Dissolution	Elastomer (ACM)	60	60	60	60
Sonication	Filler in acetone	-	-	-	20
	The rest of components	-	-	5	5
Magnetic stirring	The rest of components in acetone	-	15	-	-
	ACM solution and recipe components	25	10	10	10
Pouring into moulds					
Acetone evaporation		24 h	24 h	24 h	24 h

Finally, the resulting solution was poured into the moulds with Teflon® coating (90 mm in diameter), and loosely covered with lid in order to reduce acetone evaporation rate thus avoiding formation of bubbles in the film. However, vacuum (for instance, -0.5 bar for 4 hours) can be applied successfully for the same purposes. Thickness of the samples can be controlled by the amount of solution poured into moulds.

3.2.2. Mixing in internal mixer

ACM, CO and GECO samples were compounded in laboratory scale measuring mixer (Brabender® W 50 driven by Brabender Plasti-Corder®). It has two roller blades (tangential rotors) and neat mixing chamber volume (NCV) of about 55 cm^3. The recipes of the compounds are presented in ***Table 3.8*** - ***Table 3.10***.

As the fill factor was experimentally set to 0.85, and density of the compound was varying due to different elastomer, filler and oil densities, the size of batch was estimated according to the formula from [60] p. 511:

$$\text{Batch weight (g)} = \text{NCV} \times \text{fill factor} \times \text{compound density} \quad (3.1)$$

***Table 3.8**. ACM compound recipes.*

Component	**Function**	**Amount, phr**			
		Chlorine cure-site (AR715)		Dual cure-site (4051EP)	
ACM	Elastomer	100	100	100	100
Sodium stearate	Curative, chlorine acceptor	3	3	3	3
Sulphur	Curative, activator	0.3	0.3	0.3	0.3
Stearic acid	Retarder	-	-	0.5	0.5
Fomblin® or MIDEL® oil	Plasticizer	0/2/5	-	0/2/5	-
TP or TO	Filler	-	5	-	10

***Table 3.9**. GECO compound recipes.*

Component	**Function**	**Amount, phr**		
		TMTD-accelerated		CBS-accelerated
GECO (T3108)	Elastomer	100	100	100
Zinc oxide	Activator, acid acceptor	5	5	5
Stearic acid	Activator, process aid	2	2	2
TMTD	Accelerator	1	1	-
CBS	Accelerator	-	-	1
Sulphur	Curative	1	1	1
Fomblin® or MIDEL® oil	Plasticizer	0/1/2/5/10/15	-	-
BT, or TP, or TO	Filler	-	5/10/15/20	-

***Table 3.10**. CO compound recipe.*

Component	**Function**	**Amount, phr**	
CO (H45)	Elastomer	100	100
Calcium carbonate	Acid acceptor	5	5
Triazine	Curative	1	1
Fomblin® or MIDEL® oil	Plasticizer	0/2/5	0.25[§§]
BT, or TP, or TO	Filler	-	5

The oil-filled and reference neat rubber samples were compounded in a short-time single-pass mix. The mixing efficiency of filled elastomeric samples was not good enough to obtain proper filler distribution in a short cycle mixing that led to an extended mixing times. Due to the absence of the cooling system in the mixer, the time for single-pass mixing of particle filled compounds was chosen so that significant temperature rise was avoided. The mixing orders are presented in ***Table 3.11***.

[§§] MIDEL® oil is added in order to ease processing and improve removal from the mixer, as this rubber compound tends to stick to the metal parts of the mixer

Table 3.11. *Compounding order.*

Time	Component	Settings
Neat and oil-filled ACM (4051EP and AR715)		
0 min	elastomer	40 ˚C, 70 rpm
1 min	(oil)	70 rpm
1 min 30 s	retarder, curatives	70 rpm
3 min 30 s	dumping	up to 65 ˚C
Particle-filled ACM(4051EP)		
0 min	elastomer	40 ˚C, 60 rpm
1 min	filler	70 rpm
2 min 30 s	curative	70 rpm
4 min 30 s	dumping	up to 75 ˚C
Particle-filled ACM(AR715)		
0 min	elastomer	40 ˚C, 70 rpm
1 min	filler	70 rpm
2 min 30 s	curative	70 rpm
3 min 30 s	dumping	up to 65 ˚C
Neat and oil-filled GECO		
0 min	elastomer	40 ˚C, 60 rpm
1 min	ZnO	60 rpm
1 min 15 s	stearic acid	60 rpm
1 min 45 s	(oil)	60 rpm
3 min 30 s	curative, accelerator	60 rpm
	dumping	up to 75 ˚C
Particle-filled GECO		
0 min	elastomer	40 ˚C, 60 rpm
1 min	ZnO	60 rpm
1 min 15 s	stearic acid, filler	60 rpm
3 min	curative, accelerator	60 rpm
5 min	dumping	up to 65 ˚C
Neat and oil-filled CO		
0 min	elastomer	40 ˚C, 60 rpm
1 min	$CaCO_3$	
1 min 30 s	(oil)	60 rpm
1 min 45 s	curative	60 rpm
3 min 30 s	dumping	60-70 ˚C
Particle-filled CO		
0 min	elastomer	40 ˚C, 60 rpm
1 min	$CaCO_3$	60 rpm
1 min 30 s	filler, oil	60rpm
3 min 45 s	curative	60 rpm
5 min 30 s	dumping	up to 65 ˚C

3.2.3. Mixing on mill

Samples were prepared in Leibniz Institute of Polymer Research in Dresden, Germany on a laboratory scale two-roll mixing mill according the formulation presented in ***Table***

3.12. After mixing the elastomer, filler and oil was added on mill and then followed by the final addition of curatives. The reference sample was prepared on mill with neither oils nor fillers.

Table 3.12. *Recipe of ACM compound prepared on mill.*

Component	**Function**	**Amount, phr**
		Dual cure-site (4051EP)
ACM	Elastomer	100
Sodium stearate	Curative, chlorine acceptor	3
Sulphur	Curative, activator	0.3
Stearic acid	Retarder	0.5
Fomblin® or MIDEL® oil	Plasticizer	0.25
BT	Filler	5/10/20

3.3. Curing and determination of curing time

Curing characteristics of rubbers were studied in Advanced Polymer Analyser (APA), APA2000 from Alpha Technologies. APA2000 is an oscillating parallel-plate rheometer constructed to measure dynamic mechanical properties of polymers before, during and after cure. It measures complex torque S* transmitted through the sample, and software separates its real part S' that is used for drawing a curing curve. Time to a given per cent state-of-cure (x) is obtained for corresponding torque level calculated according to the formula:

$$t_{Cx} \rightarrow \frac{x}{100}(M_H - M_L) + M_L \qquad (3.2)$$

where M_H – maximum torque, M_L – minimum torque, while the example curing curve and t_{cx} determination is shown in ***Figure 3.1***. However, some curing times (e.g. t_{c90} and t_{c50}) are calculated automatically in APA2000. The tests were carried out at the same day when the mixing was performed. The temperature profiles were set to 160 and 175˚C with the test time of 20 minutes.

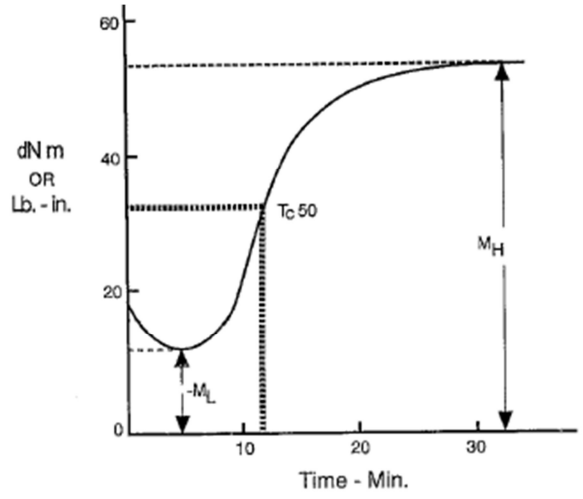

Figure 3.1. *The example of curing curve and curing time determination [60].*

Most of synthetic rubbers show an equilibrium torque level M_H, or plateau, while natural rubber usually show reversion after maximum torque level is attained. ACM elastomers commonly exhibit a "marching modulus", when no maximum torque level is achieved. In such case t_{cx} can be calculated based on M_H for a certain time, or suitable curing time can be established after mechanical tests based on the required properties. [63] After proper curing times were determined, the samples were vulcanized according to the data from ***Table 3.13***. ACM samples prepared on mill were cured at 180 ˚C for 15 minutes. Furthermore, in order to study the effect on crosslink density on the properties of composites, ACM compound prepared on mill was also cured for 3, 5, 8, 10 and 12 minutes with specimen thickness of about 1 mm.

Table 3.13*. Curing times in press at 175 ˚C.*

Elastomer	**Thickness**	**Curing time, min**
ACM (prepared in internal mixer)	~ 0.2 mm	15
	~ 1 mm	15
GECO (with TMTD)	~ 1 mm	3.5
GECO (with CBR)	~ 1 mm	15
CO	~ 1 mm	15

Samples fabricated by solution casting method were carefully released from moulds avoiding stretching and cured in ventilated oven at 175 ˚C for 30 minutes. Samples mixed in internal mixer were cured in MKH hydraulic press with electrically heated plates in 1 mm thick aluminium moulds, or without moulds in order to obtain about 0.2 mm thick films.

3.4. Determination of crosslink density

The crosslink density *N'* expressed by number of moles of crosslinks per unit volume is determined by equilibrium swelling measurement in solvent (here: toluene, in ambient conditions) from the equation:

$$N' = \frac{v}{2} \tag{3.3}$$

At the same time, *v*, number of effective network chains, is calculated according to the applied Flory-Rehner equation [103;104]:

$$\upsilon = -\frac{1}{V_s}\frac{\ln(1-v_r)+v_r+\chi v_r^2}{v_r^{1/3}-v_r/2} \tag{3.4}$$

where v_r – is volume fraction of rubber, V_s – is the molar volume of solvent and χ – is the Flory-Huggins polymer-solvent interaction parameter. For toluene, V_s = 106.2 g/mol. For the systems "acrylic rubber-toluene", "CO-toluene" and "GECO-toluene" Flory-Huggins interaction parameter needs to be calculated according the equation [105;106]:

$$\chi = \frac{V_s}{RT}\left(\delta_s - \delta_p\right)^2 + k \tag{3.5}$$

where R is the gas constant (R= 8.3144621[J/mol K]), T – temperature in Kelvins, k – the constant (k = 0.35), δ_s and δ_p- Hildebrand solubility parameter of solvent and polymer respectively. For toluene, $\delta_s = 18.2\ MPa^{1/2}$, $\delta_p = 19.21\ MPa^{1/2}$ for CO, $\delta_p = 18.46\ MPa^{1/2}$ for GECO and for polyethylacrylate $\delta_p = 18.27\ MPa^{1/2}$. By using δ_p for polyethylacrylate we eliminate the effect of crosslink sites in acrylic rubber on solubility parameter; solubility parameter for acrylic rubber is not available in references. This method takes into account both the existing chemical and physical crosslinks. If necessary, density of each type of network can be obtained as described elsewhere [107].

Taking into consideration insoluble components in rubber compound (curative, accelerator, acid acceptor, etc.) the volume fraction of rubber in the swollen vulcanizate is [108;109]:

$$v_r = \frac{(m_d - m_0\varphi)/\rho_r}{(m_d - m_0\varphi)/\rho_r + (m_s - m_d)/\rho_s} \tag{3.6}$$

where m_s and m_d are the weight of the swollen and dried specimen respectively, m_o – the initial weight of the specimen, φ – the mass fraction of insoluble components in the compound, ρ_s = 0.87 g/cm^3 is the density of solvent (toluene) and ρ_r is the calculated density of rubber compound.

However, if vulcanizates contain reinforcing fillers, v_r can be calculated using Kraus expression [104]:

$$\frac{v_r}{v_{rf}} = 1 - (3c\left(1 - v_r^{1/3}\right) + v_r - 1)\frac{\phi}{1-\phi} \tag{3.7}$$

where v_{rf} is the volume fraction of filled rubber in the swollen gel calculated according to the formula (3.6), ϕ – volume fraction of filler in the unswollen filled rubber and c is the filler-rubber interaction parameter. The fillers used in the current study are generally referred to as non-reinforcing fillers, but the addition of ceramic particles may lead to an increase in some mechanical properties. [71;85]

Due to the challenging determination of filler-rubber interaction parameter for the studied systems it is not included into the scope of the study. In case any of the filler shows reinforcing action, v_r can be estimated from the ratio of swelling values (Q) of the corresponding compounds [110]:

$$\frac{v_r}{v_{rf}} = \frac{Q_f}{Q_0} \tag{3.8}$$

where Q_0 is swelling value of unfilled rubber and Q_f is the swelling value of a filled one. Swelling value is defined as grams of solvent per gram of rubber hydrocarbon [111]:

$$Q = \left(\frac{m_s - m_d}{m_0}\right)\frac{F}{100} \tag{3.9}$$

where *F* is *formula weight*, meaning total weight of rubber together with compounding ingredients based on hundred parts of rubber. Moreover, from this equation, apparent crosslink densities of elastomeric compounds can be calculated as *1/Q*.

For the determination of crosslink density three specimens (10x10 mm) of the sample were weighed and then immersed in 150 mL of toluene at 20 ˚C for 96 hours in order to obtain equilibrium swelling. The saturated swollen specimens were removed from solvent, wiped quickly with filter paper and weighed. Specimens were weighed again after 48 hour drying in air. Crosslink densities were generally determined according to the equation (3.3) in moles of crosslinks per cubic meter of the material.

3.4.1. Determination of bound rubber

Bound rubber value (BRV) can be used for the estimation of filler-rubber interaction. It describes the amount of elastomer trapped or occluded by aggregated filler particles. The larger BRV means higher filler-rubber interaction. [103;110;112-114] Two 0.5 g samples were placed into filter paper bags and immersed in toluene for 72 h. The solvent was renewed every 24 h. The bags were weighed both wet and after 24 h of drying. BRV is calculated according to the formula:

$$BRV = \frac{m_1 - (m_2 - m_3)}{m_1} \quad (3.10)$$

where $m_1 = m_s \times \frac{100}{F}$ is the weight of rubber in sample, *F* – formula weight, m_s – weight of initial sample, m_2 - weight of rubber gel together with filter paper bag and m_3 – weight of dried gel with filter paper bag. Determination of BRV is made in order to choose proper formula from the abovementioned for the calculation of crosslink densities of various samples.

3.5. Mechanical testing

Tensile test is one of the most common mechanical tests for rubber compounds. It is especially important for the current study to obtain Young's modulus and M_{100} in order to estimate actuation properties of the material. TS and elongation at break give information about mechanical performance.

According to standard ISO 37:2005, larger dumbbell pieces are preferable for tensile testing, as smaller ones may give higher values for tensile properties. For the solution-casted compositions, dimensions of the sample were limited and, therefore, only miniature dumbbell test pieces could be used. Other specimens were cut off from the sheets with the same mould that was used for solution-casted samples in order to obtain comparable tensile test results. Due to the small thicknesses (0.2 – 0.5 mm) of solution-casted and ACM samples with dual cure-sites, tensile testing cannot be performed according to the standard. For the test, thin dumbbell test pieces had a test length of 10

mm and were tested at 200 mm/min rate. Testing of 1 mm thick samples of epichlorohydrin and ACM with chlorine cure-sites was conducted according to ISO 37:2005 with standard specimen type 4 at 200 mm/min rate of traverse. Messphysik MIDI 10-20/4x11 equipment with a long travel extensometer and 1 kN maximum load-cell was used in all performed tensile tests.

Young's (elastic) modulus shows a relation of tensile stress to strain and it is applicable only for purely elastic deformation. Unlike metals, Young's modulus (Y) is not usually calculated for rubbers, as elastomeric strain-stress curve shows high strains and almost no linear portion. Nevertheless, determination of elastic modulus is of high importance for the current work, as also for the other works in the field of electrically activated elastomeric actuators.

Several methods of determining Y for elastomers is available in literature. Omnès et al. [113] calculates Y from the stress-strain curves fitted by six-order polynomial function at strains below 0.09. Similar polynomial fitting was applied by Molberg et al. [52]. In most of the articles, elastic modulus is determined as a slope of the stress-strain curve at certain elongation (5% [11;35;98], up to 30% [110] and higher [51]), in some – by regression analysis at 0 to 40 % elongation, as no linear region was available on the tensile curve [55]. Also modulus values are often obtained for certain pre-strain value [11;115]. For most of the methods, values obtained from tension and compression are slightly different [40] and depend on the testing rates used (50 – 500 mm/min). However, large number of works mentions neither test rate, nor method for determining Young's modulus that make comparison of the results impossible. In some cases it is unclear which physical quantity is referred to as "modulus" ("elastic modulus", "Young's modulus") - whether that is Young's modulus discussed above, or elastic modulus obtained from dynamic mechanical analysis, or even stress at certain per cent elongation, as shown in [46]. These problems have already been discussed in literature [5], but clear standardized terms and testing methods are still not available.

Here, Young's modulus is determined from the slope of stress-strain curves in the linear region (at 5% elongation) because at 200 mm/min rate required by standard for the determination of other tensile properties, amount of data points at lower elongation can be insufficient. Such method allows comparing Young's modulus of the material within current study. Finally, stress at 100% (M_{100}) and 200 % (M_{200}) elongation are important values for this study because most of actuator materials require pre-straining up to 100% and more before the test. The median result of three tests is reported for each of the value.

3.6. Electrical testing

Electrical testing is crucial for materials applied in DEAs, as their performance depends a lot on the dielectric properties of elastomeric film. Testing for the electric breakdown was conducted at High Voltage laboratory at TUT by K. Lahti and J. Puikko. Dielectric

constants were determined at the Laboratory No10 for luminescence, relaxation and electrical properties of polymeric systems at the Institute of Macromolecular Compounds, Russian Academy of Sciences (IMC RAS) in St. Petersburg with the assistance of N. V. Afanas′eva.

3.6.1. Determination of dielectric constant

Dielectric testing is widely used for polymeric dielectrics. It is extremely sensitive to the structure of polymers, nature and amount of polar groups it their chains and various types of molecular motion. Moreover, different inclusions within the material affect the results of dielectric testing a lot.

The tests were conducted at Laboratory 10 of IMC RAS using an automatic LCR-meter 4270 by Wayne Kerr. In order to measure loss tangent ($tg\delta$) and capacitance C, the sample was fixed in a measuring cell as shown in ***Figure 3.2***. Measuring cell is constructed of brass electrodes insulated by 10-15 mm thick Teflon discs and connected to LCR-meter by clamped wires. Upper movable cylindrical electrode, 10 mm in diameter, is attached to the screw that allows changing the distance between electrodes. However, such system fails to set exactly the same test pressure for the samples with different thicknesses because the upper electrode is moved manually thus depending on the operator. Therefore, measuring cell with integrated micrometre was tested in order to avoid the abovementioned problem. Although it allowed using same electrode pressure for all the samples and reduced the error arising from the thickness determination, such measuring cell showed very big error of unknown nature in the results and was not used further.

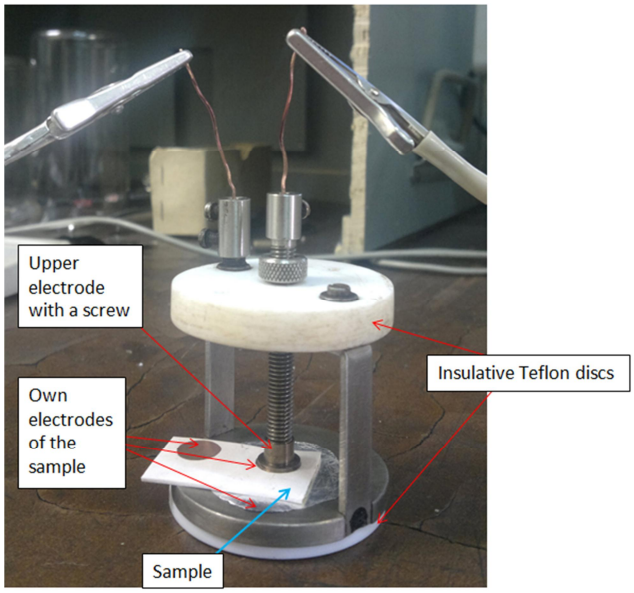

Figure 3.2. *Measuring cell with sample in assembly.*

For precise permittivity determination it is very important to have good contact between the sample and upper electrode where the voltage is applied. Therefore, each

sample has its own set of secondary electrodes. Upper, or measuring, one is a circle cut from a conductive copper tape (0.1 mm thick, with carbon-based adhesive layer), while lower circular electrode of larger diameter is made of aluminium foil.

The sample was chosen so that the fluctuation of its thickness was lower than few per cents. The thickness was measured by a micrometre. LCR-meter measured the capacitance of the samples, and after that dielectric permittivity of the specimens was calculated by software according to the following formula:

$$\varepsilon' = 14.4\frac{hC}{d^2}, \tag{3.11}$$

where h – thickness of the sample in cm, d – diameter of the measuring electrode, C – capacitance of the sample in pF. Loss factor was determined from the measured quality factor Q_f:

$$tg\delta = \frac{1}{Q_f} \tag{3.12}$$

Finally, dielectric losses were calculated from equation (2.10). Dielectric permittivity and loss factor of the samples were determined for the 120 Hz – 610 kHz range and solely at 1 kHz. The accuracy of the device was checked on two resistors with known resistance, as described in user manual, and on polyimide thin film with known dielectric permittivity. The error of the device is about 0.1 %. Maximum error from thickness determination and calculations is 5 %. Four parallel tests were conducted, and the median value was determined.

3.6.2. Testing for breakdown strength

According to the standard IEC 60243-1, all the samples were preconditioned for 24h at +23˚C, 50% relative humidity. During the testing of solution-casted samples, 100mm rod-rod electrodes (DC, positive polarity) were utilized and samples were immersed in dielectric oil during the test. Testing rate was set to 250 V/s and the test was performed until the breakdown of the sample occurred. Four parallel tests were conducted, and the median value was determined.

3.7. Microscopy

Microscopic images of the studied elastomeric sheets allow evaluating the distribution of fillers and unused curatives within the material. This can be a useful tool when explaining, for instance, the effect of fillers and pores on dielectric permittivity. Study was conducted on Zeiss ULTRAplus scanning electron microscope.

Chosen samples were immersed in liquid nitrogen and then broken in halves in order to obtain cross-section surface to study. Then samples were placed into metallic sample supporting springs and glued to the sample-holder. Same carbon-based glue was also applied into sides of the specimen and left to dry-up. Finally, samples were carbon-coated and studied at 500, 1000, 2000, 5000 and 10000 magnification. Such magnification was chosen because of the much different particle size of the fillers and the unknown size of possible voids inside the material. Two different spots of each sample were viewed.

4. Results and discussions

Here the experimental results are presented and discussed. The results are viewed concerning preparation techniques, mechanical and electrical testing. Moreover, experimental data is compared with values obtained from theoretical calculations. Conclusions are drawn after every subchapter.

4.1. Preparation techniques

Solution casting and conventional rubber mixing methods of sample preparation were chosen to be tested because of number of advantages they provide. Solution casting is preferable method for laboratory-scale production because it requires no specific knowledge, large equipment and is easy to perform with small amounts of materials. On the other hand, conventional preparation methods of rubber samples require more specific knowledge and special equipment, but can offer much shorter production times and require no solvents. In this chapter, comparison is made between the samples made of ACM rubber with dual cure-sites which were prepared in different ways mentioned above.

Visually, samples prepared by solution casting are shiny and have uneven surface with multiple inclusions of aggregated curatives and few visible bubbles. Samples fabricated by simple solution casting have no visual differences to those where sonication was used. Rubber specimen prepared on mill is less shiny with even surface and no visible inclusions, while sample made in internal mixer has dull and smooth surface. Samples can be seen in ***Figure 4.1***.

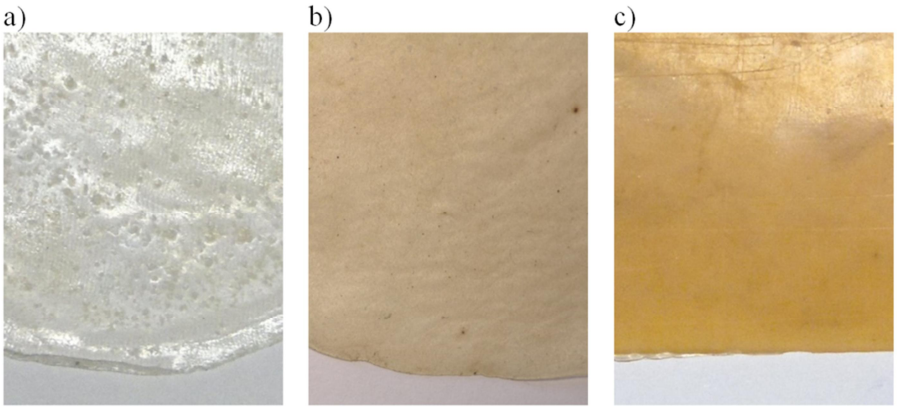

Figure 4.1. *ACM samples with dual cure-sites fabricated by a) solution casting; b) mixing in internal mixer; c) mixing on two-roll mill.*

4.1.1. Tensile properties

Some difficulties in determination of tensile properties were related to the small thickness of the samples and their increased adhesion to the metal clamps of the testing equipment. Next, some error can arise from thickness determination and differences in thickness between the samples. Moreover, solution-casted samples showed remarkably large deviation in the determined values within the tested specimens that can be related to uneven distribution of curatives and presence of clumps. It is also assumed that crosslink density was varying within the sample. ***Figure 4.2*** shows important properties of ACM samples prepared by different methods.

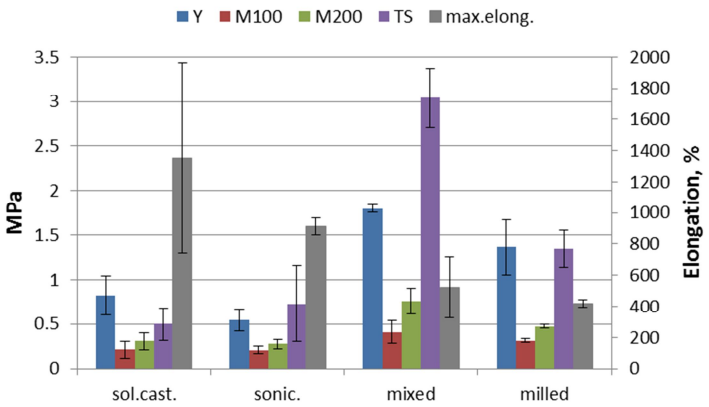

Figure 4.2*. Tensile properties (with standard deviations) of ACM with dual cure-sites prepared by different methods.*

Here, tensile properties vary a lot depending on a selected fabrication method. Moreover, deviation from average is significant for most properties. For the solution-casted samples, possible presence of residual acetone or inhomogeneity of the specimen could be a reason for such deviation. First, remarkably increased elongation at break and low tensile strength (TS) of solution-casted samples indicates low crosslink density of the material that is possibly due to problems with distribution of the curatives, as well as differences in curing methods. Curing in press is progressing faster than in ventilated oven. This hypothesis is supported by the TS and maximum elongation values obtained for the ACM prepared on mill and cured for 3 minutes; they are 0.96±0.04 MPa and 1410±48 % respectively. However, lower elongation at break but higher TS of the sonicated sample compared to another solution-casted one may mean that sonication positively affected the distribution of the curatives. Further study of the crosslink densities suggests the same. Stress at 100 % and 200 % elongation is comparably same for solution-casted samples.

Second, samples prepared in internal mixer obviously have very high Young's modulus and tensile strength, as well as other tensile properties compared to the samples fabricated by milling. For these samples crosslink densities should be of the same order of magnitude because of the similar curing processes. However, milled

samples were cured at 5 ˚C higher temperature than those mixed in internal mixer, and the pressure during curing is unknown. These factors should affect the tensile properties of the compounds.

4.1.2. Dielectric properties

Dielectric properties of sonicated solution-casted sample are compared to the dielectric properties of materials prepared in internal mixer and on two-roll mill. Relative dielectric permittivities and losses are seen in ***Figure 4.3***.

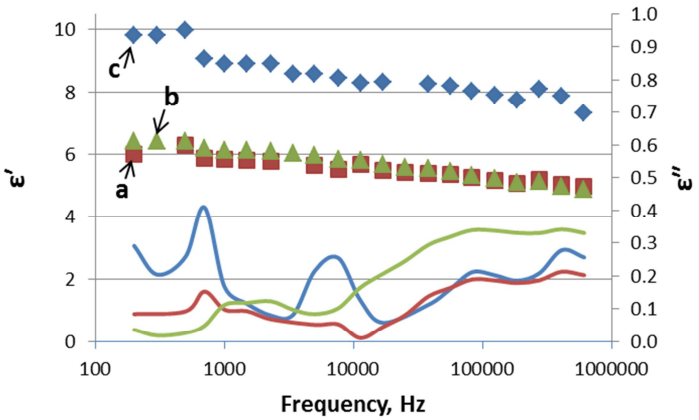

Figure 4.3*. Relative dielectric permittivity and dielectric losses (solid lines of corresponding colours) of a) solution-casted sample b) sample mixed in internal mixer and c) milled sample.*

Solution-casted and samples mixed in internal mixer have almost no difference in relative dielectric permittivity, and its dependence on the frequency in comparably low. Moreover, no notable peaks in dielectric losses are seen for these samples meaning that no relaxation processes occur in this spectrum. However, average dielectric losses of solution-casted sample at low frequencies are higher than for mixed one possibly due to poorer intramolecular structure of the specimen and uneven distribution of curatives. Furthermore, milled sample show obviously higher dielectric constant that is more dependent on frequency. Finally, clear peaks are seen in dielectric losses accompanied by corresponding change in slope of dielectric constant. Such peaks exist at same frequencies for all the measured milled specimens. This fact may lead to the conclusion that sample prepared on mill has multiple number of air-filled pores. The resistivity curves are shown in ***Figure 4.4***. Similarly to the dielectric permittivity, resistivity of solution-casted and mixed sample is almost the same, while sample prepared on mill has somehow lower electrical resistivity.

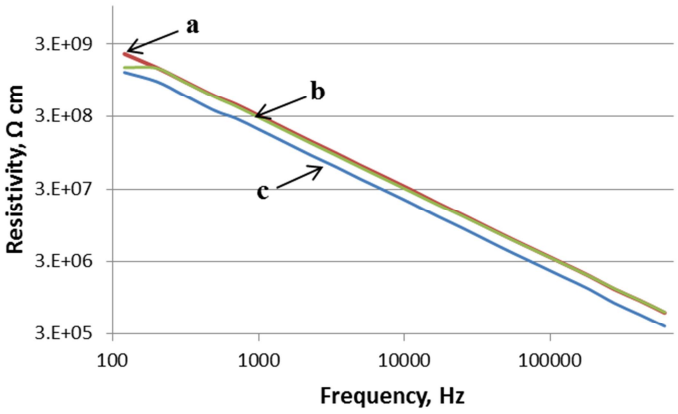

***Figure 4.4**. Resistivity (logarithmic scale) of ACM samples with dual cure-sites of a) solution-casted sample, b) sample mixed in internal mixer and c) milled sample.*

4.1.3. Conclusions

It is obvious that conventional rubber mixing methods are beneficial over solution casting methods. They provide better uniformity of samples resulting in more homogenous properties. Moreover, mixing and milling methods allow automation and are faster than solution casting methods. However, it is worth mentioning that on the early material development stage other solution-based fabrication methods can be tested, for example, substrate dipping and spraying techniques, as described in some works [117]. Such methods should result in obtaining thin elastomeric films of good quality with reduced fabrication time compared to the solution-casting methods used in the current work. Although differences in electrical and mechanical properties of the samples prepared in internal mixer and on mill are possibly related to the increased porosity of the latter one, more detailed investigation is needed in order to determine the reason for that.

Repeatability of the experiments is low for samples prepared by solution casting methods and described in the current work, and it is impossible to control any mechanical or dielectric properties for such samples. Conventionally mixed samples show more repeatable results, while possible reason for the differences between mixed and milled sample is examined in next chapters.

4.2. Neat rubbers

Conventional mixing method was chosen for further sample preparation. Here, dependence of properties on elastomer type is discussed only for the samples prepared in internal mixer. Moreover, properties of GECO samples with two different accelerators are compared. Different samples are shown in ***Figure 4.5***.

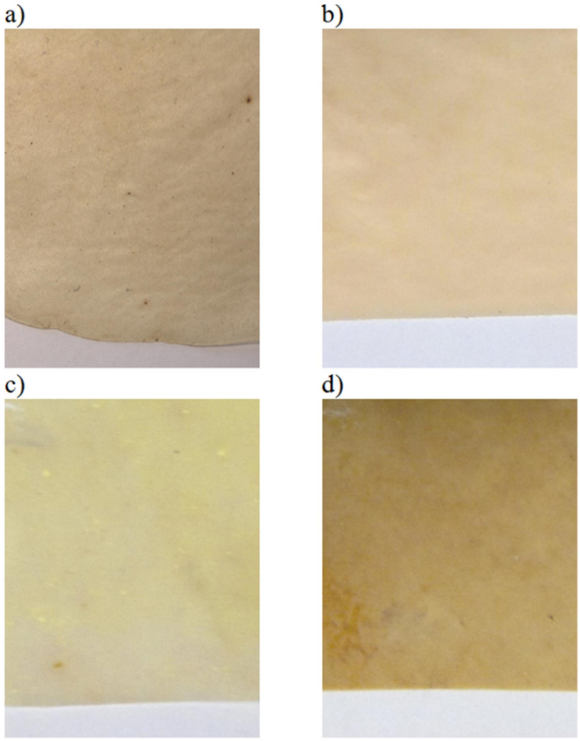

***Figure 4.5**. Unfilled rubbers: a) ACM (dual); b) ACM (chlorine); c) CO; d) GECO.*

ACM samples seem to be more uniform, while relatively large triazine particles can be seen in CO sample meaning that properties of the material will deviate and the sample cannot be evenly cured. Such problem could be related to the mixing process, when shear forces in mixer were too weak to break the clumps. Moreover, CO was excessively sticking to the mixing rotors and chamber that possibly complicated distribution of recipe ingredients even more.

4.2.1. Determination of curing time

Acrylic rubbers show marching modulus that is typical for this type of rubbers. In CO torque is usually increasing slowly and steadily with time. The obtained rheographs can be seen in ***Figure 4.6***. Curing behaviour of ACM with chlorine cure-sites was not tested, but it is known that it has “marching” curing curve and generally slower vulcanization process than ACM with dual cure-sites. However, a retarder was added to ACM (dual), and it was decided to set curing time of both ACM rubbers to 15 minutes. In CO samples no scorching is seen, and the curve is reaching no plateau. Therefore, curing times were set arbitrary for the same 15 minutes for ACM and CO rubbers.

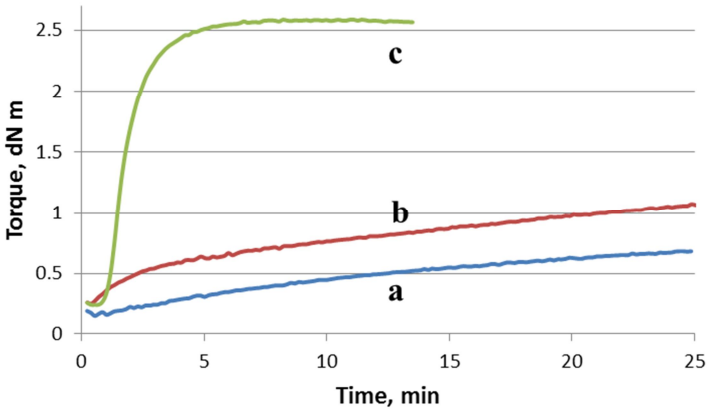

***Figure 4.6**. Curing curve at 175 ˚C of unfilled a) ACM with dual cure-sites; b) CO; c) GECO with TMTD accelerator.*

Moreover, the curing behaviour of GECO with two different accelerators was studied at 160 ˚C and 175 ˚C. The curing curves are presented in ***Figure 4.7***. Curing process starts much later with CBS accelerator than TMTD, especially at 160 ˚C, and the slope of the curve is more flat indicating a slower curing process. Compounds containing TMTD have good scorch and short curing time. Although curing with TMTD at 175 ˚C to the optimum level is fast, curing at 160 ˚C would allow tuning the crosslink density of the compound more accurately that can be useful in future experiments.

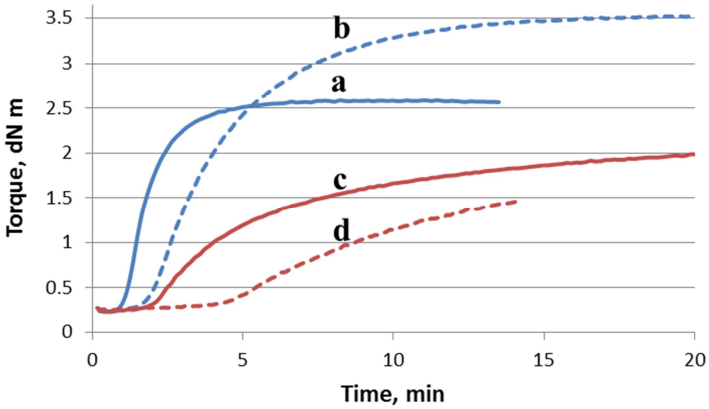

***Figure 4.7**. Curing curves of GECO samples at 160 ˚C (dashed line) and 175 ˚C (solid line) with different curatives: a, b) TMTD; c, d) CBS.*

4.2.2. Tensile properties

Tensile properties of unfilled rubbers are shown in ***Figure 4.8***. Deviation of the results within the specimens is high for ACM rubbers, especially for maximum elongation values. That could be related to the presence of voids inside the material, or poor distribution of curatives resulting in the variation in number of crosslinks within the sample, or instrumental error arising from testing. Hence, the reason for high deviation

is most likely related to the manufacturing process (unsuitable mixing cycle, low fill factor or mixing temperature, etc.) or the testing equipment. The increased fill factor and addition of curatives after cooling down the masterbatch would lead to higher shear forces during mixing thus facilitating the dispersion of the curing agents and possibly reducing the deviation in tensile properties within the sample. Same suggestions are valid for CO sample, except for the fill factor has to be generally lower for epichlorohydrin rubbers than for ACMs in order to control heat built-up. Finally, certain amount of curatives is unused in CO because of the visible large inclusions of triazine. These factors negatively affect tensile and other properties of the materials.

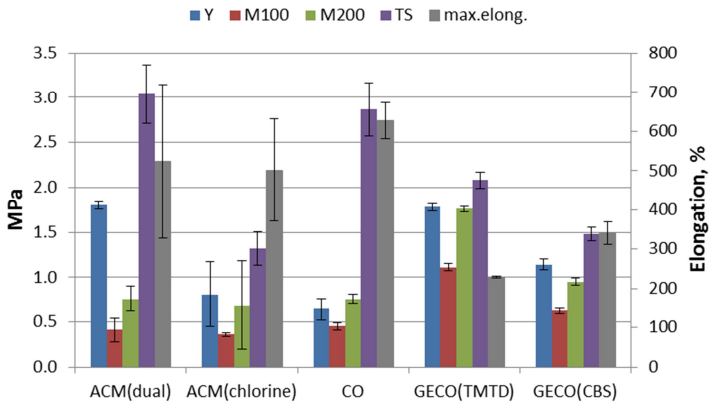

***Figure 4.8**. Tensile properties (with standard deviations) of neat rubbers.*

Young's modulus, stress at 100 and 200 % elongation and tensile strength of GECO with TMTD accelerator are notably higher than those properties of GECO with CBS and can be related to the differences in curing process and TMTD being more active accelerator than CBS. For the DEA application, CO shows better tensile properties than GECO sample – lower Y, M_{100} and M_{200}, as well as higher TS and maximum elongation.

From ***Figure 4.9*** it is seen that maximum elongation decreases with increase in curing time that is related to the corresponding increase in crosslink density. No significant changes are seen in stress at 100 and 200 % elongation, but tensile strength and Young's modulus have maximum at 10 minutes of curing. Such behaviour could not mean that the optimum state of cure is reached after 10 minutes at 175 ˚C, because the compound has a slow soap/sulphur curing system containing a retarder. Thus, more detailed investigation of the effect of curing time on mechanical properties needs to be performed together with microscopic analysis of the structure. Reduction of the tensile properties may be the sign of multiple internal defects in the sample.

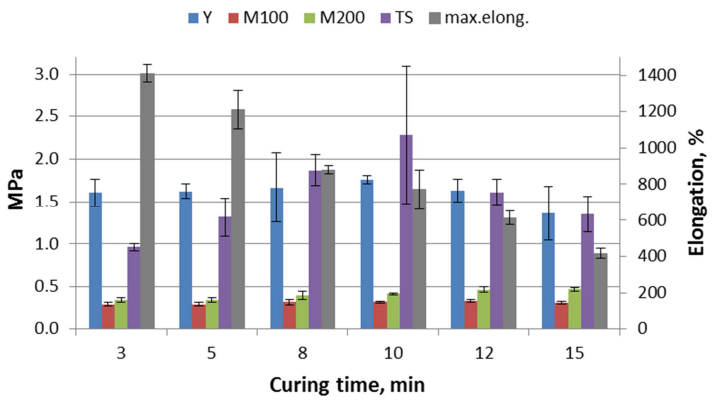

***Figure 4.9**. Tensile properties (with standard deviations) of ACM with dual cure-sites prepared on mill depending on the curing time.*

4.2.3. Dielectric properties

Dielectric constants and losses of various materials are presented in ***Figure 4.10*** - ***Figure 4.11***. ACM with only chlorine cure-sites has somehow higher dielectric permittivity compared to the dual cure-site ACM. According to the dielectric data, it is impossible to determine whether the type of cure-site has an effect on relative permittivity and losses of the ACM rubbers or those differences are related to the microscopic structure and morphology of the sample. Moreover, dielectric permittivity of ACM (chlorine) is higher than the average reported for acrylic rubbers (4 – 7) at 1kHz [3;44;52;65] meaning that sample structure should definitely have an effect on it.

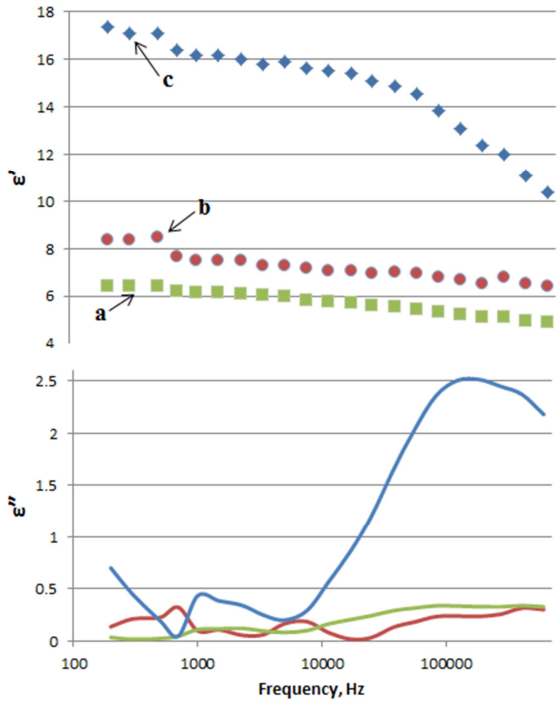

***Figure 4.10**. Relative dielectric permittivity (ε') and dielectric losses (ε'', solid lines of corresponding colours) of a) ACM with dual cure-sites, b) ACM with chlorine cure-sites and c) CO sample.*

CO is known to have comparably high dielectric constant that is related to the chemical structure of the highly polar polymer. High dielectric losses of CO sample at higher frequencies accompanied with the change of permittivity slope are related to relaxation process of unknown nature. Comparison with pure polyepichlorohydrin can help understanding if that relaxation related to the polymer itself, or, for example, to the large inclusions of triazine. More test points and tested specimens are required in order to determine whether relaxation occurs in CO and ACM (chlorine) at lower frequencies.

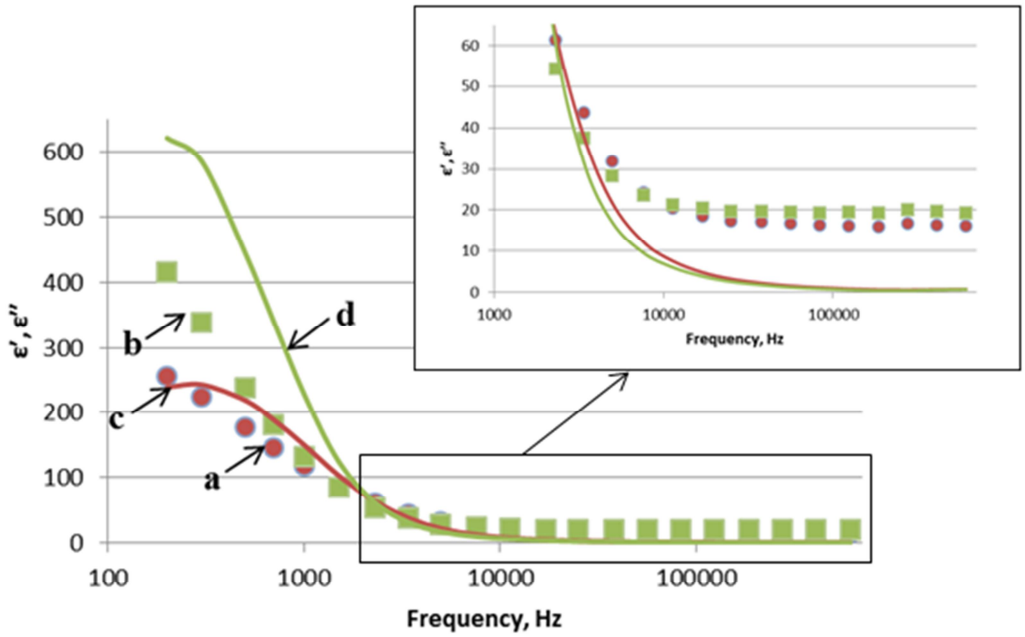

Figure 4.11. *Relative dielectric permittivity (a) and dielectric losses (c) of GECO with TMTD accelerator; relative dielectric permittivity(b) and dielectric losses (d) of GECO with CBS accelerator.*

GECO samples have very high ε′ and ε″ most likely due to the higher conductivity (lower resistivity) of the compounds that can be seen from ***Figure 4.12***. Both resistivity slope changes and dielectric losses of GECO rubbers increase significantly at about 10 kHz. CO sample has lower resistivity than tested ACM rubbers, but stays in dielectric region at lower frequencies, while GECO falls into semi-conductive one (below 10^8 Ω cm). Moreover, the slope of GECO curve changes at lower frequencies with resistivity depending less on the frequency that can be a sign of arising DC conductivity. The type of accelerator used with GECO rubber has little effect on material's resistivity.

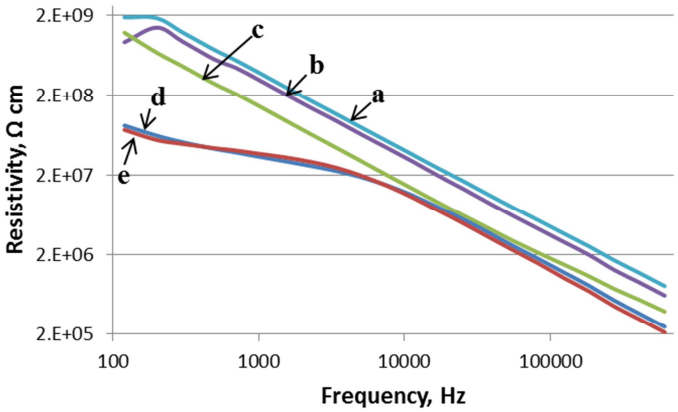

***Figure 4.12**. Volume resistivity (logarithmic scale) of neat rubber samples: a) ACM with dual cure-sites, b) ACM with chlorine cure-sites, c) CO, and GECO with d) TMTD accelerator or e) CBS accelerator.*

4.2.4. Conclusions

Much attention should be paid to the manufacturing of ACM and CO samples. Possible changes can include cooling of the masterbatch before addition of curatives and better control of the temperature. Moreover, optimal fill factor should be determined experimentally. These arrangements can improve the distribution of the curatives and lead to better reproducibility and less deviation of the test results. Another solution may be to use commercial package with curative dispersion. Finally, during the curing process, pressure of the press per cm^2 of rubber should be kept at the same level for all the samples, although it is sometimes difficult to calculate the area of the sheet in advance.

Concerning basic tensile properties, DEA materials need to have low elastic modulus, high elongation and moderate to high tensile strength. When comparing the properties of ACM rubbers, ACM (dual) has comparably high modulus and just moderate dielectric properties, while tensile strength of another ACM type might be too low. Among polyepichlorohydrin samples, CO would have obvious benefits over GECO, especially if problem with curative distribution is solved. Finally, when comparing the activators, the choice is made for TMTD because it provides faster curing and lower dielectric losses at frequencies below 1 kHz compared to the compounds containing CBS. However, increased conductivity, high elastic modulus and low maximum elongation make current GECO samples difficult to be applied in DEAs.

4.3. Composites

In order to create a composite with stable and homogenous properties, attention should be paid to the dispersion of filler particles within the rubber matrix. As expected, samples prepared by solution casting had poor filler dispersion that can be noted even visually. This is related to poor sedimentation stability of the suspension in acetone and

much time required for specimen to solidify. All of the filled samples were made by the sonication-assisted solution casting method, and only ACM(dual) with 5 phr of BT prepared by conventional solution casting was used for the comparison reasons. Visually, sonicated sample had better uniformity than another one. For the sonicated material, distribution of particles is more even for the least amount of filler of the smaller particle size (5 phr of TO and BT), and the least uniform for the sample with the highest load of filler with the largest particle size (20 phr of TP). In the latter case, the separate layer of TP is present at the bottom of the sample. All solution-casted composites had shiny upper and dull bottom surfaces.

Most of the filled samples prepared in internal mixer seem to be homogenous. However, large spherical TP particles are visualized in materials containing this filler. That can be explained by the overall large particle size of the filler. Distribution of fillers will be discussed more in **Chapter 4.5**. As mentioned in previous chapter, CO samples contain triazine clumps that are still present in the structure after addition of fillers or oils.

Addition of oils to ACM rubber with dual cure-sites resulted in samples with reduced uniformity and appearance of stains, especially when Fomblin® oil was used. “Bleeding” of oils was noticed at loadы over 5 phr for all the rubbers. Finally, after 3-4 months of storage, oil migrated to the surface from GECO filled with 5 phr of MIDEL®. For filled ACM elastomers use of plasticizer is limited to about 5 phr, but polyepichlorohydrin allow incorporation of 10-30 phr of oils, such as DOP (dioctyl phthalate) or DOA (dioctyl adipate) [66;69].

4.3.1. Curing

As seen from ***Figure 4.13***, addition of oils has some plasticizing effect on ACM rubber with dual cure-sites. MIDEL® reduce torque level less than Fomblin® oil, and all the materials show similar marching curve.

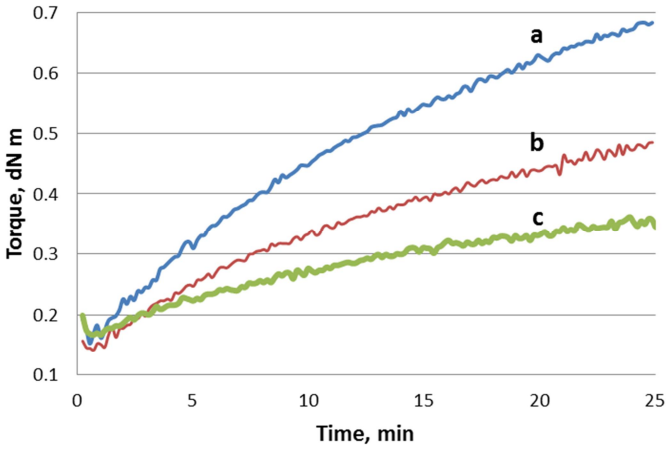

Figure 4.13*. Curing curves of acrylic rubber at 175 ˚C with a) no oil; b) 5 phr of MIDEL® oil c) 5 phr of Fomblin® oil.*

Curing curves of oil-filled GECO are shown in ***Figure 4.14***. When comparing the effect of oil incorporation to GECO, it is seen that here Fomblin® increases the torque. MIDEL® oil reduces the torque a bit in the beginning of the curing process, but then maintains it at the level of unfilled GECO. Nevertheless, presence of 5 phr oils has almost no effect on t_{90} time.

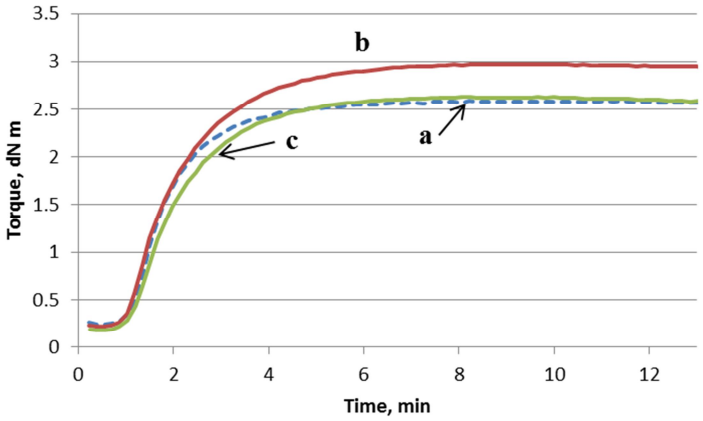

Figure 4.14*. Curing curves of GECO with TMTD accelerator at 175 ˚C with a) no oil; b) 5 phr of Fomblin oil; c) 5 phr of MIDEL oil.*

Finally, addition of fillers leads to increase in maximum torque level due to increased viscosity. Optimal cure time, however, is almost unaffected by that, as seen from ***Figure 4.15***. Addition of TO leads to a small increase in t_{90}. The onset of vulcanization is not affected by the introduced fillers and oils.

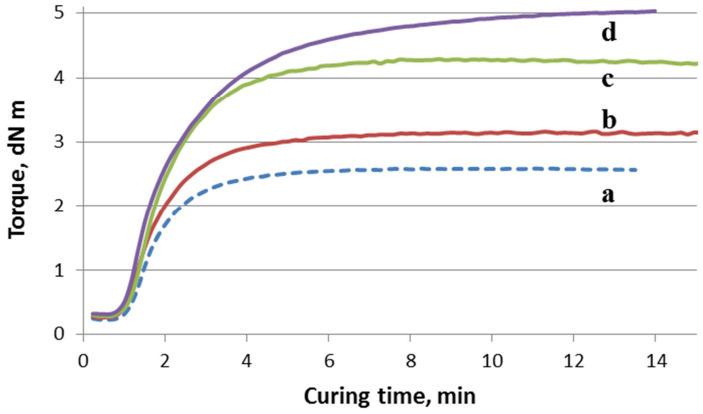

Figure 4.15*. Curing curves of GECO with TMTD accelerator at 175˚C with a) no filler; and with 20 phr of b) BT; c) TP; d) TO.*

4.3.2. Tensile properties

Tensile properties of the composites are discussed based on the sample preparation method. Although it was concluded in previous chapters that solution-casted samples have poorest structure and visible inhomogeneous distribution of particles, results of the

mechanical tests of such composites will be discussed here shortly for a comparison reason.

4.3.2.1. Solution-casted samples

Tensile properties of samples prepared by sonication-assisted solution casting are seen in ***Figure 4.16***. High deviation of the results is related to uneven thickness of the material arising from the fabrication method and poor distribution of the particles related to poor sedimentation stability of filler particles in acetone. Sedimentation stability was noticed to increase with decreasing the particle size of the filler (TP → TO). Standard deviation bars are not shown in the picture for clarity. ACM/TO composites are only available with 5 phr load of filler.

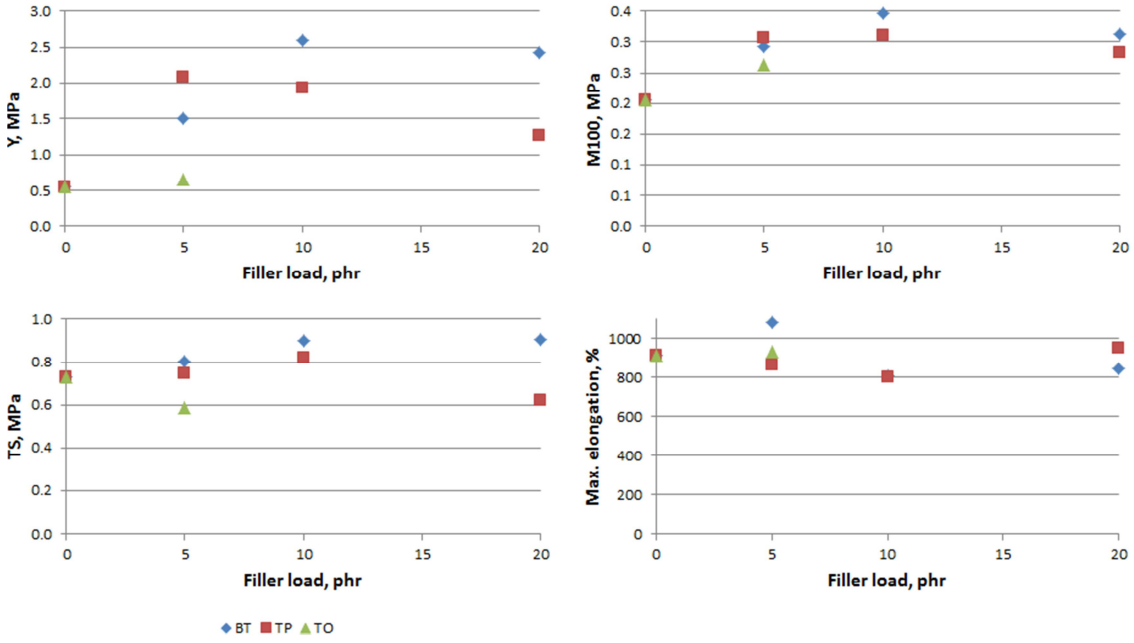

Figure 4.16. *Tensile properties of ACM (dual) composites prepared by sonication-assisted solution casting method.*

It is seen that addition of BT and TP led to certain increase in Young's modulus and M_{100} especially for low filler load. At higher load of TP the mentioned properties show regression, but are still higher than the initial level. However, increase in TS caused by BT and TP was followed by some decrease in the property at 20 phr of TP. This can be related to worse sedimentation stability of tantalum pentoxide compared to barium titanate resulting in filler distribution gradient. Anyway, TS of all solution-casted samples is very low – below 1 MPa, and the addition of TO shows the lowest TS value. High elongation at break of all the samples can be related to the very low crosslink density of the compounds.

4.3.2.2. Conventionally mixed samples

Effect of fillers on tensile properties of rubbers is first shown in ***Figure 4.17*** with an example of BT-filled ACM with dual cure-sites prepared on mill. Here, addition of BT resulted is increase in elastic modulus and tensile strength, while no significant changes in M_{100} were noticed. Moreover, maximum elongation increased, especially at 5 phr load.

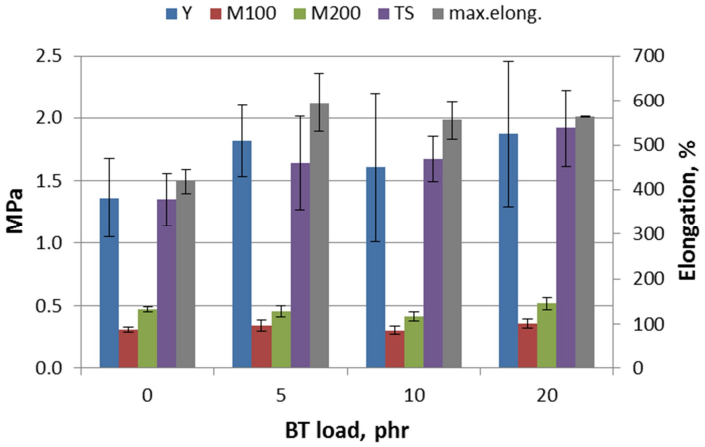

Figure 4.17*. Tensile properties (with standard deviations) of ACM with dual cure-sites depending on the BT load.*

According to the results of bound rubber determination (BRV), neither of fillers is reinforcing. Therefore, the observed changes in properties can be related to the possible defects in internal structure of the unfilled rubber, uneven distribution of the particles in composites or changes in crosslink densities. The results of dielectric tests from **Chapter 4.1.3** indicate possible presence of pores in this unfilled ACM sample explaining its comparably low mechanical properties.

At small loads of TO, elastic modulus and stress at 100% elongation of the ACM rubbers decreases as seen from ***Figure 4.18***, same behaviour is frequently reported in literature, for example, by Yang et al. [35], and can be related to the decreased crosslink density of such materials. It will be discussed in more details later in the next chapter.

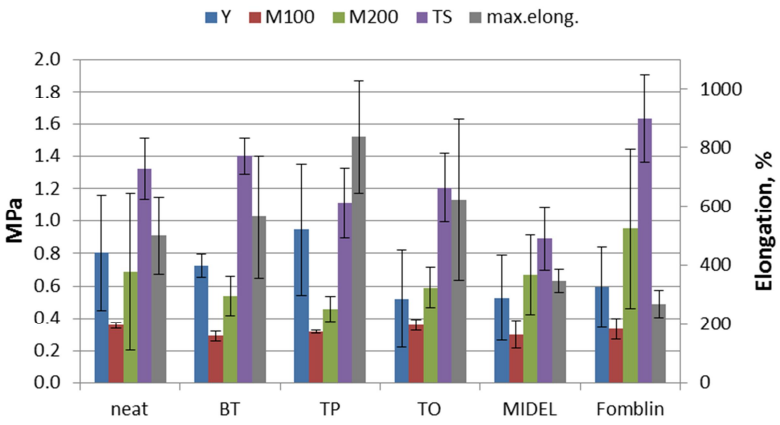

***Figure 4.18**. Tensile properties (with standard deviations) of ACM with chlorine cure-sites with 5 phr of fillers/oils.*

Young's modulus and maximum elongation of different rubbers filled with 5 phr of particles and oils is presented in ***Figure 4.19 - Figure 4.20***. Generally, compounds with any kind of fillers/oils have lower or the same elastic modulus, but addition of TP and MIDEL® oil led to some increase in that property.

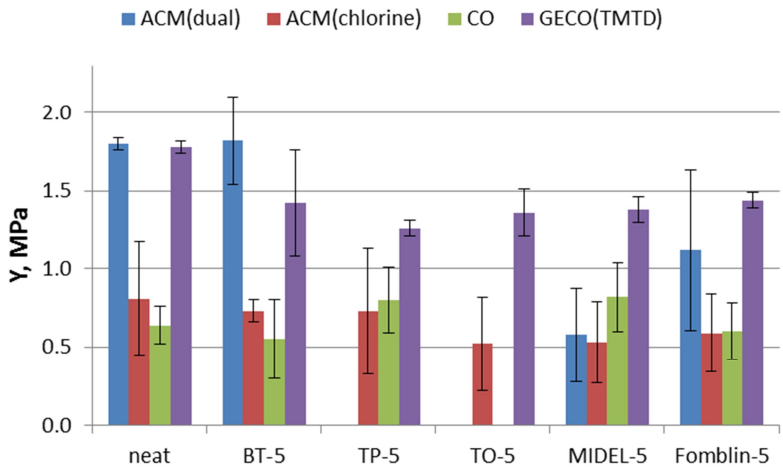

***Figure 4.19**. Young's modulus of various rubbers at 5 phr filler or oil load.*

Moreover, addition of 5 phr of oils to ACM rubbers resulted in reduced elongation at break. As tensile strength of some compounds increased, that all may mean that chosen oils do not work successfully as plasticizers. High deviation of the results within the specimen is possibly a sign of poor dispersion of recipe chemicals or defective material structure.

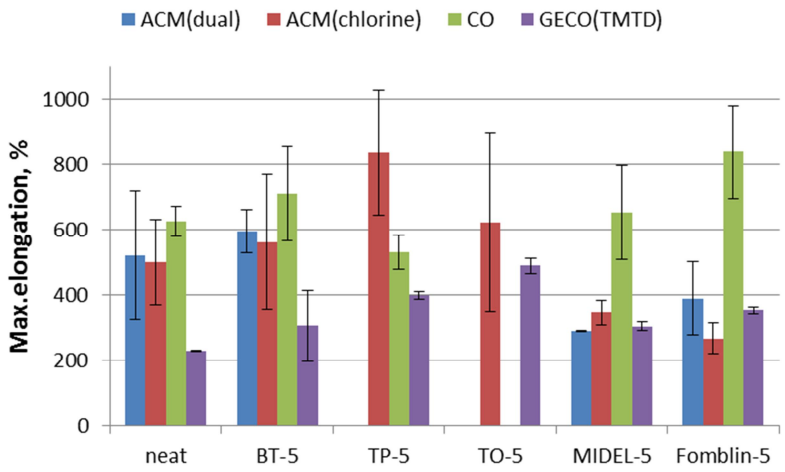

***Figure 4.20**. Maximum elongation of various rubbers with 5 phr filler or oil load.*

Mechanical properties of filler- and oil-loaded GECO are shown in ***Figure 4.21*** and ***Figure 4.22*** respectively. Standard deviation bars are not added to the graphs for clarity reasons. Addition of up to 20 phr of any filler or oil to GECO rubber resulted in lower Young's modulus, except for the 20 phr of TO that increased modulus to about 2.2 MPa. Moreover, M_{100} and M_{200} were reduced after addition of fillers and oils. Particle-filled composites also showed higher TS increasing with increase in filler load (TP, BT), as well as GECO with incorporated MIDEL® oil. Remarkably, test results for TO at different concentrations are much more chaotic than those of other fillers. This can be related to the problems with dispersion of nano-sized materials. It is impossible to distinguish any trend in the tensile behaviour of TO-filled GECO rubbers.

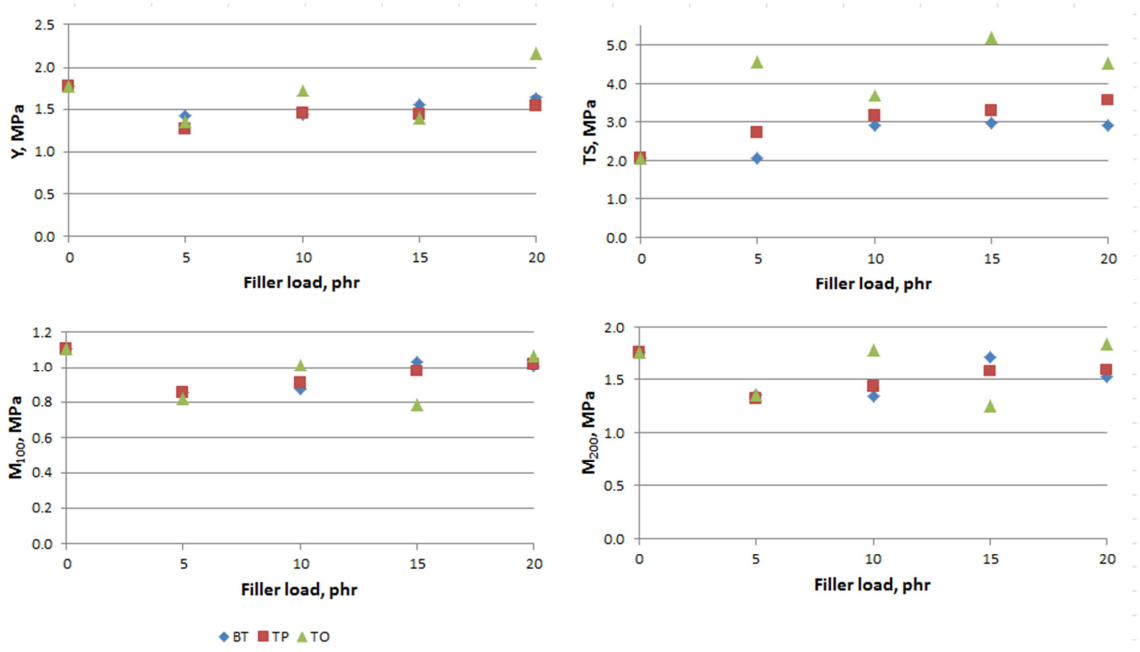

***Figure 4.21**. Mechanical properties of filler-loaded GECO rubbers.*

Similar behaviour is seen from ***Figure 4.22*** with different oil loads, especially for MIDEL® containing rubbers. Moreover, MIDEL® oil is less compatible with GECO

than Fomblin® because at 5 phr load it migrated to the surface of the sample after few month of storage.

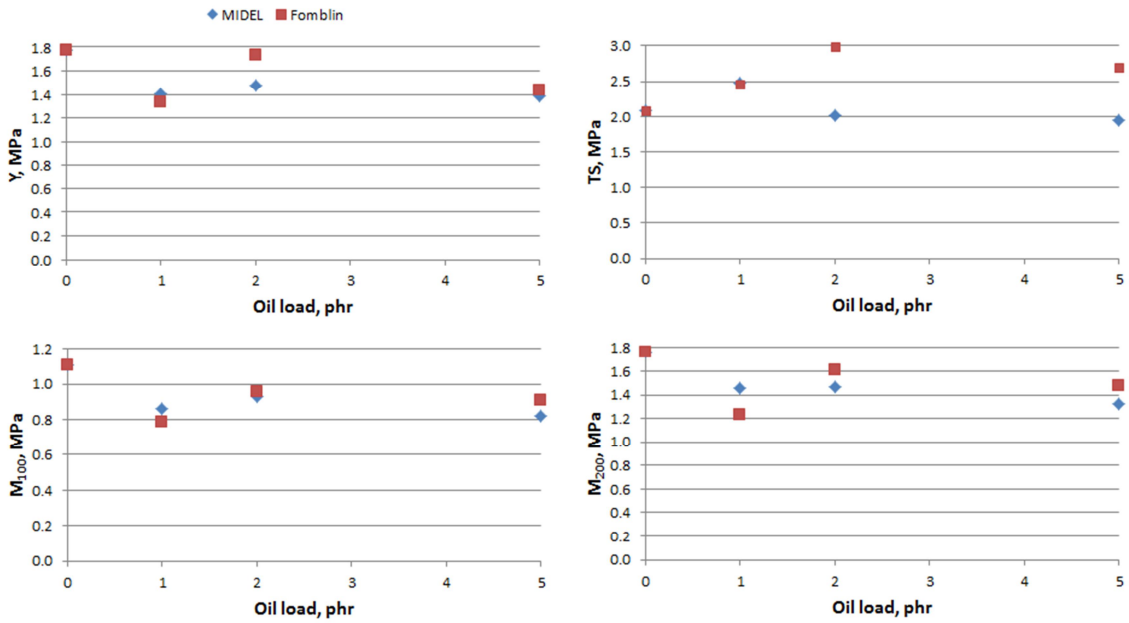

***Figure 4.22**. Mechanical properties of oil-filled GECO.*

Addition of different amount of fillers resulted in improved maximum elongation of GECO rubbers, as seen from ***Figure 4.23***, although introduction of ceramic particles usually leads to the increased stiffness of the compound and reduced elasticity. Such increase in elongation at break can have a relation to the higher tensile strength of the filled samples. Same assumptions could be valid also for MIDEL® containing GECO materials, but addition of Fomblin® seems to have plasticizing effect on such rubbers.

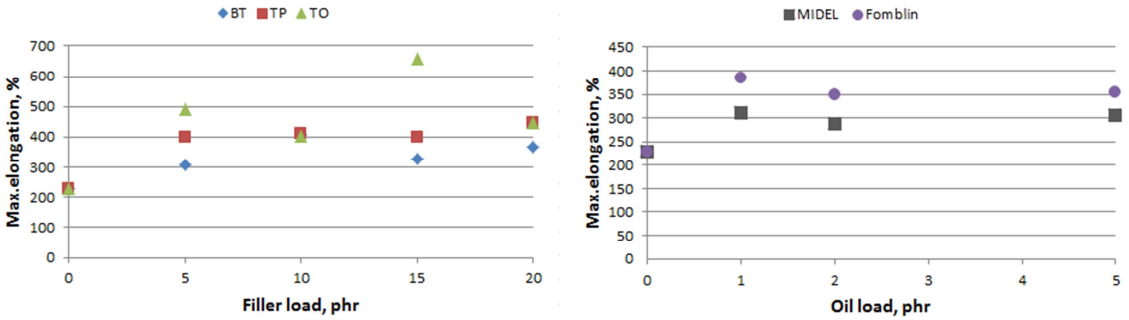

***Figure 4.23**. Maximum elongation of GECO samples.*

4.3.3. Breakdown strength

Only solution-casted samples were tested for the maximal electric field they can withstand. The results are shown in ***Figure 4.24***. No clear correlation is noticed between composition of the material and its breakdown field. Deviation of the results is high, as in most of the other tests, due to the poor distribution of fillers and curatives. Breakdown strength of polyepichlorohydrin samples was not determined because of

much higher conductivity of GECO rubbers. However, determination of maximal electric field CO samples can withstand is recommended for future research.

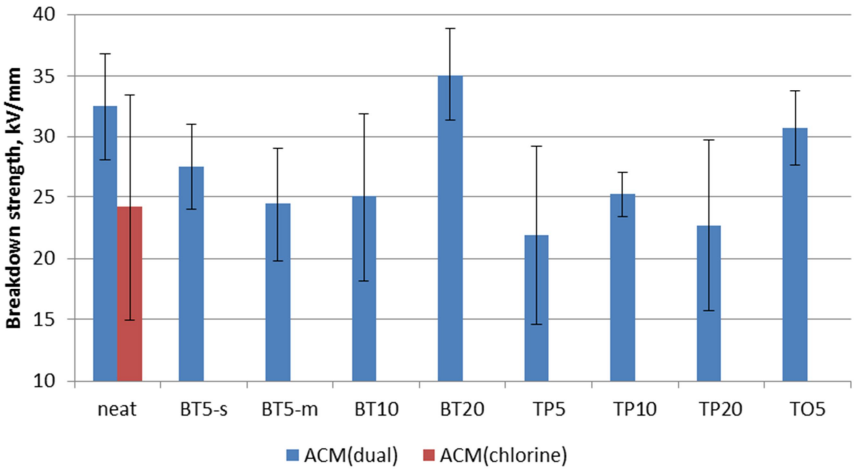

***Figure 4.24**. Breakdown strength of solution-casted*[***] *samples (with standard deviation).*

Solution-casted samples have the poorest quality compared to the samples prepared by other techniques. It is known that breakdown strength of the material depends a lot on amount of pores, presence of fillers and distribution of particles. Due to the better particle distribution and elimination of voids, it is assumed that breakdown strength of conventionally mixed rubbers should be same or better than that of corresponding solution-casted samples. Moreover, electric field applied during actuation tests should not exceed 10-15 kV/mm for the material to have perspectives as DEA. Therefore, all the tested compounds satisfy the aims of the current work from the viewpoint of breakdown strength.

Finally, although dielectric breakdown test is informative at the early development stage of suitable dielectric elastomer, the results of such test are usually arbitrary and do not reveal the real property of the actuator material because EMI phenomena is not included into this evaluation. Therefore, breakdown voltage determined with rigid electrodes should be used mostly for eliminating the materials with obviously low breakdown properties. Test with stretchable electrodes or at different prestrain rates would be more informative, but those are basically actuation tests.

4.3.4. Dielectric constant

For more clear presentation of the results, relative dielectric permittivities and losses are shown at one frequency. Although for DEA application it would be better to view dielectric properties at 1-10 Hz, the used equipment did not allow using such low

[***] Neat ACM(chlorine) and BT5-m are prepared by conventional solution-casting, while other specimens by sonication assisted one.

frequencies. The values are shown in ***Figure 4.25-Figure 4.27*** at the frequency of 1 kHz that is a standard one.

According to ***Figure 4.25***, addition of 5 phr of fillers to ACM rubbers with chlorine cure-sites and those obtained by solution-casting resulted in small increase in dielectric permittivity. Moreover, dielectric loss was reduced for ACM (chlorine). Other composites had poorer relative dielectric permittivity than the corresponding unfilled rubbers. Detailed study of the structure of the sample and more information about fillers is needed in order to justify the possible reasons for that.

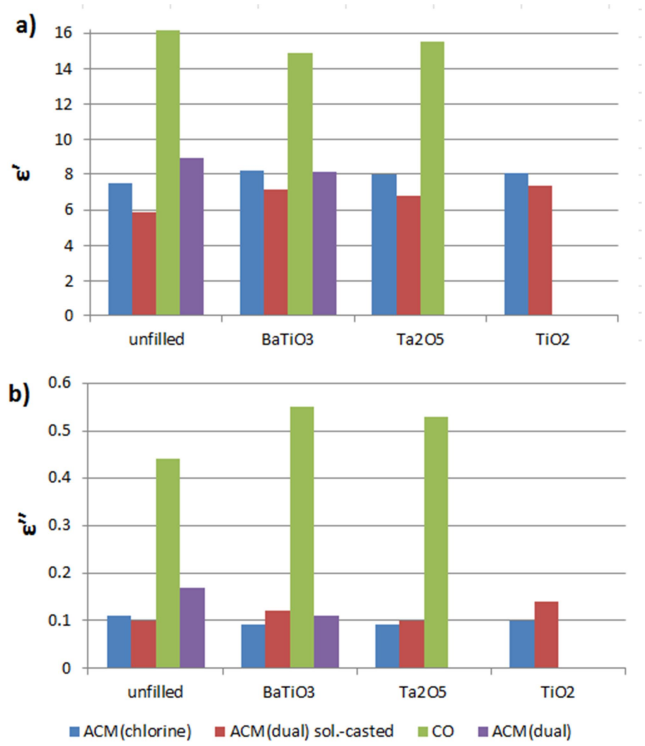

Figure 4.25*. Relative dielectric permittivity (a) and losses (b) of various composites containing 5 phr of fillers; measured at 1 kHz.*

Similar picture concerning CO composites is seen from ***Figure 4.26***, where addition of transformer oils led to a decrease in dielectric constant and increase in losses. According to the theory [21], at the temperatures above glass transition, dielectric constant of the plasticized compound should increase in case oil is compatible with elastomer and has real plasticizing effect. Hence, determination of glass transition temperature of the compounds of interest could be informative for the current study, and should be performed in future.

However, as addition of oils to CO rubbers did not decrease Y, poor plasticizing action can be assumed. It can also be related to lower polarity of the oils. Moreover, addition of oils could lead to the changes in comformations of macromolecular chains making them stiffer, but that would not explain the increase in dielectric losses. Therefore, oils possibly behaved like low-ε′ fillers in CO leading to the decrease of overall dielectric constant and increase in dielectric loss. Nevertheless, the obtained type

of behaviour is different than predicted theoretically, and requires investigation deeper than the extent of the current thesis. The opposite changes in ε′ values of ACM composites predicted by the theory are more promising for DEA applications.

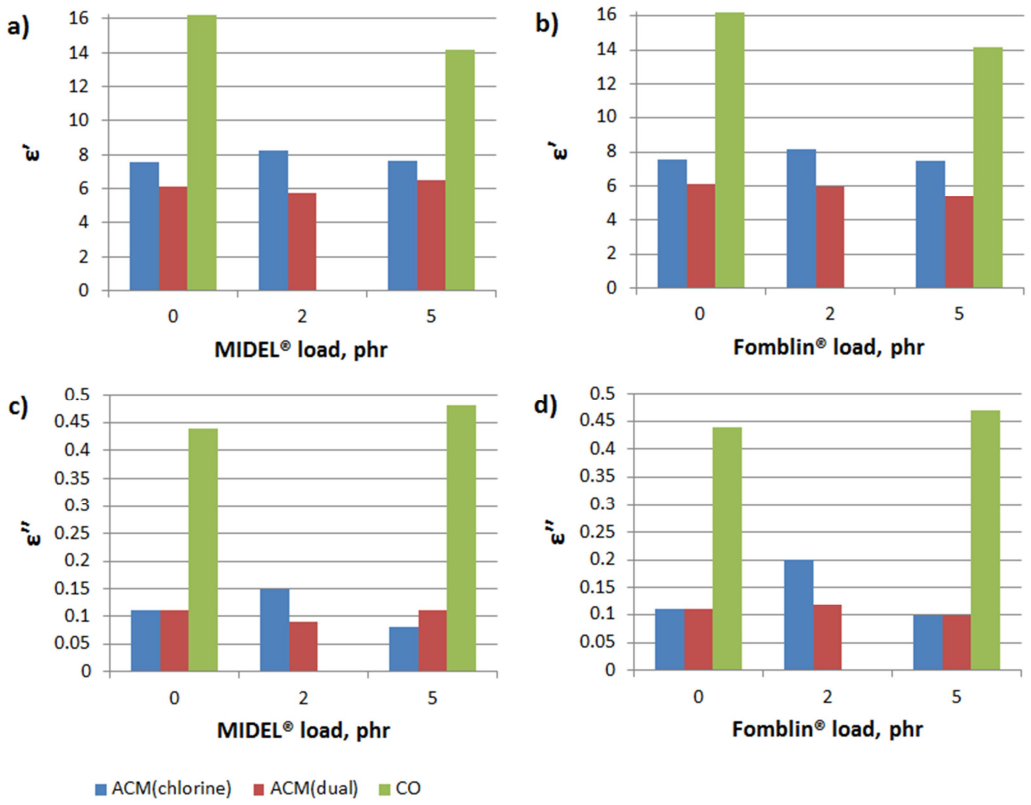

Figure 4.26*. Relative dielectric permittivity (a, b) and losses (c, d) of various composites containing transformer oils; measured at 1 kHz.*

Generally, addition of fillers to GECO rubber resulted in lower dielectric constant and correspondingly lower dielectric loss. Such changes correlate well with changes in the electric conductivity of the composites discussed later in this chapter. Addition of small amount of oils resulted in significantly increased dielectric loss in materials, as seen from ***Figure 4.27***. Therefore, none of the tested transformer oil could be recommended to be used with GECO rubbers.

Changes in material's resistivity are especially important for GECO samples because of semi-conductive nature of the compound (resistivity below 10^8 Ω cm). Reduced conductivity together with high dielectric constant would be beneficial for DEA application. Dependence of the resistivity on the filler type and amount is shown in ***Figure 4.28*** in logarithmic scale. Resistivity curves of other composites are not presented here because they are much less important and informative. Generally, addition of ceramic filler led to some increase in materials resistivity. Addition of 5 phr of BT or TO into GECO matrix led to more significant improvement at low frequencies, while further addition of filler gradually decreased electrical resistivity to the initial level. As for GECO filled with TP, addition of larger amount of dielectric particles resulted in reduced conductivity with increased filler load.

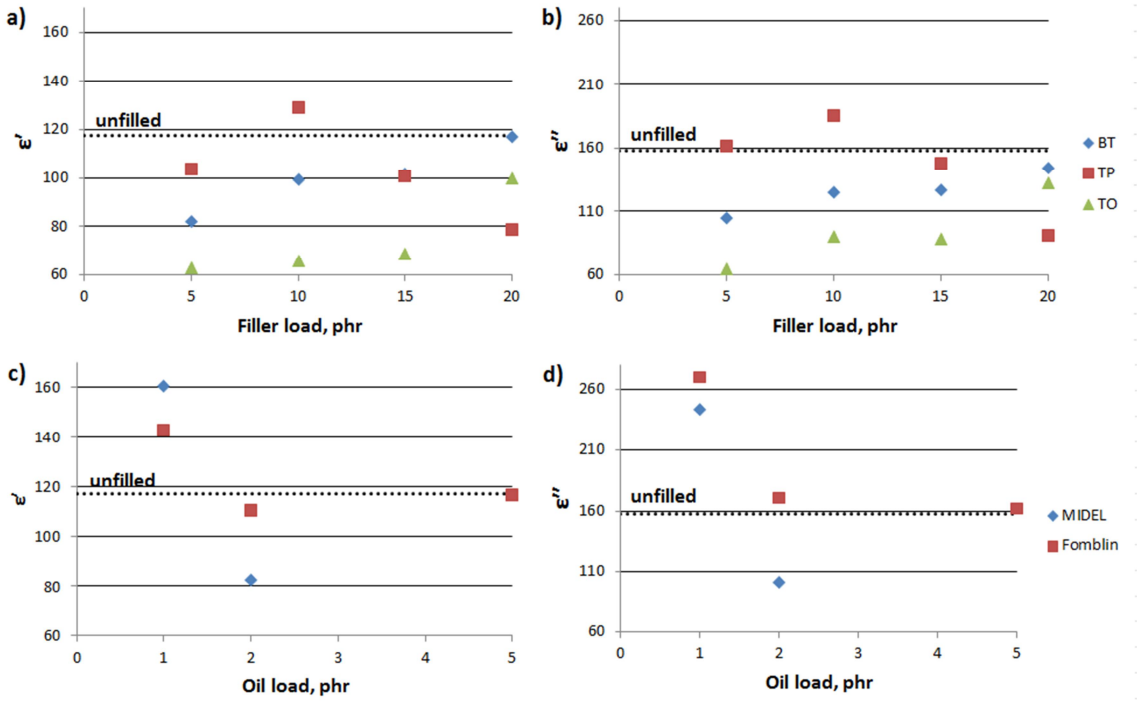

Figure 4.27. *Relative dielectric permittivity (a, b) and losses (c, d) of various GECO composites; measured at 1 kHz.*

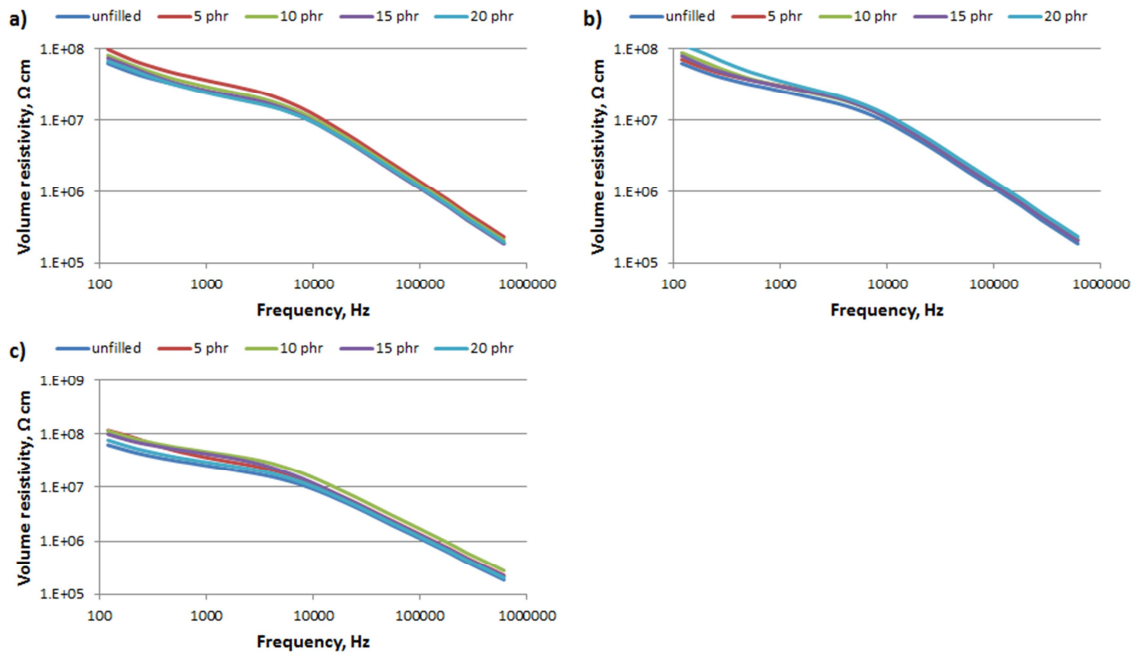

Figure 4.28. *Volume resistivity of GECO rubbers filled with a) BT; b) TP; c) TO depending on a frequency and a filler load.*

At the same time, introduction of small amounts of oil did not lead to remarkable changes neither in values nor in the shape of the curve. Resistivity curves of oil-filled GECO compounds are sown in logarithmic scale in ***Figure 4.29***.

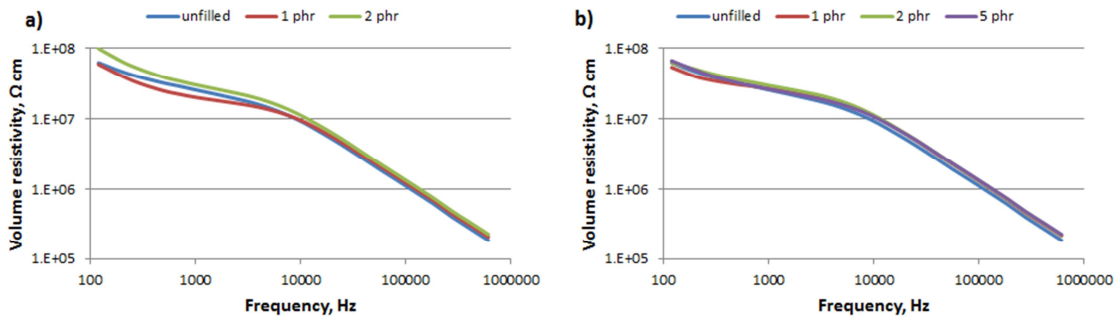

***Figure 4.29**. Volume resistivity of GECO rubbers filled with a) MIDEL® oil; b) Fomblin® oil depending on a frequency and a filler load.*

4.3.5. Fitting to dielectric composite mixing rules

By applying equations (2.22) – (2.28) from **Chapter 2.3** it is possible to estimate how well our theoretical expectations correlate with practical results. In case the correlation is found, it will be possible to calculate necessary amount of filler required to obtain a certain dielectric permittivity of the composite. Therefore, comparing experimental results with classical composite mixing rules is common practise in the DEA research field [35;70].

From the all composites studied, only dual cure-site ACM filled with BT can be fitted to dielectric composite mixing rules because other ACM and CO composites have no variation in filler load. Finally, various particle-filled GECO materials are left outside due to their lower electrical resistivity. GECO composites are closer to semi-conductors in their dielectric properties and dielectric composite mixing rules cannot be applied to them. Oil-filled compounds also were not compared to the classical mixing rules because most of the theories assume that added dielectric fillers are spherical in shape, have similar size and higher dielectric constant than the matrix. In this case, oils are unlikely to be spheres, the scale of inclusions in unknown, and the dielectric constant of any of the used oil is smaller than of rubber. The solution-casted samples have visually poor surface and bulk quality together with low homogeneity resulting in thickness variation and uneven distribution of fillers and crosslinking.

In order to compare BT-filled ACM with classical dielectric mixing rules it was assumed that dielectric constant of barium titanate is 1000, while the real value is unknown. According to ***Figure 4.30***, experimentally measured dielectric permittivity of ACM(dual)/BT composites does not fit to the predicted range, as it is lower than of initial rubber. Thus, fitting should be repeated after obtaining samples with same porosity level and after the exact dielectric constant of the filler is known.

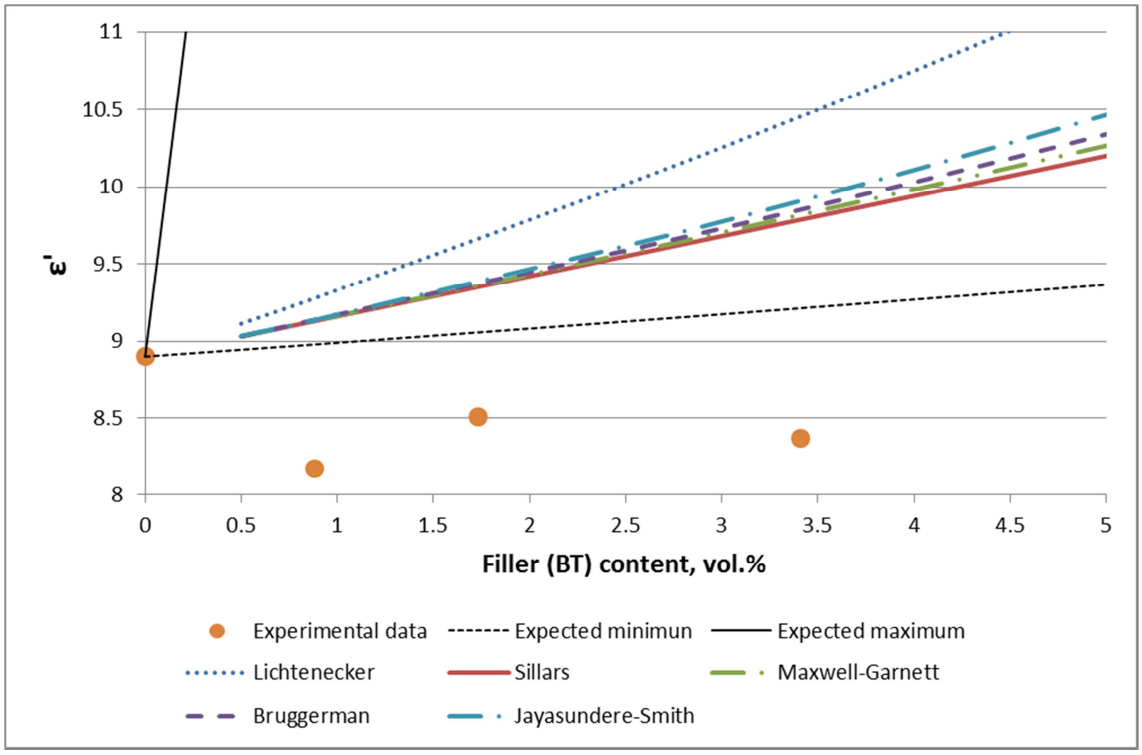

***Figure 4.30**. Fitting experimental dielectric permittivity of BT-filled ACM with dual cure-sites to classical dielectric mixing rules.*

4.3.6. Conclusions

All the obtained composites suffer from relatively poor dispersion of filler particles. Therefore, more attention should be paid to the fabrication process by adjusting the mixing parameters and possibly compound recipes. Generally, addition of fillers has little effect on mechanical properties of the compounds, and often results in slightly reduced elastic modulus. In most cases, fillers increase dielectric constant of ACM rubbers, but lead to a reduction of that property in polyepichlorohydrin. Addition of TP to GECO rubbers leads to reduction of electrical conductivity and dielectric loss factor. At the same time, transformer oils have poor plasticizing effect for most of the tested rubbers, especially GECO.

Generally the use of classical mixing rules allows estimating the dielectric properties of the composites that are being developed and it can be a useful tool when planning a composite with certain dielectric constant. In the current case, fitting to the mixing rules fails due to some problems with the studied material. Moreover, the fitting is done under the assumption that filler particles are spherical, and the real permittivity of BT used is unknown. Determination of exact dielectric constant of filler could be the next step in the research.

4.4. Effect of crosslink density

Crosslink densities of some samples were calculated in order to obtain more information about the studied materials. Determined crosslink densities of ACM samples with different curing times agree well with the theory - crosslink density increases steadily with longer curing, as seen from ***Figure 4.31***.

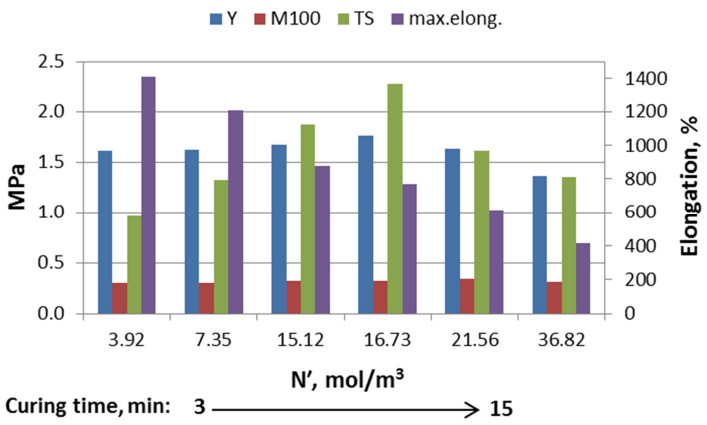

Figure 4.31. *Mechanical properties of ACM with dual cure-sites in relation to curing times and accompanying change in crosslink density.*

The test for determining BRV revealed that there was no rubber-filler gel present meaning that neither of filler is reinforcing. Thus, crosslink densities were calculated based on that information and with assumption that fillers are distributed evenly inside the matrix. Change in crosslink density has little correlation with mechanical properties of the material. Some experimental data is shown in ***Figure 4.33*** - ***Figure 4.34***. Generally, the use of white fillers is not recommended by the manufacturer due to their unknown effect on the curing process. For instance, it is known that presence of TO affects curing process of ACM rubbers and decreases the crosslink density of the composite [35].

For titania, interaction of TO-induces radicals with curatives or with polymer itself leading to the chain scission can be among possible reasons of reduced crosslink density [35]. TO is known for its active surface containing adsorbed water, hydrogen, oxygen and other molecules [86]. Moreover, according to MSDS of TO, its pH = 3.5-4.5 meaning that it could have a retarding action towards ACM rubbers. Addition of BT seem to have similar effect on ACM with dual cure-sites, as seen from ***Figure 4.32***, but the nature of such effect cannot be determined within the scope of the current work. The decrease in crosslink density can explain increased elongation at break that is often reduced with addition of fillers. However, no trend is seen in relation of crosslinking to the change in mechanical properties of these compounds.

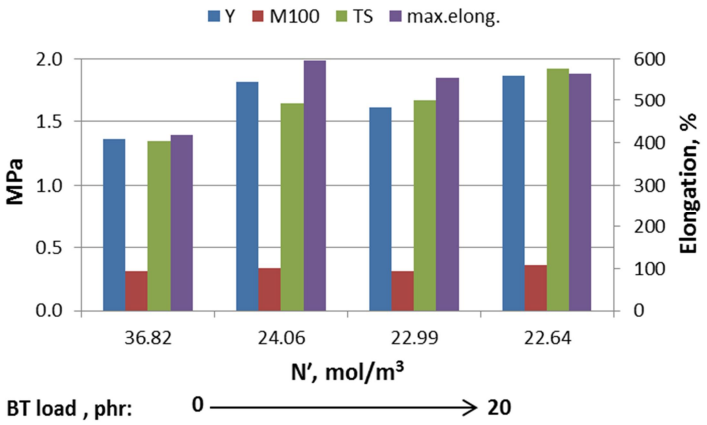

***Figure 4.32**. Mechanical properties of ACM with dual cure-sites loaded with 0, 5, 10, 20 phr of BT in relation to the crosslink density.*

From ***Figure 4.33*** it is seen that compounds with 5 phr of different fillers have the same crosslink density that is just slightly smaller than that of unfilled rubber. Addition of filler led to an increase in tensile strength of all ACM rubbers, and that was not expected to happen because of non-reinforcing nature of fillers and lowered crosslink density. Obviously, addition of transformer oils had an effect on curing process, but the nature of this phenomenon was not studied.

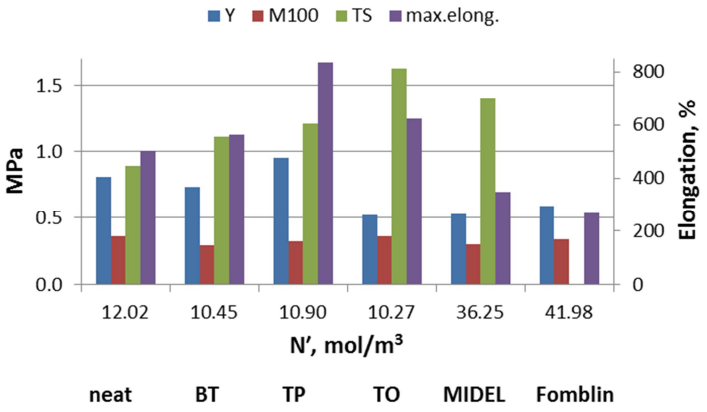

***Figure 4.33**. Mechanical properties of ACM (chlorine) with various fillers/oils in relation to the crosslink density.*

In the case of the effect of crosslink density on the mechanical properties of GECO shown in ***Figure 4.34***, no clear trend is seen. Similarly to previously discussed compounds, in order to investigate the correlation, more data at varying concentrations of fillers is needed, as well as the details of surface activity and pH values of the fillers.

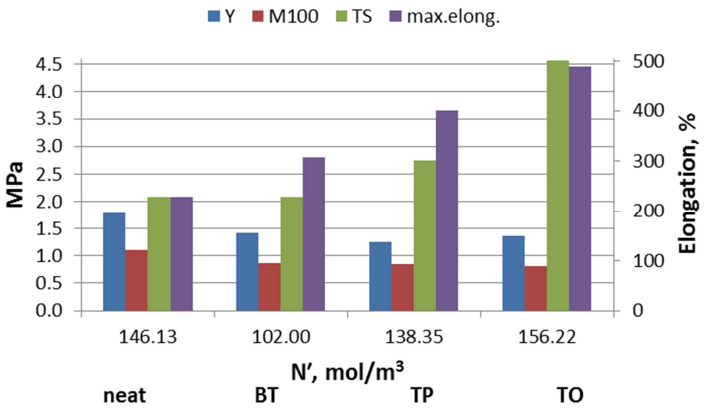

***Figure 4.34**. Mechanical properties of GECO with 5 phr of different fillers in relation to crosslink density.*

The effect of crosslink density on dielectric properties was studied by evaluating the properties of ACM rubber with dual cure-sites cured for 3 to 15 minutes. The current study revealed that, for the unknown reason, increase in crosslink density leads to the increase in relative dielectric permittivity. The relation is shown in ***Figure 4.35***. Generally, polymers with increasing crosslinking tested at temperatures above T_g show some reduction in dielectric constant that is related to the more ordered system and macromolecules that are less free to move in the applied electric field [21]. Increase in dielectric properties in such conditions would mean contaminated or disordered material. However, contamination is unlikely to show steady increase in dielectric permittivity with curing time. Therefore, such effect could be explained by voids and other structural defects that appear in material with increase in crosslink density.

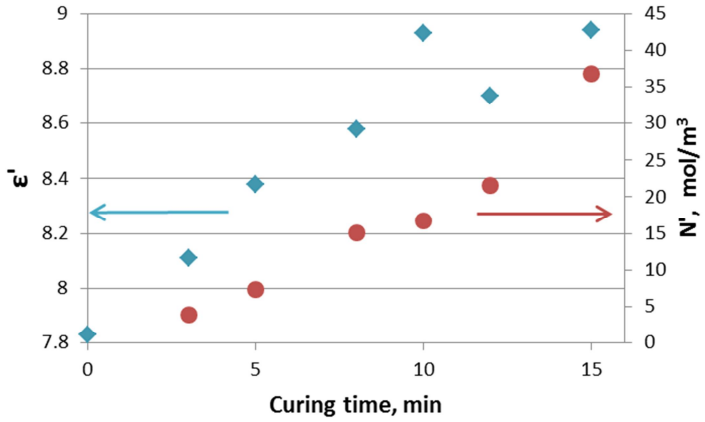

***Figure 4.35**. Effect of curing time on crosslink density and relative dielectric permittivity (at 1 kHz) of ACM unfilled rubber with dual cure-sites.*

4.4.1. Conclusions

Crosslink density has a pronounced effect on the properties of some tested rubbers, especially unfilled. While its effect on mechanical properties is widely studied in

literature, relation of the degree of crosslinking to the dielectric properties of speciality rubbers and the morphology of the sample is not fully investigated. Moreover, the possible influence of fillers on the crosslinking process should be taken into consideration. Currently, no clear relations between rubber types, amount and type of incorporated filler and mechanical/dielectric properties of the studied materials is seen. Although the importance of crosslink density for DEA materials can be overestimated in the current work, more information about surface activity, dielectric constants and pH values of the fillers can be useful for further studies.

4.5. Microscopy

SEM pictures provide information about presence and size of pores in the materials. They also allow evaluating the dispersion of particles and their agglomerates. For example, ***Figure 4.36*** reveals that ACM sample mixed on mill has large amount of pores of about 300 nm in size. With addition of BT the amount of pores decreases significantly, but their size stays relatively unchanged.

Finally, ***Figure 4.37*** shows the selected samples with 10 phr of fillers. BT and TO tend to form agglomerates, which is common problem for nanosized materials, such as TO. The size of BT powder is less than 2 μm, as declared by the manufacturer, and its uneven particle distribution can be related to inefficient mixing. However, improved filler dispersion is stated not to have effect on dielectric permittivity of material [118]. The largest particles of TP can reach about 250 μm and can be noticed visually especially if they form aggregates, but such large particles were not seen at the fracture surface. The SEM image possibly shows some smaller TP inclusions in the material. Remarkably, just very few voids can be seen in ACM filled with TP compared to the samples filled with same amount of BT or TO.

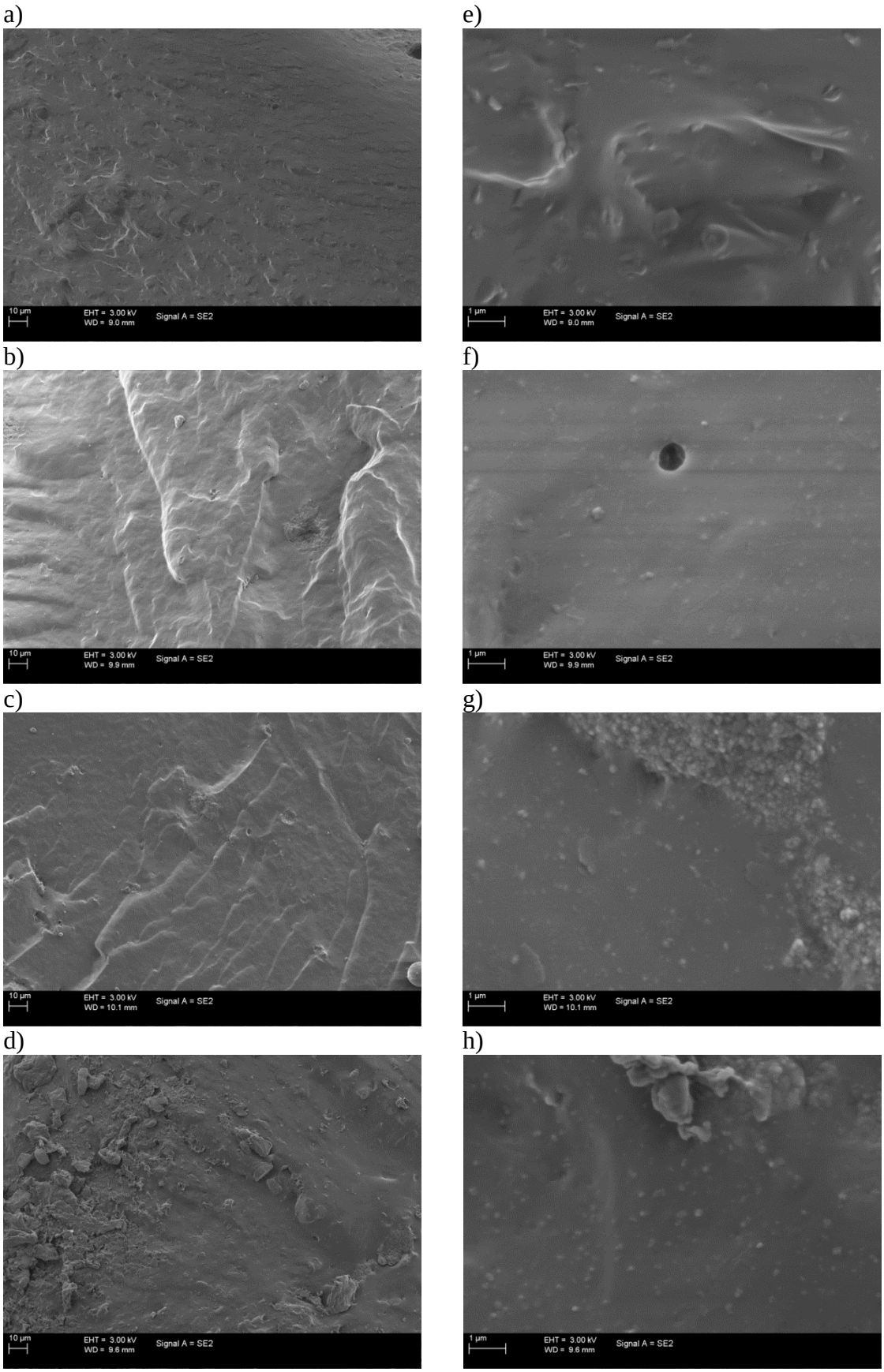

***Figure 4.36**. SEM images of unfilled ACM (a, e) and ACM with 5 phr (b, f); 10 phr (c, g); 20 phr (d, h) of barium titanate.*

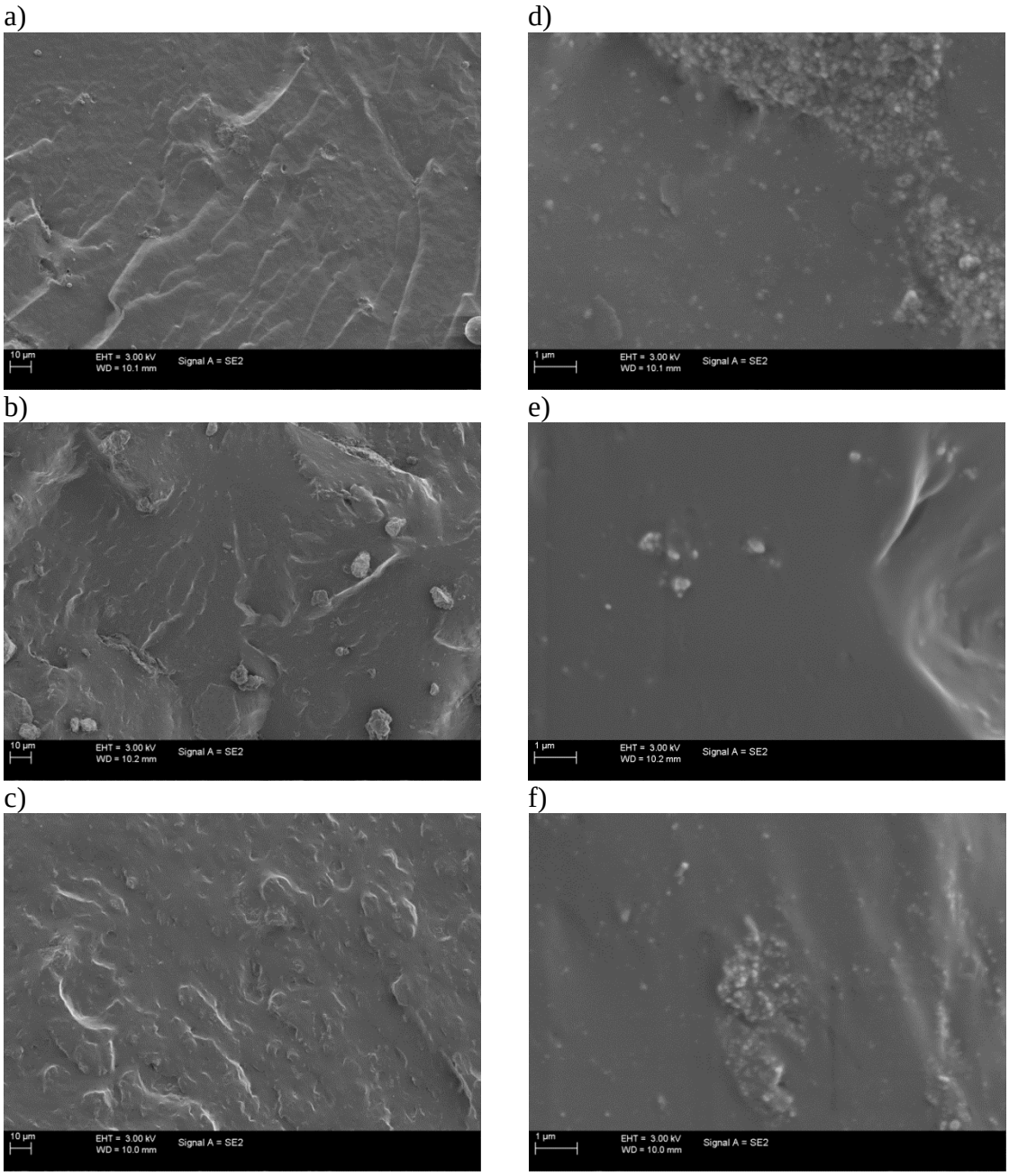

Figure 4.37*. SEM images of ACM compound containing 10 phr of BT (a, d), TP (b, e) and TO (c, f) with different magnification.*

4.5.1. Conclusions

Scanning electron microscopy provides good supplementary information for the research that helps in explaining the result of mechanical and dielectric testing. It is helpful to detect the pores inside the sample, while other methods (e.g., comparing theoretically calculated density to the experimentally determined one) may be more inaccurate. However, SEM cannot give much information about the fillers that are so much different in particle size, when same magnification is used for all the samples.

4.6. Evaluation of materials

For the proper evaluation of actuation materials, real actuation tests should be performed in addition to the presented test methods. Preliminary theoretical estimation of actuation behaviour is also possible, for example, by applying Maxwell pressure equation and the following thickness strain formula. In order to estimate actuation behaviour of tested materials with Maxwell's equation, it should be assumed that dielectric materials are ideal meaning that stretching has no effect on their dielectric behaviour. Otherwise, more sophisticated modelling should be performed that stay outside the scope of current work.

From **Chapters 2.1.5 - 2.1.6**, it is clear that performance of real DEAs is limited by electrical breakdown strength, EMI, prestraining and elasticity of the material in addition to the already mentioned dielectric and mechanical properties. The simplest way to compare materials in their possible actuation performance is to calculate the ε'/Y ratio, like it was done in some works [50;61]. Here, actuation properties of tested materials are estimated based on assumption that they are ideal not prestrained dielectrics with dielectric strength higher than maximum applied electric field and showing no EMI. Finally, it is worth mentioning that real actuation behaviour is usually poorer than estimated one.

Attention should also be paid to the dielectric losses in material and elasticity of composites. First, low dielectric losses generally mean better actuation performance at a given electric field. That is related to less energy dissipated in each cycle and lower heat build-up. Compared to the material with high losses, it may also mean lower actuation electric field and improved life-time. Furthermore, high losses can arise from increased conductivity of materials, and for DEA material it is important to stay in high resistivity range. Second, elastic materials with higher maximum elongation can be preferred over materials with similar other properties (ε'/Y ratio, dielectric loss factor (tgδ), tensile strength, etc.) because they allow larger prestaining and may result in better actuation strains and electromechanical stability. ***Figure 4.38*** shows evaluation of neat elastomeric materials prepared in internal mixer. Values of the loss factor are not shown, because they are comparably same for ACMs and CO rubbers (0.02-0.03), and reach 1.34 for GECO samples.

Based on this evaluation, ACM with chlorine cure-sites and CO are expected to have better actuation performance than other tested elastomers. According to the data from ***Figure 4.39***, TP shows poorest properties among fillers for both ACM and CO. Addition of oils may be beneficial for ACM, but lead to decrease in ε'/Y ratio for CO samples. Finally, loss factor was decreased from 0.02 to 0.01 when 5 phr of filler or oil was introduced into ACM matrix, while no significant changes were seen for CO. No data is available for CO/TO samples because of the problems with its preparation mentioned earlier in **Chapter 3.2**.

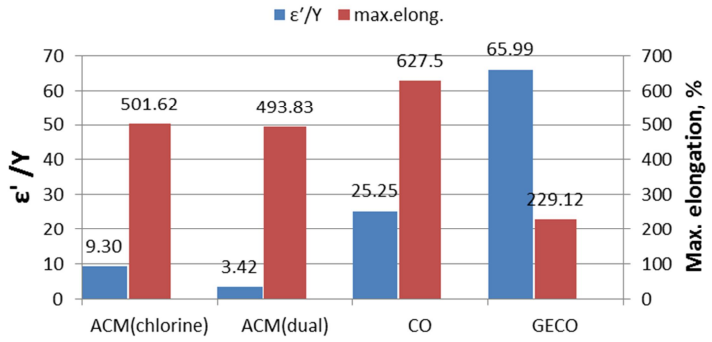

***Figure 4.38**. Evaluation of unfilled elastomers of different types.*

Samples prepared by solution-casting methods are excluded from the material evaluation because of obviously poor properties related to the distribution of particles and curatives, as well as to disadvantages in fabrication.

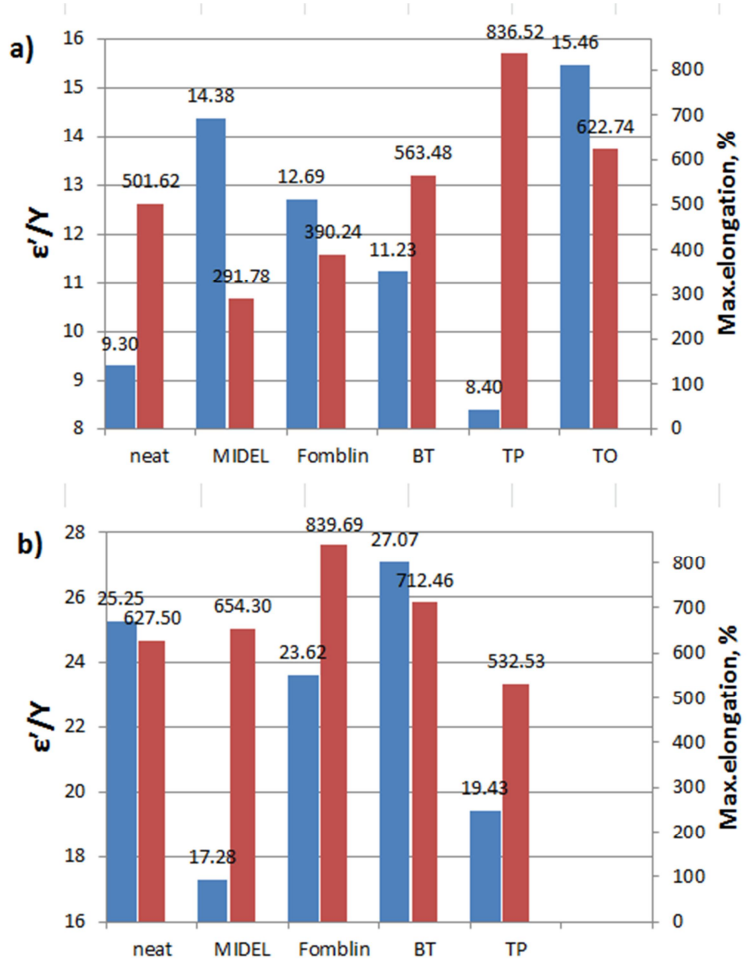

***Figure 4.39**. Evaluation of selected elastomers with 5 phr fillers/oils; a) ACM(chlorine); b) CO.*

4.6.1. Conclusions

Among the samples prepared in internal mixer, ACM with chlorine cure-sites and CO rubbers are believed to have the best perspectives for the application in DEAs. BT and TO can be used further, but transformer oils do not perform satisfactory and can be replaced by some conventional plasticizers in the future research. However, before excluding TP from the further studies, it could be important to test TP with smaller particle size. Finally, only actuation tests can reveal the real performance of the materials because the response of the dielectric materials to the applied electric field is dependent on numerous factors and cannot be predicted just by mechanical and dielectric properties of the material.

5. General conclusions and further work

The current work aims to investigate the effect of material type and preparation method, as well as type and amount of different fillers and plasticizers on the mechanical and dielectric properties of the selected elastomers. These goals contribute to the further development of the superior material for DEA application. As the result of the conducted research, not much improvement was obtained in the elastomeric material concerning its applicability for DEA. However, current work showed its importance at the initial stage of the research. Here, different methods of sample preparation and dielectric testing were investigated and compared revealing the most promising ones. The most suitable techniques and materials were pointed out together with the suggestions about improving them. Moreover, deeper understanding of dielectric phenomena was obtained, as well as enlarged knowledge of practical aspects related to the dielectric testing.

First, the study revealed that conventional rubber mixing is beneficial over solution casting methods, as it provides better uniformity of samples resulting in more homogenous properties and is generally faster than solution casting technique. The observed differences in mechanical properties of the samples prepared in internal mixer and on mill can be related to the increased porosity of the latter one, as revealed in SEM images. More detailed investigation is needed, and preparation conditions leading to creation of pores should be determined. Among the samples prepared in internal mixer, neat ACM with chlorine cure-sites and CO rubbers show more suitable properties for the DEA applications because of their low elastic modulus and high enough dielectric permittivity. However, ACM and CO samples, both neat and filled, suffered from significant deviations of mechanical and dielectric properties within the sample that is related to the poor distribution of curatives and filler particles during mixing. When porosity was not affecting the results, addition of fillers to ACM rubbers resulted in some increase in dielectric constant and reduced elastic modulus, especially for TO. For the unknown reason, CO samples loaded with different types of fillers had reduced dielectric permittivity. Investigation of the microscopic structure of those materials could be helpful in finding reason for that. Although current GECO samples have increased conductivity and high elastic modulus, addition of fillers, for instance, 20 phr of TP resulted in significantly reduced conductivity as well as decreased elastic modulus and dielectric loss factor. At the same time, dielectric constant of such material was much higher than that of the other rubbers.

Among the fillers, BT and TO seem to be more preferable for further studies, but transformer oils do not perform satisfactory with the selected rubbers and could be replaced by some conventional plasticizers, for example, DOP or DOA in the future. Moreover, it could be important to test same fillers with different particle size, as

dielectric properties of the filler are related to this parameter. Furthermore, higher loads of fillers should be mixed with the selected rubbers.

Next, crosslink density has a pronounced effect on the properties of some tested rubbers, especially unfilled ones. The effect of crosslinking on the dielectric properties of speciality rubbers and the morphology of the sample is not fully investigated. Although its importance can be overestimated, possible influence of fillers on the curing process should be taken into consideration. Therefore, more information about surface activity, dielectric constants and pH values of the fillers could be useful for further research on the field.

Finally, only actuation tests can reveal the real performance of the materials, because the response of the dielectric materials to the applied electric field is dependent on numerous factors and cannot be predicted just by mechanical and dielectric properties of the material. However, recommendations for the further research include:

- The conventional rubber mixing process should be adjusted in order to obtain better dispersion of fillers and curatives. The possible changes involve, for example, increased fill factor for ACMs that can reach 0.95, lower mixing temperatures and different mixing scheme. Another solution may be to use commercially available curative dispersion packages.
- Other solution-based fabrication methods could be tested, for example, substrate dipping and spraying techniques. Such methods should result in obtaining thin elastomeric films of good quality with reduced fabrication time compared to the solution-casting methods used in the current work. Here the attention should be paid to the applied solvent, dispersion of the particles in solution, viscosity of the solution and drying conditions.
- It is assumed that further addition of dielectric fillers can improve electrical resistivity of GECO material by disrupting the percolation paths between ethylene oxide (EO) units that are responsibly for conductivity of GECO rubbers. Moreover, GECO with low content of EO could be used as matrix. At the same time, mechanical properties of such material could be adjusted by lowering the crosslink density.
- Fillers of different particle sizes and loads can be tested with the studied rubbers after mixing process is modified successfully. Moreover, fillers can be added to the conventionally plasticized rubbers. It could be important to precondition the fillers that tend to absorb water, like TO, before the mixing in order to exclude its effect on the results.
- Real actuation tests should be performed for the selected material, and test can be performed with stretchable electrodes at different prestrain rates. Moreover, determination of dielectric breakdown strength of CO is important.

References

1. Xia F, Jiang L. Bio-inspired, smart, multiscale interfacial materials. *Advanced Materials* 2008; 20 (15) : 2842-2858.

2. Pelrine R, Kornbluh RD, Pei Q, et al. Dielectric elastomer artificial muscle actuators: toward biomimetic motionProc. SPIE 4695, Smart Structures and Materials 2002: Electroactive Polymer Actuators and Devices (EAPAD), 126July 102002126-137126-137.

3. Brochu P, Pei Q. Advances in dielectric elastomers for actuators and artificial muscles. *Macromolecular Rapid Communications* 2010; 31 (1):10-36.

4. Löwe C, Zhang X, Kovacs G. Dielectric elastomers in actuator technology. *Advanced Engineering Materials* 2005; 7 (5):361-367.

5. Shankar R, Ghosh TK, Spontak RJ. Dielectric elastomers as next-generation polymeric actuators. *Soft Matter* 2007; 3 (9):1116-1129.

6. Bar-Cohen Y, ed. *Biomimetics: Nature-based innovation. Chapter 6. Electroactive polymer actuators as artificial muscles.* CRC Press; 2011. Bar-Cohen Yoseph, ed. Electroactive Polymer Actuators as Artificial Muscles.

7. Mirfakhrai T, Madden JDW, Baughman RH. Polymer artificial muscles. *Materials Today* 2007; 10 (4) : 30-38.

8. Kim KJ, Tadokoro S, eds. *Electroactive polymers for robotic applications: Artificial muscles and sensors.* Springer; 2007.

9. Gallone G, Galantini F, Carpi F. Perspectives for new dielectric elastomers with improved electromechanical actuation performance: Composites versus blends. *Polymer International* 2010; 59 (3):400-406.

10. Chen L, Liu C, Liu K, et al. High-performance, low-voltage, and easy-operable bending actuator based on aligned carbon nanotube/polymer composites. *ACS Nano* 2011; 5 (3) : 1588-1593.

11. Stoyanov H, Kollosche M, Risse S, McCarthy DN, Kofod G. Elastic block copolymer nanocomposites with controlled interfacial interactions for artificial muscles with direct voltage control. *Soft Matter*. 2011; 7 (1):194-202.

12. Carpi F, Rossi DD, Kornbluh R, Pelrine R, Sommer-Larsen P, eds. *Dielectric elastomers as electromechanical transducers: Fundamentals, materials, devices, models and applications of an emerging electroactive polymer technology.* 1st edition ed. Academic Press; 2008.

13. Stoyanov H. *Soft nanocomposites with enhanced electromechanical response for dielectric elastomer actuators.* [D.Sc. thesis]. University of Potsdam; 2010.

14. Kofod G. *Dielectric elastomer actuators.* [Ph.D. thesis]. The Technical University of Denmark; 2001.

15. Birks JB, ed. *Modern dielectric materials.* London: Heywood&Company; 1960.

16. Maliakal A. Chapter 3.2 dielectric materials: Selection and design. In: Bao Z, Locklin J, eds. *Organic field-effect transistors.* CRC Press; 2007:229-251.

17. Van Krevelen DW, Te Nijenhuis K. Chapter 11 - Electrical properties. In: Krevelen DWV, Nijenhuis KT, eds. *Properties of polymers (fourth edition).* Amsterdam: Elsevier; 2009:319-354.

18. Riande E, Díaz-Calleja R. *Electrical properties of polymers.* NY: Marcel Dekker; 2004:649.

19. Сканави ГИ. *Физика диэлектриков (область слабых полей).* Том 1. Москва-Ленинград: Государственное издательство технико-технической литературы; 1949:500. [Skanavi GI. *Physics of dielectrics (in weak fields).*Vol.1. Moscow-Leningrad; 1949:500]

20. Kao KC. Chapter 4 - Ferroelectrics, piezoelectrics, and pyroelectrics. In: *Dielectric phenomena in solids.* San Diego: Academic Press; 2004:213-282.

21. Перепечко ИИ. *Введение в физику полимеров.* Москва: Химия; 1978:312. [Perepechko II. *Introduction to polymer physics.* Moscow: Khimiya; 1978:312]

22. Jonscher AK. Dielectric relaxation in solids. *J Phys D* 1999 ;32 (14) :R57 .

23. Havriliak SJ, Havriliak SJ. *Dielectric and mechanical relaxation in materials: Analysis, interpretation, and application to polymers.* Göttingen: Hanser Gardner Publications; 1997:508.

24. Kao KC. 8 - Electrical aging, discharge, and breakdown phenomena. In: *Dielectric phenomena in solids.* San Diego: Academic Press; 2004:515-572.

25. Niu X, Stoyanov H, Hu W, Leo R, Brochu P, Pei Q. Synthesizing a new dielectric elastomer exhibiting large actuation strain and suppressed electromechanical instability without prestretching. *Journal of Polymer Science Part B: Polymer Physics* 2013;51 (3):197-206.

26. Zhao X, Suo Z. Theory of dielectric elastomers capable of giant deformation of actuation. *Phys Rev Lett* 2010; 104 (17):178302.

27. Kollosche M, Kofod G. Electrical failure in blends of chemically identical, soft thermoplastic elastomers with different elastic stiffness. *Appl Phys Lett* 2010; 96 (7):071904-071904-3.

28. Yuan W, Hu LB, Yu ZB, et al. Fault-tolerant dielectric elastomer actuators using single-walled carbon nanotube electrodes. *Adv Mater* 2008; 20 (3):621-625.

29. Yuan W, Brochu P, Ha SM, Pei Q. Dielectric oil coated single-walled carbon nanotube electrodes for stable, large-strain actuation with dielectric elastomers. *Sensors and Actuators A: Physical* 2009; 155 (2):278-284.

30. Chun K, Oh Y, Rho J, et al. Highly conductive, printable and stretchable composite films of carbon nanotubes and silver. *Nat Nano* 2010; 5 (12):853-857.

31. Sekitani T, Nakajima H, Maeda H, et al. Stretchable active-matrix organic light-emitting diode diaplay using printable elastic conductors. *Nature Materials* 2009; 8 (6): 494 - 499.

32. Rosset S, Shea HR. Flexible and stretchable electrodes for dielectric elastomer actuators. *Applied Physics A* 2013; 110 (2):281-307.

33. Bozlar M, Punckt C, Korkut S, et al. Dielectric elastomer actuators with elastomeric electrodes. *Appl Phys Lett* 2012; 101 (9):091907.

34. Hsien Low S, Lynn Shiau L, Lau G. Large actuation and high dielectric strength in metallized dielectric elastomer actuators. *Appl Phys Lett* 2012; 100 (18):182901.

35. Yang D, Tian M, Dong Y, Kang H, Gong D, Zhang L. A high-performance dielectric elastomer consisting of bio-based polyester elastomer and titanium dioxide powder. *J Appl Phys* 2013; 114 (15).

36. Zhou J, Hong W, Zhao X, Zhang Z, Suo Z. Propagation of instability in dielectric elastomers. *Int J Solids Structures* 2008; 45 (13):3739-3750.

37. Suo Z, Zhao X, Greene WH. A nonlinear field theory of deformable dielectrics. *J Mech Phys Solids* 2008; 56 (2):467-486.

38. Plante J, Dubowsky S. On the performance mechanisms of dielectric elastomer actuators. *Sensors and Actuators A: Physical* 2007; 137(1):96-109.

39. Plante J, Dubowsky S. Large-scale failure modes of dielectric elastomer actuators. *Int J Solids Structures* 2006; 43 (25–26):7727-7751.

40. Pelrine R, Kornbluh R, Joseph J, Heydt R, Pei Q, Chiba S. High-field deformation of elastomeric dielectrics for actuators. *Materials Science and Engineering: C* 2000 ;11 (2) :89-100.

41. Shankar R, Ghosh TK, Spontak RJ. Electromechanical response of nanostructured polymer systems with no mechanical pre-strain. *Macromolecular Rapid Communications* 2007; 28 (10):1142-1147.

42. Simpson RB. *Rubber basics.* iSmithers Rapra Publishing; 2002.

43. Nam J, Choi HR, Koo JC, Lee YK, Kim KJ. Dielectric elastomers for artificial muscles. In: Kim K, Tadokoro S, eds. *Electroactive polymers for robotic applications.* Springer London; 2007:37-48.

44. Choi HR, Jung KM, Koo JC, Nam JD, Lee YK, Cho MS. Electrostatically driven soft polymer actuator based on dielectric elastomer. *Key Engineering Materials* 2005; 297-300:622-627.

45. Chuc NH, Koo JC, Lee YK, Nam J, Choi HR. Artificial muscle actuator based on the synthetic elastomer. *International Journal of Control, Automation and Systems* 2008; 6 (6):894-903.

46. Tangboriboon N, Datsanae S, Onthong A, Kunanuruksapong R, Sirivat A. Electromechanical responses of dielectric elastomer composite actuators based on natural rubber and alumina. *Journal of Elastomers and Plastics* 2013;45 (2):143-161.

47. Kunanuruksapong R, Sirivat A. Highly electroresponsive polymer blends of polyaniline nanoparticles and chloroprene rubbers. *Advances in Polymer Technology* 2013;32 (S1):E556–E571.

48. Intanoo P, Sirivat A, Kunanuruksapong R, Lerdwijitjarud W. Electromechanical properties of ethylene propylene diene elastomers: Effect of ethylene norbornene content. *Materials Sciences and Applications* 2011;2 (5):307-313.

49. Intanoo P, Sirivat A, Kunanuruksapong R, Lerdwijitjarud W, Kunchornsup W. Electroactive polymer actuator ffom highly doped permethylpolyazine dispersed in ethylene propylene diene elastomer. *Journal of Polymer Research* 2012; 19 (10):1-10.

50. Yang D, Tian M, Kang H, et al. New polyester dielectric elastomer with large actuated strain at low electric field. *Materials Letters* 2012; 76:229-232.

51. Goswami K, Galantini F, Mazurek P, Daugaard AE, Gallone G, Skov AL. Reinforced poly(propylene oxide): A very soft and extensible dielectric electroactive polymer. *Smart Mater Struct* 2013; 22 (11):115011.

52. Molberg M, Leterrier Y, Plummer CJG, et al. Frequency dependent dielectric and mechanical behavior of elastomers for actuator applications. *Journal of Applied Physics* 2009;106 (5):054112.

53. Shankar R, Ghosh TK, Spontak RJ. Electroactive nanostructured polymers as tunable actuators. *Advanced Materials* 2007;19 (17):2218-2223.

54. Liu R, Wang J, Li Q, Li S, Zhang S, Ding X. Copper phthalocyanine oligomer grafted acrylic elastomer nanocomposites with high dielectric constants. *J Appl Polym Sci* 2014;131 (6):[np].

55. Michel S, Zhang XQ, Wissler M, Löwe C, Kovacs G. A comparison between silicone and acrylic elastomers as dielectric materials in electroactive polymer actuators. *Polymer International* 2010;59 (3) 391-399.

56. Wissler M. *Modeling dielectric elastomer actuators.* [Doctor of Sciences thesis]. Swiss Federal Institute of Technology in Zurich; 2007.

57. Koh SJA, Li T, Zhou J, et al. Mechanisms of large actuation strain in dielectric elastomers. *Journal of Polymer Science Part B: Polymer Physics* 2011;49 (7):504-515.

58. Biggs J, Danielmeier K, Hitzbleck J, et al. Electroactive polymers: Developments of and perspectives for dielectric elastomers. *Angewandte Chemie International Edition* 2013;52 (36):9409-9421.

59. Matoba Y, Shoji S, Ikeda Y. Conductivity of crosslinked poly(epichlorohydrin-co-(ethylene oxide)-co-(allyl glycidyl ether)) compositions under ambient circumstances for its application to an electrophotographic system. *J Appl Polym Sci* 2005;98 (2):825-830.

60. Dick JS, ed. *Rubber technology: Compounding and testing for performance.* 2nd ed. Hanser Gardner Publications; 2009.

61. Yang D, Zhang L, Liu H, Dong Y, Yu Y, Tian M. Lead magnesium niobate-filled silicone dielectric elastomer with large actuated strain. *Journal of Applied Polymer Science* 2012;125 (3):2196-2201.

62. Franta I, ed. *Elastomers and rubber compounding materials. Manufacture, properties and applications.* Elsevier; 1989.

63. Morton M, ed. *Rubber technology.* 3rd edition ed. Chapman&Hall; 1995.

64. Starmer PH, Wolf FR. Acrylic elastomers, survey. In: *Encyclopedia of polymer science and technology.* John Wiley & Sons, Inc.; 2002.

65. Di Lillo L, Schmidt A, Carnelli DA, et al. Measurement of insulating and dielectric properties of acrylic elastomer membranes at high electric fields. *J Appl Phys.* 2012;111 (2):024904.

66. Klingender RC. Chapter 5. Polyacrylate Elastomers—Properties and applications. In: Klingender RC, ed. *Handbook of specialty elastomers.* CRC Press; 2008:155-192.

67. Wootthikanokkhan J, Burford RP, Chaplin RP. Effect of curing agent on interfacial adhesion in acrylic polymer-based laminates. *Journal of Applied Polymer Science* 1998;67 (7):1277-1284.

68. Vial TM. Elastomers, synthetic. Acrylic elastomers. In: Mark HF, Kirk RE, Othmer DF, Seaborg GT, eds. *Kirk-othmer encyclopedia of chemical technology.* Vol 8. 3rd ed. Wiley & Sons, Inc.; 1979:459-469, 930 pp.

69. Klingender RC. Chapter 7. Polyepichlorohydrin elastomer. In: Klingender RC, ed. *Handbook of specialty elastomers.* CRC Press; 2008:245-288.

70. Gallone G, Carpi F, De Rossi D, Levita G, Marchetti A. Dielectric constant enhancement in a silicone elastomer filled with lead magnesium niobate–lead titanate. *Materials Science and Engineering: C* 2007;27 (1):110-116.

71. Wetzel B, Haupert F, Friedrich K, Zhang MQ, Rong MZ. Impact and wear resistance of polymer nanocomposites at low filler content. *Polymer Engineering & Science* 2002; 42 (9):1919-1927.

72. Li Y, Huang X, Hu Z, Jiang P, Li S, Tanaka T. Large dielectric constant and high thermal conductivity in poly(vinylidene fluoride)/barium titanate/silicon carbide three-phase nanocomposites. *ACS Appl Mater Interfaces* 2011; 3 (11):4396-4403.

73. Nowotny J. Chapter 3. Basic properties of TiO2. In: *Oxide semiconductors for solar energy conversion. Titanium dioxide.* CRC Press; 2011:145–163.

74. Nelson JK, ed. *Dielectric polymer nanocomposites.* Springer US; 2010.

75. Nalwa HS, ed. *Handbook of low and high dielectric constant materials and their applications.* Academic Press; 1999; No. Volume 1: Materials and Processing. Volume 2: Phenomena, Properties and Applications. (Two-Volume Set).

76. Parker RA. Static dielectric constant of rutile (TiO2), 1.6-1060Â°K. *Phys Rev* 1961; 124 (6):1719-1722.

77. Pavlovic AS. Some dielectric properties of tantalum pentoxide. *J Chem Phys* 1964; 40 (4):951-956.

78. Lin J, Masaaki N, Tsukune A, Yamada M. Ta2O5 thin films with exceptionally high dielectric constant. *Applied Physics Letters* 1999; 74 (16):2370-2372.

79. Kim P, Jones SC, Hotchkiss PJ, et al. Phosphonic acid-modified barium titanate polymer nanocomposites with high permittivity and dielectric strength. *Advanced Materials* 2007; 19 (7):1001-1005.

80. Tuttle BA, Voigt JA, Sipola DL, Olson WR, Goy DM. Chemically prepared lead magnesium niobate dielectrics. *MRS Proceedings* 1997;495:185.

81. Jesurani S, Kanagesan S, Velmurugan R, Kalaivani T. Phase formation and high dielectric constant of calcium copper titanate using sil-gel route. *Journal of Materials Science: Materials in Electronics* 2012; 23 (3):668-674.

82. Carpi F, Gallone G, Galantini F, De Rossi D. Silicone/poly(hexylthiophene) blends as elastomers with enhanced electromechanical transduction properties. *Advanced Functional Materials* 2008; 18 (2) : 235-241.

83. Risse S, Kussmaul B, Krüger H, Kofod G. Synergistic improvement of actuation properties with compatibilized high permittivity filler. *Advanced Functional Materials* 2012;22 (18):3958-3962.

84. Muscat J, Swamy V, Harrison NM. First-principles calculations of the phase stability of TiO2. *Phys Rev B* 2002; 65 (22):224112.

85. Katz HS, Milewski JV, eds. *Handbook of fillers for plastics.* 2nd ed. New York: Van Nostrand Reinhold Company; 1987.

86. Diebold U. The surface science of titanium dioxide. *Surface Science Reports* 2003; 48 (5–8):53-229.

87. Kuo D, Chang C, Su T, Wang W, Lin B. Dielectric properties of three ceramic/epoxy composites. *Mater Chem Phys* 2004;85 (1):201-206.

88. Tsurumi T, Sekine T, Kakemoto H, et al. Evaluation and statistical analysis of dielectric permittivity of BaTiO3 powders. *J Am Ceram Soc* 2006; 89 (4):1337-1341.

89. Smith MB, Page K, Siegrist T, et al. Crystal structure and the paraelectric-to-ferroelectric phase transition of nanoscale BaTiO3. *J Am Chem Soc* 2008; 130 (22):6955-6963.

90. Böse H, Uhl D, Flittner K, Schlaak H. Dielectric elastomer actuators with enhanced permittivity and strain Proc. SPIE, Electroactive Polymer Actuators and Devices (EAPAD) March 24 2011-79762J.

91. Liu Y, Liu L, Zhang Z, Leng J. Dielectric elastomer film actuators: Characterization, experiment and analysis. *Smart Materials and Structures* 2009; 18 (9):095024.

92. Zibrov IP, Filonenko VP, Sundberg M, Werner P-. Structures and phase transitions of*B*-Ta2O5 and*Z*-Ta2O5: Two high-pressure forms of Ta2O5. *Acta Crystallographica B* 2000; 56:659-665.

93. Zhao H, Wang D, Zha J, Zhao J, Dang Z. Increased electroaction through a molecular flexibility tuning process in TiO2-polydimethylsilicone nanocomposites. *Journal of Materials Chemistry A* 2013 (9):3140-3145.

94. Hao L, Shi Z, Zhao X. Mechanical behavior of starch/silicone oil/silicone rubber hybrid electric elastomer. *React Funct Polym* 2009; 69 (3):165-169.

95. Chuc NH, Doan VT, Park JK, et al. The effects of additives on the actuating performances of a dielectric elastomer actuator. *Smart Materials and Structures* 2009; 18 (1):015006.

96. Böse H, Uhl D, Rabindranath R. Novel DEA with organically modified silicone elastomer for permittivity enhancementProc. SPIE, Electroactive Polymer Actuators and Devices (EAPAD)8340 April 26 2012 -83402E.

97. Ludeelerd P, Niamlang S, Kunaruksapong R, Sirivat A. Effect of elastomer matrix type on electromechanical response of conductive polypyrrole/elastomer blends. *Journal of Physics and Chemistry of Solids* 2010; 71 (9):1243-1250.

98. Liu H, Zhang L, Yang D, et al. A new kind of electro-active polymer composite composed of silicone elastomer and polyethylene glycol. *Journal of Physics D: Applied Physics* 2012; 45 (48):485303.

99. Herbert JM. *Ferroelectric transducers and sensors.* Vol 3. Gordon&Breach; 1982:438.

100. Zeon Chemicals L.P. ZEON: 2013 product guide. *Bulletin.* 2013:15.

101. C5-10 fatty acids esters with pentaerythritol. chemBlink Online Database of Chemicals from Around the World Web site. http://www.chemblink.com/products/68424-31-7.htm. Updated 2103. Accessed 9/11, 2013.

102. CAS no 69991-67-9. GuideChem. Chemical trading quide. Web site. http://www.guidechem.com/cas-699/69991-67-9.html. Updated 2013. Accessed 9/11, 2013.

103. Sahoo B, Naskar K, Tripathy D. Conductive carbon black-filled ethylene acrylic elastomer vulcanizates: Physico-mechanical, thermal, and electrical properties. *J Mater Sci* 2012 ;47 (5) :2421-2433.

104. Gent AN, ed. *Engineering with rubber - how to design rubber components.* 2nd ed. Hanser Publishers; 2001.

105. Orwoll RA, Arnold PA. Polymer-solvent interaction parameter X. In: Mark J, ed. Springer New York; 2007:233-257.

106. Schuld N, Wolf BA. Polymer-solvent interaction parameters. In: Mark J, ed. Springer New York; 1999:VII/247-265.

107. Sekkar V. Comparison between crosslink densities derived from stress-strain data and theoretically data evaluated through the a-model approach for a polyurethane network system based on hydroxyl terminated polybutadiene and isophorone-diisocyanate. *J Appl Polym Sci* 2010; 117 (2):920-925.

108. Xu H, Han J, Fang L, Shen F, Wu C. Effect of grafted carbon black on properties of vulcanized natural rubber. *Polymer Bulletin* 2007; 58 (5-6):951-962.

109. Chen Y, Xu C. Crosslink network evolution of nature rubber/zinc dimethacrylate composite during peroxide vulcanization. *Polymer Composites* 2011; 32 (10):1505-1514.

110. Bhattacharya M, Bhowmick AK. Polymer–filler interaction in nanocomposites: New interface area function to investigate swelling behavior and young's modulus. *Polymer* 2008; 49 (22):4808-4818.

111. Tiwari M, Datta RN, Talma AG, Noordermeer JWM, Dierkes WK, van Ooij WJ. Comparative study of plasma-thiophene and -acetylene coated silica in SBR and EPDM reinforcement. *Rubber Chem Technol* 2009; 82 (5):473-491.

112. Poikelispää M, Das A, Dierkes W, Vuorinen J. Synergistic effect of plasma-modified halloysite nanotubes and carbon black in natural rubber-butadiene rubber blend. *Journal of Applied Polymer Science*. 2012.

113. Omnès B, Thuillier S, Pilvin P, Grohens Y, Gillet S. Effective properties of carbon black filled natural rubber: Experiments and modeling. *Composites Part A: Applied Science and Manufacturing* 2008; 39 (7):1141-1149.

114. Leblanc JL. Elastomer-filler interactions and the rheology of filled rubber compounds. *J Appl Polym Sci* 2000;78 (8):1541-1550.

115. Ha SM, Yuan W, Pei Q, Pelrine R, Stanford S. Interpenetrating polymer networks for high-performance electroelastomer artificial muscles. *Adv Mater* 2006; 18 (7):887-891.

116. Meththananda IM, Parker S, Patel MP, Braden M. The relationship between shore hardness of elastomeric dental materials and young's modulus. *Dental Materials* 2009; 25 (8):956-959.

117. Araromi OA, Conn AT, Ling CS, Rossiter JM, Vaidyanathan R, Burgess SC. Spray deposited multilayered dielectric elastomer actuators. *Sensors and Actuators A: Physical* 2011; 167 (2):459-467.

118. Mc Carthy DN, Risse S, Katekomol P, Kofod G. The effect of dispersion on the increased relative permittivity of TiO2 /SEBS composites. *J Phys D* 2009; 42 (14):145406.

Appendix 1: Comparison of biological muscles and available actuator materials

Table A. 1. *Comparison of actuator materials [3].*

Type (specific)	Maximum strain	Maximum pressure	Specific elastic energy density	Elastic energy density	Coupling efficiency k^2	Maximum efficiency	Specific density	Relative speed (full cycle)
	%	MPa	$J \cdot g^{-1}$	$J \cdot cm^{-3}$	%	%		
Dielectric elastomer (acrylic with prestrain)	380	7.2	3.4	3.4	85	60–80	1	Medium
Dielectric elastomer (silicone with prestrain)	63	3	0.75	0.75	63	90	1	Fast
Dielectric elastomer (silicone—nominal prestrain)	32	1.36	0.22	0.2	54	90	1	Fast
Electrostrictive polymer [P(VDF–TrFE)]	4.3	43	0.49	0.92	–	≈80 (est.)	1.8	Fast
Electrostatic devices (integrated force array)	50	0.03	0.0015	0.0025	50 (est.)	>90	1	Fast
Electromagnetic (voice coil)	50	0.1	0.003	0.025	–	>90	8	Fast
Piezoelectric ceramic (PZT)	0.2	110	0.013	0.1	52	>90	7.7	Fast
Piezoelectric single crystal (PZT-PT)	1.7	131	0.13	1	81	>90	7.7	Fast
Piezoelectric polymer (PVDF)	0.1	4.8	0.0013	0.0024	7	–	1.8	Fast
Shape memory alloy (TiNi)	>5	>200	>15	>100	5	<10	6.5	Slow
Shape memory polymer (polyurethane)	100	4	2	2	–	<10	1	Slow
Thermal (expansion—Al, dT = 500 K)	1	78	0.15	0.4	–	<10	2.7	Slow
Conducting polymer (PANI)	10	450	23	23	<1	<5 (est.)	≈1	Slow
Ionic gels (polyelectrolyte)	>40	0.3	0.06	0.06	–	30	≈1	Slow
Magnetostrictive (terfenol-D)	0.2	70	0.0027	0.025	–	60	9	Fast
Natural muscle (human skeletal)	>40	0.35	0.07	0.07	–	>35	1	Medium
Natural muscle (peaks in nature)	100	0.8	0.04	0.04	–	40	–	Slow–fast

Table A. 2. *Comparison of classes of muscle-like materials with natural muscles [2].*

Actuator	Strain	Actuation Pressure	Density	Efficiency	Speed (fast AND slow)
Natural Muscle	●	●	●	●	●
Electromagnetic	●	●	○	●	○
Piezoelectric	○	●	◐	●	●
Shape Memory Alloy	◐	●	◐	○	○
Magnetostrictive	○	●	○	●	○
Electrostatic	●	○	●	●	●
Dielectric Elastomers	●	●	●	●	●
○ = Poor		◐ = Fair		● = Good	